UNIVERSIDAD NACIONAL AUTÓNOMA DE MÉXICO

PROGRAMA DE MAESTRÍA Y DOCTORADO EN INGENIERÍA

ENERGÍA – SISTEMAS ENERGÉTICOS

DIFFUSION PROCESSES IN NUCLEAR REACTORS WITH MATHEMATICAL MODELING OF FRACTIONAL ORDER

TESIS

QUE PARA OPTAR POR EL GRADO DE:

DOCTOR EN INGENIERÍA

PRESENTA:

ÉRICK GILBERTO ESPINOSA MARTÍNEZ

DR. JUAN LUIS FRANÇOIS LACOUTURE, Facultad de Ingeniería-UNAM

DRA. CECILIA MARTÍN DEL CAMPO MÁRQUEZ, Facultad de Ingeniería-UNAM

DR. NADER MALEKI MOGHADDAM, Universidad de Teherán

DR. GILBERTO ESPINOSA PAREDES, UAM-Iztapalapa

CIUDAD UNIVERSITARIA, CD. MX. DICIEMBRE 2021

JURADO ASIGNADO:

Presidente:	Dra. Martín del Campo Márquez Cecilia
Secretario:	Dr. Quezada García Sergio
1 er Vocal:	Dr. Francois Lacouture Juan Luis
2 do Vocal:	Dr. Espinosa Paredes Gilberto
3 er Vocal:	Dr. Polo Labarrios Marco Antonio

Lugar donde se realizó la tesis: CIUDAD UNIVERSITARIA, FACULTAD DE INGENIERÍA

TUTOR DE TESIS:

JUAN LUIS FRANÇOIS LACOUTURE

FIRMA

For Mérida & Nicolás, who shine on.

ACKNOWLEDGMENTS

I wish to thank to my family, for their support, and especially my parents who have never turned their back on me.

To all my professors and colleagues, who have shared their knowledge and have challenged me to give all my effort.

To The National Autonomous University of Mexico (UNAM) for giving me the chance to perform my postgraduate studies.

And finally, to the citizens of MEXICO whom through their taxes make possible to CONACyT to grant scholarships to perform postgraduate studies.

RESUMEN

En la presente tesis doctoral se desarrolla un novedoso modelo matemático puntual de orden fraccional para el estudio y análisis simultáneo de los procesos de transporte de calor y neutrones en reactores nucleares. Con el fin de lograrlo, el primer paso fue llevar a cabo una revisión literaria exhaustiva, la cual se realizó hasta la conclusión del presente trabajo. Lo siguiente, fue el desarrollo del modelo de la cinética neutrónica puntual fraccional de tiempo-espacio (TSFNPK por sus siglas en inglés), el cual considera dos exponentes de difusión anómalos (dos exponentes distintos de orden fraccional), uno que incluye estados de la memoria pasados (memoria de tiempo no local); y el otro, efectos de memoria espaciales (memoria espacial local). Adicionalmente se exploran métodos de solución, encontrando que el método de Edwards et al. (2002) tiene la mejor aproximación de solución para la ecuación diferencial de orden fraccional presentada. El modelo fue evaluado para obtener los intervalos en los que los exponentes de difusión fraccional producen los resultados más cercanos a los datos comparados. Al final, el acoplamiento del modelo TSFNPK se llevó a cabo en un código numérico de un Reactor de Agua Supercrítica (SCWR), se comparó con datos de la literatura y se encontraron resultados similares.

ABSTRACT

In this PhD thesis is presented a novel zero-dimensional mathematical model of fractional order for the analysis and study of the simultaneous heat and neutron transport processes in nuclear power reactors. In order to achieve this, the first step was to perform an extensive literature review, which was carried out until the fulfillment of the thesis. Following, a Time-Space Fractional Neutron Point Kinetics (TSFNPK) mathematical model was derived, which considers two-anomalous diffusion exponents (two different exponents of fractional order), one which includes memory past states (non-local time memory) and the other, space memory effects (local space memory); additionally, solution methods were explored, the Edwards et al. (2002) method was found to be the best solution approach for the present fractional differential equation. The model was assessed in order to obtain the intervals in which the fractional diffusion exponents yielded the results closest to compared data. At the end, the coupling of the developed TSFNPK model was accomplished in a Supercritical Water Reactor (SCWR) numerical code, results were compared to those of literature finding close agreement to some of them.

INDEX

NOMENCLATURE

A_f	Flow area	$\left[\mathrm{m}^2\right]$
B_g^2	Geometric buckling	$\left[\mathrm{m}^{-2}\right]$
B_g^{k+1}	Fractional geometric buckling	$\left[\mathrm{m}^{-(\kappa+1)}\right]$
Cp	Heat capacity	$\left[\mathrm{kg\,m^2\,s^{-2}\,K^{-1}}\right]$
D_m	Mass transfer diffusion coefficient	$\left[\mathrm{cm}^2/\mathrm{s}\right]$
D_n	Neutron diffusion coefficient	$\left[\mathrm{cm}\right]$
D_{th}	Thermal diffusivity	$\left[\mathrm{m}^2/\mathrm{s}\right]$
f	Friction factor	Dimensionless
$F(z)$	Axial power factor	Dimensionless
G	Mass flux	$\left[\mathrm{kg/m^2\,s}\right]$
H_∞	Convective heat transfer coefficient	$\left[\mathrm{W/m^2K}\right]$
k	Thermal conductivity	$\left[\mathrm{W\,m^{-1}\,K^{-1}}\right]$
k_{eff}	Effective multiplication factor	Dimensionless
k_∞	Infinite multiplication factor	Dimensionless
n	Neutron density	
l	Neutron lifetime	$\left[\mathrm{s}\right]$
ℓ	Characteristic length	$\left[\mathrm{cm}\right]$
L	Neutron difussion length	$\left[\mathrm{cm}\right]$

L_a	Characteristic length of the system	$[\mathrm{cm}]$
P_H	Heated perimeter	$[\mathrm{m}]$
P	Neutronic power	
P_0	Nominal power	
P_{NL}	Non-leakage probability	Dimensionless
$\vec{q}$	Heat flux vector	$\left[\mathrm{W\,m^{-2}}\right]$
q'''	Internal heat generation	$\left[\mathrm{W\,s^{-1}}\right]$
S	Neutron source	$\left[\mathrm{cm^{-3}s^{-1}}\right]$
t	Time	$[\mathrm{s}]$
T	Temperature	$[\mathrm{K}]$
V_f	Fuel volumen	$\left[\mathrm{m^3}\right]$
w	Thermal propagation velocity	$\left[\mathrm{m s^{-1}}\right]$

Greek letters and Special Characters

$\mathbf{J}$	Diffusion flux	$\left[\mathrm{mol\,m^{-2}s^{-1}}\right]$
$\mathbf{J}_n$	Neutron current density	$\left[\mathrm{cm^{-2}s^{-1}}\right]$
Σ_a	Macroscopic absorption cross section	$\left[\mathrm{cm^{-1}}\right]$
Σ_f	Macroscopic fission cross-section	$\left[\mathrm{cm^{-1}}\right]$
Σ_{tr}	Macroscopic transfer cross-section	$\left[\mathrm{cm^{-1}}\right]$

ϕ	Neutron flux	$\left[\mathrm{cm}^{-2}\mathrm{s}^{-1}\right]$
υ	Neutron velocity	$\left[\mathrm{cm}\,\mathrm{s}^{-1}\right]$
γ	Mean number of fission neutrons	Dimensionless
β	Fraction of delayed neutrons	Dimensionless
ρ_κ	Neutron leakage	Dimensionless
ρ_m	Density	$\left[\mathrm{kg}\,\mathrm{m}^{3}\right]$
ρ_n	Reactivity	Dimensionless
τ_0	Relaxation time	$[\mathrm{s}]$
τ_α	Fractional relaxation time	Dimensionless
λ	Decay constant	$\left[\mathrm{s}^{-1}\right]$
Λ	Neutron generation time	$[\mathrm{s}]$

Subindexes and Superindexes

α	Time dependent fractional diffusion exponent or related
κ	Space dependent fractional diffusion exponent or related
w	Wall
b	Bulk
n	Nuclear related
m	Mass related

Mathematical Operators and Functions

Γ	Gamma function
B	Beta function

$\hat{B}^{1/2}$	Square root of the matrix
D_α	Fractional time derivative
D_t^α	Caputo fractional derivative
Erf	Error function
$Erfc$	Complementary error function
E_α	Mittag-Leffler function
E_t	Mellin-Ross function
r	Cylindrical radial coordinate
W	Wiener process
∇	Gradient operator

Acronyms

2EFPKE	Two Energy Groups Fractional Point Kinetics Equations
ADE	Anomalous Diffusion Exponent
ANN	Artificial Neural Network
ATWS	Anticipated Transient Without SCRAM
BWR	Boiling Water Reactor
CFNPK	Corrected Fractional Neutron Point Kinetics
EFDM	Explicit Finite Difference Method
EFNPK	Extended Fractional Neutron Point Kinetics
FDE	Fractional Differential Equations
FPID	Fractional Proportional Integral Derivative
F-ROM	Fractional Reduced Order Model
F-SNPK	Fractional-Space Neutron Point Kinetics
FNPK	Fractional Neutron Point Kinetics

IAEA	International Atomic Energy Agency
MCNP	Monte Carlo N-Particle Transport Code
NFDE	Spatial-Fractional Diffusion Equation
NPP	Nuclear Power Plant
NSFDM	Nonstandard Finite Difference Method
PID	Proportional Integral Derivative
QBS	Quintic B-Spline
ROIOSMC	Reduced-Order Integer-Order Sliding Mode Controller
ROFOSMC	Reduced-Order Fractional-Order Sliding Mode Controller
SCWR	Supercritical-Water-Cooled Reactor
SFDM	Standard Finite Difference Method
TFTE	Time Fractional Telegraph Equation
TSFNPK	Time-Space Fractional Neutron Point Kinetics

1. INTRODUCTION

The transport phenomena and neutron point kinetics models are usually presented as positive integer Partial Differential Equations; however, since 1695, when L'Hopital addressed a letter to Leibniz inquiring the result when y is not an integer, fractional calculus, Fractional Differential Equations (FDE) or Differentiation and Integration to an arbitrary order has been studied. These studies have been applied in several areas in the last 30 years (physics, signal processing, fluid mechanics, viscoelasticity, mathematical biology, electrochemistry, among others), but not in nuclear technology until recent years (Debnath, 2003). These fractional derivatives provide (it has been proved in other areas) exceptional description of memory and hereditary properties of materials and different processes such as, but not limited to diffusion; compared to classical models where these properties are neglected, especially in dynamical systems. The paradigm of having a simple mathematical model that can predict energy and neutron transport in a highly absorbent and heterogeneous medium, such as in a Nuclear Reactor core, could be solved with FDE.

In the energy and mass transport phenomena, the molecular transport mechanism is described as a constitutive equation with the form,

$$\mathbf{J}_m = -D_m \nabla \phi \tag{1.1}$$

where $\mathbf{J}$ is the diffusion flux, D is the diffusion coefficient which represents a scale parameter among the molecular behavior and the continuum hypothesis, and $\nabla \phi$ is the flux driving force.

Analogously, for mass transport, the concentration gradient is the driving force of the flux, and for energy transport, the temperature gradient. The energy balance equation in transitory regimen of a nuclear fuel with energy source by volume unit can be expressed as,

$$\rho_m Cp \frac{\partial T}{\partial t} + \nabla \cdot \vec{q} = q''' \tag{1.2}$$

where ρ_m is the density and Cp is the heat capacity, T is the temperature, t is the time, $\vec{q}$ is the heat flux vector, and q''' is the internal heat generation. The constitutive equation analogously with Eq. (1.1) is $\vec{q} = -k\nabla T$, where k is the thermal conductivity; when substituted to Eq. (1.2), yields,

$$\rho_m Cp \frac{\partial T}{\partial t} - k\nabla^2 T = q''' \tag{1.3}$$

In the classical diffusion theory, the Fourier's Law of heat conduction describes the relation among the heat flux and the temperature gradient, and considers that the heat propagation velocity is infinite, due that the propagation time is zero. When heat transfer includes events of extremely high temperature gradients, extremely high heat fluxes or an extremely short transitory length, the heat propagation velocity is finite, and the heat flux conduction is propagative, not diffusive. Especially in highly unstable situations the parabolic heat conduction equation fails. In such situations the Fourier's Law fails (Lewandowska and Malinowski, 2006), this yields to paradoxical results. Therefore, in literature numerous attempts of formulate a new model exists (Joseph and Preziosi, 1989, 1990; Ozisik and Tzou, 1994; Tzou, 1997). Nowadays, the most used is the heat conduction hyperbolic model introduced by Vernotte (1958) and Cattaneo (1958), independently,

$$\tau_0 \frac{\partial \vec{q}}{\partial t} + \vec{q} = -k\nabla T \tag{1.4}$$

where τ_0 is a relaxation time. This model, which contains, memory effects, is widely accepted due to its simplicity and efficacy. If, we substitute (1.4) in (1.2), yields,

$$\tau_0\left(\rho_m Cp\frac{\partial^2 T}{\partial t^2}\right)+\rho_m Cp\frac{\partial T}{\partial t}-\frac{k}{\rho_m Cp}\nabla^2 T=+q'''+\tau_0\frac{\partial q'''}{\partial t} \tag{1.5}$$

The resulting governing equation has a hyperbolic nature, with the relaxation time, and it is known as the non-Fourier heat conduction equation; it can be associated with the telegraph equation, where the thermal propagation velocity is given by,

$$w=\sqrt{\frac{D_{th}}{\tau_0}}\,,\quad ;\qquad D_{th}=\frac{k}{\rho Cp} \tag{1.6}$$

where D_{th} is the thermal diffusivity. If $\tau_0=0$, which is the parabolic Fourier's equation, Eq. (1.6) results in the infinite paradox velocity. The non-Fourier effect is more attractive in engineering practical problems such as conduction in heterogeneous systems, fast heat processes and slow conduction processes. Recently, numerous heat conduction non-Fourier problems have been investigated, such as, the problem of the thermal resistance at the interfase by Lor and Chu (2000); reaction heat conduction in the solid phase by Antaki (1998); and non-Fourier heat conduction in a finite media under superficial heating under impulses by Araki (2000).

In nuclear reactor applications the term $\tau_0\frac{\partial^2 T}{\partial t^2}$ in the nuclear fuel has effects that could be important in the safety transient analysis which translates in power excursion peaks as well as turbine trip, or isolation of the steam lines, while the physical interpretation of the term $\frac{\tau_0}{\rho Cp}\frac{\partial q'''}{\partial t}$ suggests that it exists a heat transfer effect due to a rapid change in the source

term, i.e., neutron power affected by changes in the reactivity, mainly by Doppler and void fraction effects.

In the present thesis, the aim is to develop a heat transfer and neutron flux coupled model to describe all typical and atypical transients in BWRs. The specific objectives are listed as follows. 1. A thorough literature review to know the state-of-the-art of fractional calculus applied to the analysis of nuclear reactors. 2. From the derivation of a Fractional Neutron Diffusion Equation Model (FNDEM), obtaining a TSFNPK model, proposing analytical and numerical solutions, evaluate such model performing numerical experiments with different diffusion exponents of fractional order. 3. Deriving a TSFNPK model with temperature feedback effects, proposing numerical solutions and evaluating it with numerical experiments with different diffusion exponents of fractional order. 3. Comparing the results with classical transport theory and literature data. 4. Finally, the numerical coupling of the TSFNPK with the thermal hydraulics of a SCWR is presented.

The proposed fractional non-Fourier constitutive equation is,

$$\tau^{\alpha}\frac{\partial^{\alpha}\vec{q}}{\partial t^{\alpha}}+\vec{q}=-k\nabla T \tag{1.7}$$

where α is the time dependent fractional diffusion exponent, $0<\alpha<1$ for subdiffusive processes; $1<\alpha<2$ superdifussive processes; and $\alpha=1$ for normal diffusion. This fractional order constitutive equation is a generalization of Vernotte-Cattaneo (1958), when substituted in Eq. (1.5), the fractional order heat conduction equation is obtained, or more commonly, the fractional order telegraph equation,

$$\tau^{\alpha}\rho_m Cp\frac{\partial^{\alpha+1}T}{\partial t^{\alpha+1}}+\rho_m Cp\frac{\partial T}{\partial t}-\frac{k}{\rho_m Cp}\nabla^2 T=q'''+\tau^{\alpha}\frac{\partial^{\alpha}q'''}{\partial t^{\alpha}} \tag{1.8}$$

In most applications, the proposed fractional equation is of the form, $\frac{\partial^{\alpha} T}{\partial t^{\alpha}} = D_{\alpha} \nabla^2 T$ (e.g., Dzieliński et al., 2010; Sierociuk et al., 2013; Xiaojun y Baleanu, 2013), where Eq. (1.8) is not included in an implicit form, therefore without source term. In nuclear reactors the fractional modeling has been applied to determine the temperature fields in a Pebble nuclear fuel, which is highly heterogeneous (Espinosa-Paredes et al., 2014a). However, the implementation of these type of modeling is almost null in the nuclear field, being of great importance due that the irradiated fuels present irregularities in the geometry and microscopic cracks, where fractional order models have a huge field of application.

2. FRACTIONAL CALCULUS IN ENGENEERING

Almost all theory regarding fractional calculus was developed more than a century ago, however it was in the 21st century that most engineering applications were developed, this, in order to meet the requirements of the physical phenomena.

Complementary formulation is presented, due that this project is not of calculus/mathematical nature, but it is being used as an advanced tool in order to accomplish the objectives (Kimeu, 2009; Loverro, 2004).

2.1 Essential Functions

Before pushing into more deep concepts, such as the Riemann-Liouville and Grunwald-Letnikov definitions, it is essential to introduce other simpler mathematical definitions, the Gamma Function, the Betta Function, the error function, and the Mittag-Leffler Function. (Miller and Ross, 1993; Oldham and Spanier, 1974; Pod- lubny, 1999).

2.1.1 The Gamma Function

Known also as the Euler's Gamma Function, is inherent to fractional calculus, its most basic interpretation is the generalization of the factorial of all real numbers, by definition,

$$\Gamma(n) = \int_0^\infty t^{n-1} e^{-t} dt \qquad \text{for all} \qquad n \in \mathbb{R}^+ \tag{2.1}$$

or,

$$\Gamma(n+1) = n\Gamma(n) \qquad ; \qquad n \in \mathbb{R}^{+} \tag{2.2}$$

and,

$$\Gamma(n) = (n-1)! \qquad ; \qquad n \in \mathbb{N} \tag{2.3}$$

For this function, the value for any quantity is of the form of the integral equivalent to the same quantity n minus one time the gamma of the quantity minus one. If integrated by parts, the relation for integer values of n is the factorial definition. Figure 2.1 shows the plot of the gamma function around the value of zero, for negative integer values, the function goes to infinity.

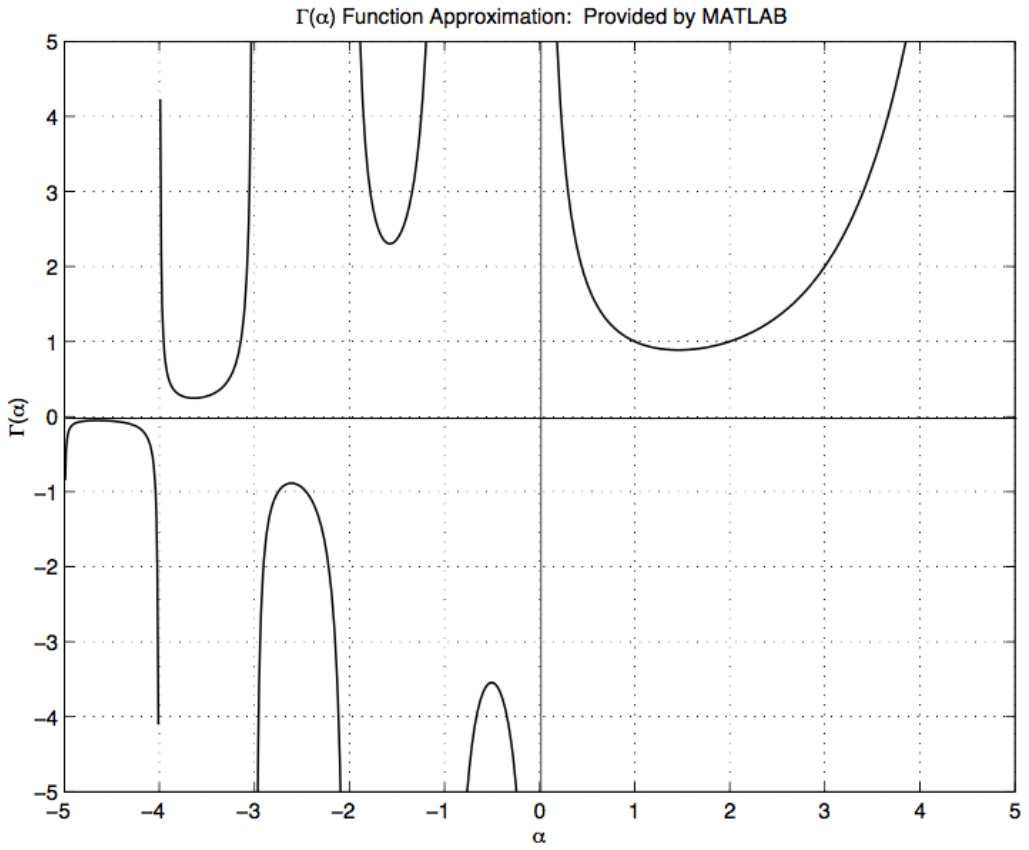

Figure 2.1. Gamma Function Approximation (MATLAB).

2.1.2 The Beta Function

This function is known as the Euler Integral of the First Kind, just as the Gamma function, it is essential to fractional calculus,

$$B(x,y)=\int_0^1 t^{x-1}(1-t)^{y-1}dt \quad ; \qquad x,y\in x\in\mathbb{R}^+ \tag{2.4}$$

Also its solution is given in terms of the Gamma function,

$$B(x,y)=\frac{\Gamma(x)\Gamma(y)}{\Gamma(x+y)} \quad ; \qquad x,y\in x\in\mathbb{R}^+ \tag{2.5}$$

2.1.3 The Error Function

The error function is given by,

$$Erf\left(n\right)=\frac{2}{\sqrt{\pi}}\int_0^n e^{-t^2}dt \qquad ; \qquad n\in\mathbb{R} \tag{2.6}$$

Its complementary function (*Erfc*) can be written in terms of the Error function,

$$Erfc\left(n\right)=1-Erf\left(n\right) \tag{2.7}$$

thus, $Erf\left(0\right)=0$ and $Erf\left(\infty\right)=1$.

2.1.4 The Mittag-Leffler Function

This function is a generalization of the exponential function, e^x, and plays a very important role in fractional calculus, the standard definition is given by,

$$E_\alpha\left(z\right)=\sum_{k=0}^{\infty}\frac{z^k}{\Gamma\left(\alpha k+1\right)} \qquad ; \qquad \alpha>0 \tag{2.8}$$

Plotting (2.8) for different α is shown in Figure 2.2.

Also, this function can be represented in two arguments,

$$E_{\alpha,\beta}\left(z\right)=\sum_{k=0}^{\infty}\frac{z^k}{\Gamma\left(\alpha k+\beta\right)} \qquad ; \qquad \alpha>0,\beta>0 \tag{2.9}$$

The latter equation is the more generalized form of the equation, although not always required with fractional differential equations.

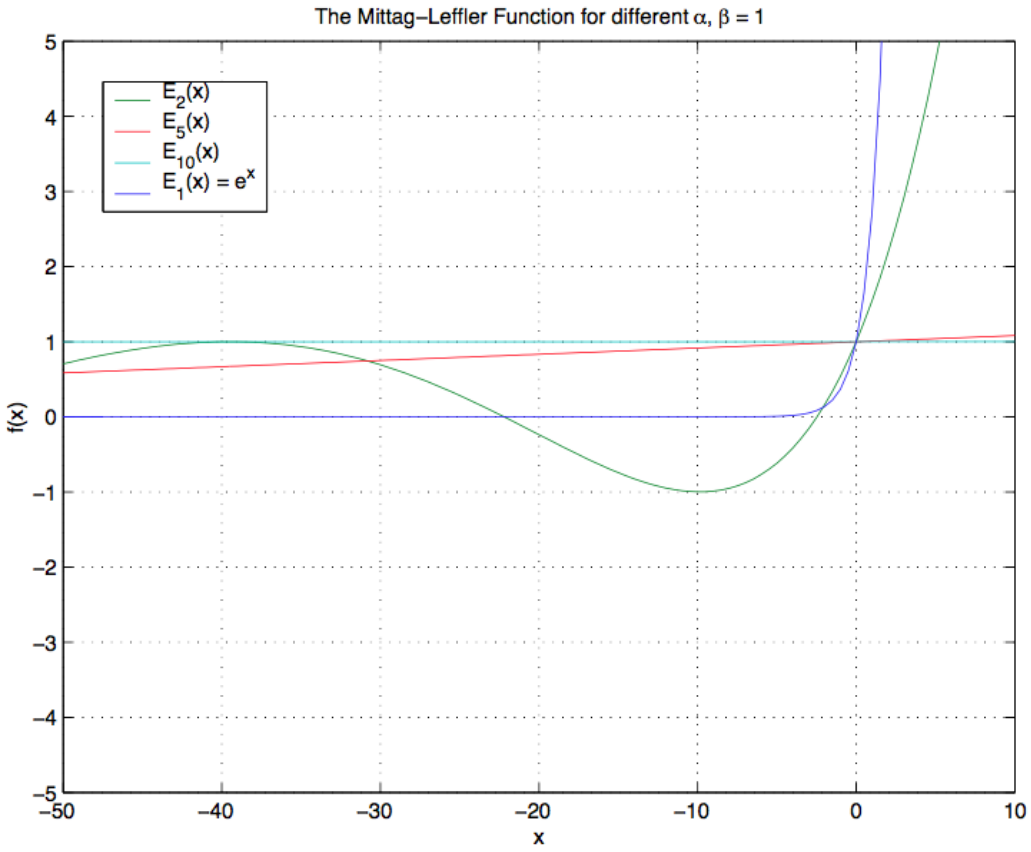

Figure 2.2. Mittag-Leffler Standard Function Approximation for different values of α (MATLAB).

2.1.5 The Mellin-Ross Function

This function appears when the fractional integral of an exponent is solved, $e^{\alpha t}$, its definition is given by,

$$E_t(v,\alpha) = t^v e^{\alpha t}\Gamma^*(v,t) \tag{2.10}$$

or,

$$E_t(v,\alpha)=t^v\sum_{k=0}^{\infty}\frac{(\alpha t)^t}{\Gamma(k+v+1)}=t^v E_{1,v+1}(at) \tag{2.11}$$

2.2 The Riemann-Liouville Fractional Integral and Derivative

In order to obtain the Riemann-Liouville definition, we consider the Riemann-Liouville n-fold integral which is given by,

$$\underbrace{\int_\alpha^t\int_\alpha^{t_n}\int_\alpha^{t_{n-1}}\cdots\int_\alpha^{t_3}\int_\alpha^{t_2}}_{n-\text{fold}} f(t_1)dt_1dt_2\cdots dt_{n-1}dt_n=\frac{1}{\Gamma(n)}\int_\alpha^t\frac{f(\tau)}{(t-\tau)^{1-n}}d\tau \tag{2.12}$$

Rewriting Eq. (2.12) of the order α, after a few steps we obtain the fractional integral which is given by,

$${}_0D_t^{\alpha}f(x)=\frac{1}{\Gamma(n-\alpha)}\frac{d^n}{dt^n}\int_0^t\frac{f(\tau)}{(t-\tau)^{\alpha-n+1}}d\tau \tag{2.13}$$

where $\Gamma(n)$ is the Gamma Function (Eq. 2.1) given by Oldham and Spanier (1974).

Recalling that differentiation is the opposite of integration, we can define the fractional derivative using the fractional integral definition, thereby if $\alpha=n-u$, where $0<\alpha<1$, n being the smallest integer greater than u, we have,

$$D^u f(x)=D^n\left[D^{-\alpha f(x)}\right] \tag{2.14}$$

2.3 The Grünwald-Letnikov Fractional Integrals and Derivative

If we have a continuous function $f(t)$, the first derivative can be expressed as,

$$\frac{d}{dt} f(t) \equiv f'(t) = \lim_{h \to 0} \frac{f(t) - f(t-h)}{h} \tag{2.15}$$

The second derivative of Eq. (2.15) yields,

$$\frac{d^2}{dt^2} f(t) \equiv f''(t) = \lim_{h \to 0} \frac{f(t) - 2f(t-h) + f(t-2h)}{h^2} \tag{2.16}$$

If we derive Eq. (2.16) once again, we obtain,

$$\frac{d^3}{dt^3} f(t) \equiv f'''(t) = \lim_{h \to 0} \frac{f(t) - 3f(t-h) + 3f(t-2h) - f(t-3h)}{h^3} \tag{2.17}$$

Generalizing this rule we obtain a formula,

$$\frac{d^n}{dt^n} f(t) \equiv f^n(t) = \lim_{h \to 0} \frac{1}{h^n} \sum_{j=0}^{n} (-1)^j \binom{n}{j} f(t - jh) \tag{2.18}$$

Considering the above equations, we can write the derivative definition of the order of α as follows,

$$D_t^{\alpha} f(t) = \lim_{h \to 0} \frac{1}{h^{\alpha}} \sum_{j=0}^{\infty} (-1)^j \binom{\alpha}{j} f(t - jh) \tag{2.19}$$

for $\binom{\alpha}{0} = 1$ and $n = \frac{t - \alpha}{h}$, where a is a real constant, we finally obtain the Grünwald-Letnikov,

$$ {}_{\alpha}D_{t}^{\alpha} f(t) = \lim_{h\to 0} \frac{1}{h^{\alpha}} \sum_{j=0}^{\left[\frac{t-\alpha}{h}\right]} (-1)^{j} \binom{\alpha}{j} f(t-jh) \tag{2.20} $$

2.4 The Caputo Fractional Derivatives

The Caputo definition was given by (Caputo, 1967; Podlubny, 1999),

$$ {}_{\alpha}D_{t}^{\alpha} f(t) = \frac{1}{\Gamma(n-\alpha)} \int_{\alpha}^{t} \frac{f^{(n)}(\tau)}{(t-\tau)^{\alpha-n+1}} d\tau \quad ; \quad n-1 < \alpha < n \tag{2.21} $$

Under homogenous initial conditions the Riemann-Liouville and the Caputo derivatives are equivalent. If the Riemann-Liouville fractional derivative is ${}^{RL}_{\alpha}D_{t}^{\alpha} t(t)$ and the Caputo definition is ${}^{C}_{\alpha}D_{t}^{\alpha} f(t)$, then the relation between them,

$$ {}^{RL}_{\alpha}D_{t}^{\alpha} t(t) = {}^{C}_{\alpha}D_{t}^{\alpha} f(t) + \sum_{k=0}^{n-1} \frac{(t-\alpha)^{k-\alpha}}{\Gamma(k-\alpha+1)} f^{(k)}(\alpha) \tag{2.22} $$

for $f^{(k)}(\alpha) = 0 \quad ; \quad (k = 0,1,\ldots,n-1)$.

The initial conditions for this derivative are in the same form as for the integer-order differential equations, being an advantage because applied problems require definitions of fractional derivatives.

2.5 Solution Schemes

2.5.1 Method of separating variables

In order to exemplify the separating variables method for fractional differential equations, the following time-fractional telegraph equation will be solved,

$$D_t^{2\alpha}u(x,t)+\alpha D_t^{\alpha}u(x,t)=k\frac{\partial^2 u(x,t)}{\partial x^2}+f(x,t) \quad ; \quad \begin{matrix} 0<x<L \\ t>0 \\ \frac{1}{2}<\alpha\le 1 \end{matrix} \tag{2.23}$$

constrained by the initial and boundary conditions,

$$\begin{matrix} u(x,0)=\phi(x)\ ; & u_t(x,0)=\Psi(x) & ; & 0\le x\le L \\ u(0,t)=\mu_1(t)\ ; & u(L,\mathrm{t})=\mu_2(t) & ; & t>0 \end{matrix} \tag{2.24}$$

$\phi(x)$ and $\Psi(x)$ are continuous functions which satisfy $\phi(0)=\mu_1(0)$, $\phi(L)=\mu_2(0)$, where $\mu_1(t)$ and $\mu_2(t)$ are nonzero functions with order-one continuous derivative. Transforming the nonhomogeneous boundary to homogeneous boundary conditions, $u(x,t)=W_1(x,t)+V_1(x,t)$ and $V_1(x,t)=\mu_1(t)+\frac{(\mu_2(t)-\mu_1(t))x}{L}$ which satisfies the boundary conditions,

$$V_1=(0,t)=\mu_1(t) \quad ; \quad V_1(L,t)=\mu_2(t) \tag{2.25}$$

substituting in Eqs. (2.23) and (2.24),

$$D_t^{2\alpha}u(x,t)+\alpha D_t^{\alpha}W_1(x,t)+V_1(x,t)=k\frac{\partial^2 W_1(x,t)+V_1(x,t)}{\partial x^2}+f(x,t) \quad ; \quad \begin{matrix} 0<x<L \\ t>0 \end{matrix} \tag{2.26}$$

$$
\begin{aligned}
&W_1(x,0)=\phi_1(x) \quad ; \quad \frac{\partial W_1(x,0)}{\partial t}=\Psi_1(x) \quad ; \quad 0\le x\le L \\
&W_1(0,t)=W_1(L,t)=0 \quad ; \quad t\ge 0
\end{aligned}
\tag{2.27}
$$

2.5.2 Laplace Transform

For this solution scheme we need to find the Laplace transform of the equation, solve for the function, and find the solution with the inverse Laplace function.

3. FRACTIONAL MODELS APPLIED TO NUCLEAR POWER REACTORS

The development of fractional order models applied to nuclear power reactors began in the present century and can be divided into two stages, an early stage which comprehends from the first ever published article in 2002 until the year 2019, and the present stage or contemporary stage of that this work is part of. The most relevant works in chronological order are shown below.

3.1 Early stage

The first published article regarding fractional order models applied to nuclear reactor analysis was from Zabadal et al. (2002), which presents a closed solution for the multidimensional transport equation using a fractional derivative, they name it as the fractional derivative transport equation solution (FDE).

Next, Amaral et al. (2003) construct an integral form for the 1D, 2D and 3D dimensional transport equation solutions to calculation of the angular flux, with the Klein-Nishina scattering kernel, isotropic scattering, and Rutherford scattering kernel. Their formulation is applied on the calculation of the angular flux for one, two and three dimensional problems and compared with numeric results available in the literature.

No other publications involving fractional calculus are reported from that year until Das & Biswas (2007) introduced and explored the fractional divergence, where it is

developed for application to the constitutive neutron diffusion equation for describing the neutron flux profile,

$$\nabla^{\alpha} \cdot \mathbf{J}_n + \Sigma_a \phi - S = 0 \tag{3.1}$$

where $\mathbf{J}_n$ is the vector current density, Σ_a is the macroscopic absorption cross section, ϕ is the neutron flux, and S is the neutron source. Rewritten in a one-dimensional form and applying the current vector given by the Fick's law,

$$-D_n \frac{d^{1+\alpha}\phi}{dx^{1+\alpha}} + \Sigma_a \phi - S = 0, \ldots 0 < \alpha < 1 \tag{3.2}$$

where D_n is the neutron diffusion coefficient.

According to them, the above equation which includes the definition of fractional divergence describes the neutron flux by not considering it as a classical point quantity, thus giving a better representation for a distributed system encompassing the process history. Therefore, really describing the reactor flux profile. However, it is important to mention that the fractional order will be different from reactor to reactor due to heterogeneity and reactor configurations.

The next year, a book by Das (2008) is published, extending the ideas of Das & Biswas (2007) regarding fractional divergence in a complete chapter, also establishing concepts such as fractional curl, fractional criticality and fractional geometrical buckling which is later explored by Espinosa-Paredes (2017), its work is mainly focused on reactor control. Meanwhile Espinosa-Paredes et al. (2008) derived a fractional P_1 equation which

covers *normal diffusion* and *anomalous diffusion*, the *non-Fickian law* for the vector of neutron current density ($\mathbf{J}_n$) applied by these authors is given by,

$$\left(\frac{3D_n}{\upsilon}\right)\frac{\partial \mathbf{J}_n(\mathbf{r},t)}{\partial t}+\mathbf{J}_n(\mathbf{r},t)=-D_n(\mathbf{r})\nabla\phi(\mathbf{r},t) \tag{3.3}$$

where the term $\left(\frac{3D_n}{\upsilon}\right)$ has units of time, and it is known as the relaxation time τ_{relax}, and υ is the neutron velocity. The latter yields the neutron fractional wave equation, considered as a time-fractional neutron flux telegrapher equation,

$$\tau_\alpha \frac{1}{\upsilon}\frac{\partial^{\alpha+1}\phi}{\partial t^{\alpha+1}}+\tau_\alpha \Sigma_a \frac{\partial^\alpha \phi}{\partial t^\alpha}+\frac{1}{\upsilon}\frac{\partial\phi}{\partial t}+\Sigma_a\phi=D\nabla^2\phi \tag{3.4}$$

where α is the time dependent fractional diffusion coefficient.

After two years without any other works, Sarder et al. (2010) presents an analytical approximation method for the solution of the fractional neutron diffusion equations with one group of delayed neutrons as a possible solution of the fractional neutron transport equation, given by,

$$\frac{1}{\upsilon}\frac{\partial^\alpha\phi(x,t)}{\partial t^\alpha}=D_n\nabla^2\phi(x,t)+(\gamma\Sigma_f-\Sigma_a)\phi(x,t)+\lambda C(x,t)$$

$$\frac{\partial^\alpha C(x,t)}{\partial t^\alpha}=\beta\gamma\Sigma_f\phi(x,t)-\lambda C(x,t) \tag{3.5}$$

where $0<\alpha<0.5$; γ is the average number of neutrons produced per fission, Σ_f the macroscopic fission cross-section, λ the decay constant, C the concentration of neutron precursors , and β the total fraction of delayed neutrons.

The next year, Espinosa-Paredes et al. (2011) derived the first form of the Fractional Neutron Point Kinetics model (FNPK),

$$\begin{aligned}&\tau_\alpha \frac{d^{\alpha+1}n(t)}{dt^{\alpha+1}} + \tau_\alpha \left[\frac{1}{l} - \frac{(1-\beta)}{\Lambda}\right]\frac{d^\alpha n(t)}{dt^\alpha} + \frac{dn(t)}{dt} \\ &= \frac{\rho(t)-\beta}{\Lambda} n(t) + \sum_{i=1}^{m} \lambda_i C_i(t) + \tau_\alpha \sum_{i=1}^{m} \lambda_i \frac{d^\alpha C_i(t)}{dt^\alpha}\end{aligned} \tag{3.6}$$

where τ_α fractional relaxation time, Λ is the neutron generation time, l the neutron lifetime in a finite reactor, ρ reactivity, and n neutron density.

Eq. (3.6) is the first fractional approximation including time memory and non-local effects, and they present its numerical solution applying the numerical method introduced by Edwards et al. (2002) which in turn considers the Diethelm (1997) method, additionally a numerical stability analysis is presented. The bases and fundamentals of fractional models for the analysis of nuclear reactors, tested with numerical experiments considering *non-leakage probability* equal to one are presented in this work and the model expands the classical neutron point kinetics, from integer derivatives to non-integer derivatives. These newly derived models are a useful tool to provide important information on reactor dynamics.

The following year a boom regarding fractional models applied to Nuclear Power Plants (NPP) analysis appears, and diverse works are published, from the numerical solution of the FNPK model, based on an explicit finite difference scheme with the Grunwald–Letnikov fractional derivative definition (Ray & Patra, 2012) applied to the analysis of the dynamics of nuclear reactors, which agreed with original results; a SIMULINK dynamical stability simulation of nuclear reactor cores (Shirazi, 2012), once again, applied to the FNPK model; sensitivity and uncertainty analyses of the anomalous diffusion exponent (ADE) in

the FNPK model (Espinosa-Paredes et al., 2012a) and to the Time-Fractional Telegrapher's Equation (Espinosa-Paredes et al. 2012b) were performed applying a Monte Carlo simulation in their methodology to determine the best value of the ADE; in the start-up of NPPs by Polo-Labarrios & Espinosa-Paredes (2012a, 2012b) which considers and external source; and, the derivation of a P1 approximation for the Transport Equation (TFTE) by Espinosa-Paredes & Polo-Labarrios (2012) finding that this derivation gives the best estimate for purely absorbing media where it is known that normally most approximations fail.

In 2013, based on the same original ideas, i.e., non-local and time memory effects, a novel fractional-space law for the vector of neutron current density was proposed by Espinosa-Paredes et al. (2013a),

$$\mathbf{J}_n(\mathbf{r},t) = -D_{n,\alpha}\,\nabla^{\alpha}\phi(\mathbf{r},t) \tag{3.7}$$

which was applied to derive the spatial-fractional diffusion equation (NFDE) and established as a new constitutive law for the neutron current density, additionally they present a detrended fluctuation analysis method to estimate the fractional coefficient.

Afterwards, Vyawahare & Nataraj (2013a) presented a simplified version of the FNPK model applied to a nuclear reactor slab geometry, considering only the term $d^{\alpha}n/dt^{\alpha}$, i.e., $\tau^{\alpha}\left[P_{NL}/l-(1-\beta)/\Lambda\right]=1$ where P_{NL} is the non-leakage probability. The same authors present the derivation of a Fractional Telegraph Equation Vyawahare & Nataraj (2013b) based on the standard continuous-time random walk method, where their main findings are that nuclear reactor cores should be modeled as sub-diffusion, values of the fractional exponent near the unity should be used on the moderator region and smaller values for highly absorbing regions such as in the control rods vicinity; they also claim that the

model is more realistic and "trouble free", thus being appropriate to achieve more efficient, safe, and reliable operation and control in NPPs. Schramm et al. (2013) solved the FNPK model applying the Adomain decomposition method and found that their results where between those of classical kinetics and results from transport approaches and also that the order of the derivative is related to a scaling of the differential with the "effective volume" which is not necessarily obtained with an integer order. Ray & Patra (2013) once again applied an explicit difference method with the Grunwald-Letnikov derivative definition to solve the first fractional order stochastic neutron point kinetic model,

$$\frac{d}{dt}\begin{bmatrix} n \\ c_1 \end{bmatrix} = \hat{A}\begin{bmatrix} n \\ c_1 \end{bmatrix} + \begin{bmatrix} q \\ 0 \end{bmatrix} + \hat{B}^{1/2}\frac{d\vec{W}}{dt} \tag{3.8}$$

$$\text{where } \vec{W}(t) = \begin{bmatrix} W_1 & (t) \\ W_2 & (t) \end{bmatrix} = \lim_{\Delta t \to 0} \frac{1}{\sqrt{\Delta t}} \begin{bmatrix} \eta_1 \\ \eta_2 \end{bmatrix}, \quad \text{and } \hat{A} = \begin{bmatrix} \frac{\rho - \beta}{l} & \lambda_1 \\ \frac{\beta_1}{l} & -\lambda_1 \end{bmatrix}$$

where W is a Wiener process and $\hat{B}^{1/2}$ is the square root of the matrix. Eq. (3.8) represents the first model of its type to be analyzed, however they only report findings regarding the numerical method.

Continuing with the chronology, Polo-Labarrios et al. (2014) presented a numerical analysis with reactivity insertion of the FNPK model, analyzing the ramp and sinusoidal reactivity insertion; their main findings are that with relatively small values of the fractional exponent, sub-diffusive effects are greater. Espinosa-Paredes et al. (2014) deal with the incorporation of temperature feedback effects to the FNPK model, where results are compared with the classical model and found that the neutron density peak is lower for the

classical model caused by anomalous diffusion which is more evident when the decreasing the anomalous diffusion exponent. Nowak et al. (2014a,b) present two works where they analyse the FNPK model with six groups of delayed neutron precursors and present results considering a bilinear system of fractional and ordinary differential equations, where they compare three different solution methods; the first one considers the discrete Grünwald-Letnikov definition of the fractional derivative, the second involves building an scheme in the FOMCON Toolbox from the MATLAB environment, and the third is the Edwards et al. (2002) method; the effect of relaxation time, order of fractional derivative and step-size on the obtained results were examined and according to numerical results, the last method turned out to be the best. Nowak & Duzinkiewicz (2014) proposed a numerical solution in a MATLAB environment with step input change and analyse the impact of the stablished parameters. Ray & Patra (2014a) present numerical simulations for solving the FNPK model applying the multi-step differential transform method, their model considers a fractional derivative in time for the neutron density and the concentration for six groups of delayed neutrons, their main finding is that the numerical method is an easier and efficient way to obtain a numerical solution and accuracy improves with the time step. In another work, Ray & Patra (2014b) performed a numerical simulation for a fractional order stationary neutron transport equation using the Haar wavelet collocation method in a homogeneous medium with isotropic scattering, resulting in a simple, easy and fast mathematical method and being more suitable, accurate and efficient than other methods. The NFDE model was subject of study by Maleki Moghaddam et al. (2014) who developed a one-dimensional numerical code to simulate the reactor code for different fractional exponents, the model is validated against the classical neutron point kinetics equation model and they found that the effective multiplication factor strongly depends on the order of the fractional derivative.

Next year the last authors expand their numerical code, Maleki Moghaddam et al. (2015a) present a 2 dimensional multigroup numerical code (NFDE-2D) and Maleki Moghaddam et al. (2015b) a 3 dimensional multigroup numerical code (NFDE-3D) to simulate anomalous diffusion phenomena in the nuclear reactors; the conclusion of these works is that when $\alpha = 0.86$, results closely approach (0.035% of relative error) to those of the transport theory and in order to choose the best order of the fractional exponent, experimental data is necessary. Moghaddam et al. (2015c) once again studied the NFDE and results were comparable to those of the transport theory, finding a maximum error of 1.7% for the classical and 0.108% for the transport theory of the k_{eff}, using Monte Carlo N-Particle Transport code (MCNP). Nowak et al. (2015) studied feedback reactivity effects in the FNPK model considering fuel and coolant temperatures applying two approximations, an algorithm based in the discrete Grünwald–Letnikov definition of the fractional derivative and building an analog scheme in the FOMCON Toolbox in MATLAB environment. Patra & Ray (2015) present the solution of a nonlinear FNPK model, expanding their 2014 works by including temperature feedback reactivity with multi-group of delayed neutrons, applying the explicit finite difference method (EFDM) for the solution, and demonstrating that this method is straightforward and effective to solve fractional order nonlinear neutron point kinetics equations. This same year, a book dealing with applications of fractional calculus in reactor dynamics is published by Ray (2015), which is basically a compendium of his works on fractional calculus applied to nuclear engineering. Finally, Vyawahare & Nataraj (2015) present their findings of their developed 2013 model, on a book chapter, including adiabatic temperature feedback effects, where the stiff system is solved with the Adams-Bashforth-

Moulton method, being self-limited in power excursions and reporting convergence issues for small values of the fractional exponent but being consistent with reactor physics.

Vyawahare & Nataraj (2016) develops two one-dimensional fractional-order two-group models with two groups, a Telegraph-Subdiffusion model and a Fractional-order model. The first analysis of the fractional terms in the mathematical models is presented by Espinosa-Paredes & Polo-Labarrios (2016) and found that the time derivative directional source term is negligible i.e., $\tau_\alpha \frac{d^\alpha \mathrm{S}}{dt^\alpha} \approx 0$, thus they simplify the FNPK model to,

$$\tau_\alpha \frac{d^{\alpha+1} n(t)}{dt^{\alpha+1}} + \frac{\tau_\alpha}{\ell} \frac{d^\alpha n(t)}{dt^\alpha} + \frac{dn(t)}{dt} = \frac{\rho(t)-\beta}{\Lambda} n(t) + \lambda c(t) \tag{3.9}$$

The same year, Aboanber & Nahla (2016a) present a corrected version of the FNPK (CFNPK) model, where the proposed version considers a non-leakage probability different from one, thus,

$$\tau_\alpha \frac{d^{\alpha+1} n(t)}{dt^{\alpha+1}} - \tau_\alpha \left[\frac{(\rho(t)-\mu)}{\Lambda} \right] \frac{d^\alpha n(t)}{dt^\alpha} + \frac{dn(t)}{dt} = \frac{\rho(t)-\beta}{\Lambda} n(t) + \sum_{i=1}^{m} \lambda_i C_i(t) + \tau_\alpha \sum_{i=1}^{m} \lambda_i \frac{d^\alpha C_i(t)}{dt^\alpha} \tag{3.10}$$

Probably motivated by the above work Espinosa-Paredes (2016) discuss the length and time scales orders of magnitude of the FNPK model, remarking that the corrected version of the FNPK model is in fact an extension of the original model. In another work, Aboanber & Nahla (2016b) derived a modified FNPK model,

$$\tau_\alpha \frac{d^\alpha}{dt^\alpha}\left[\frac{dn(t)}{dt}-\left(\frac{\rho-\beta}{\Lambda}+vDB_g^2\right)n(t)-\sum_{i=1}^{m}\lambda_i C_i(t)\right]+\frac{dn(t)}{dt}-\left(\frac{\rho-\beta}{\Lambda}\right)n(t)-\sum_{i=1}^{m}\lambda_i C_i(t)=0 \tag{3.11}$$

where $\frac{dC_i(t)}{dt}=\frac{\beta_i}{\Lambda}n(t)-\lambda_i C_i(t)$; they tested and compared it with the classical model for step, ramp, and sinusoidal reactivity, finding that, in their own words, *is the best representation of neutron density for subcritical and supercritical reactors*. Schramm et al. (2016) studied the FNPK model with a fractional Riemann-Liouville definition and temperature feedback effects, their main findings are that within the used parameters the influence of the fractional derivative is small and for temperature feedback effects these were completely suppressed due to the fractional derivative; however, their conclusions seem to contradict every work published so far which include feedback effects by temperature, e.g., Espinosa-Paredes et al. (2014) found that the fractional point kinetics model has important effects on the neutron density with feedback effects due that sub-diffusive effects are evidently appreciated, and in a more recent work this issue is addressed. This year, the first tangible applications of fractional order models applied to nuclear engineering start to appear, Cázares-Ramírez & Espinosa-Paredes (2016) applied a time-fractional telegraph equation (TFTE) during a severe accident transient in a BWR to study the Hydrogen generation and found that the Hydrogen concentration is inversely proportional to the fractional coefficient. Another application of fractional order models was published by Davijani et al. (2016), developing a reduced-order fractional-order sliding mode controller (ROFOSMC) for power control of NPPs, the proposed model was adapted in order to include temperature feedback from the lumped fuel, coolant temperatures, and the effect of Xenon concentration in the controller design; they found that compared with respect to the integer-order model

(ROIOSMC), their model has robustness against uncertainty, acceptable performance, faster response of control effort signal and a smaller tracking error as well as the ability to reject disturbance and noise signal. Sallah & Margeanu (2016) studied the effect of a fractional parameter on the neutron transport in finite disturbed reactors with quadratic scattering for shielding effectiveness in the MAVRIC shielding module in SCALE6, their aim was to study neutron energy and flux data. Another analysis of the terms in fractional point kinetics (FNPK) equations is presented by Espinosa-Paredes & Cázares-Ramírez (2016) finding that the source term is crucial for the FNPK stability and very important for the W-domain. Vyawahare et al. (2016) models the neutron fractional order telegraph equation for the application in linear control models with fractional operators, they present a fractional point reactor kinetics model, a zero power fractional order transfer function and a fractional order transfer function with temperature feedback, their model predicts sub-diffusive behavior for long-times.

In the following year more applicability begins to appear, in the work of Polo-Labarrios et al. (2017) they studied the Anticipated Transient Without SCRAM (ATWS) boron with the FNPK model, the justification for this particular transient is that boron in the reactor core produces atypical neutron absorption in combination with the intrinsic feedback mechanisms which causes anomalous diffusion effects in the neutron density behavior, the FNPK model is perfect to model the dynamic behavior, due that it considers explicitly the absorption macroscopic cross section, and time-memory with non-local effects which are not considered in the classical model. Until this time only time-fractional models applied to nuclear analysis were developed and Espinosa-Paredes (2017) introduces the first spatial-fractional point reactor model (F-SNPK),

$$\frac{dn(t)}{dt}=\left[\frac{(\rho-\beta)}{\Lambda}+\upsilon\left(DB_g^2-D_\kappa B_g^{\kappa+1}\right)\right]n(t)+\sum_{i=1}^{m}\lambda_i C_i(t),\ 0<\kappa<1 \qquad (3.12)$$

where κ is the fractional differential operator; Eq. (3.12) includes a fractional geometrical buckling, a concept first introduced by Das (2008) but that it had not been explored nor concretely proposed until this work, the physical interpretation of this term is to consider neutron leakage for any geometry and dimensions of a reactor, being more realistic from a reactor physics point of view compared to the integer model; for this fractional model the initial conditions are met if and only if the initial condition $\rho(0)=-\Lambda\upsilon\left(DB_g^2-D_\kappa B_g^{\kappa+1}\right)$ is constrained, thus considering neutron leakage as a function estimated with the anomalous diffusion exponent. Once again, the FNPK model was studied, this time by Hamada & Brikaa (2017) applying a nonstandard finite difference method (NSFDM) which according to them is desirable than the standard finite difference method (SFDM), the fractional derivative is defined in the form of Grunwald-Letnikov; numerical simulations were performed for subcritical, critical, and supercritical reactivities and results are compared with the classical solutions. Nahla & Hemeda (2017) studied the FNPK model without a relaxation time and a multi-group of delayed neutrons with Picard iteration and Padé approximations, their results show that for small sub-diffusive effects the anomalous diffusion exponent is less than one but very close to one, and for small super-diffusive effects the anomalous diffusion exponent is greater than one but very close to one. Hamada (2017a) modifies the original FNPK model and includes the time derivative of the reactivity to consider Newtonian temperature feedbacks effects,

$$\tau_\alpha \frac{d^{\alpha+1}n(t)}{dt^{\alpha+1}} + \tau^\alpha \Omega(t) \frac{d^\alpha n(t)}{dt^\alpha} + \alpha\tau_\alpha \frac{d\Omega(t)}{dt} \frac{d^{\alpha-1}n(t)}{dt^{\alpha-1}} + \frac{dn(t)}{dt}$$
$$= \frac{\rho_n(t)-\beta}{\Lambda} n(t) + \sum_{i=1}^{m} \lambda_i C_i(t) + \tau_\alpha \sum_{i=1}^{m} \lambda_i \frac{d^\alpha C_i(t)}{dt^\alpha} \tag{3.13}$$

where $\Omega(t) = \frac{\rho_n(t)-\beta}{\Lambda} - \upsilon D_n B_g^2$ or $\Omega(t) = \left(\frac{1-\rho_n(t)}{\Lambda}\right) P_{NL} - \frac{(1-\beta)}{\Lambda}$; the author uses an implicit difference method for the solution, comparing the results with previous and the normal model, his main finding is that the method is unconditionally stable; on another work Hamada (2017b) expands his modified FNPK model to a finite cylindrical reactor with similar results. Another application with the Ray & Patra (2014) model is explored by Nahla (2017) during the start-up of a nuclear reactor, their results with one group of delayed neutrons agreed with Zhang et al. (2009), but not for six groups of delayed neutrons, showing that there is no difference during the lifting of the control rods. Starting from the FNPK model, Vyawahare & Espinosa-Paredes (2017) applied a reduced order model to consider void fraction and temperature feedback effects, resulting in a Fractional Reduced Order Model (F-ROM) consisting of 5 differential equations for the analysis of BWR dynamics, their results are compared with the normal reduced order model. In the same line of research, Cázares-Ramírez et al. (2017) present the stability feedback analysis of linear FNPK models developed and analyzed by Vyawahare et al. (2017), applying root locus, location of closed-loop poles in the Riemman sheet and evaluation of step response and found that the studied FNPK models are closed-loop stable. Espinosa-Paredes et al. (2017) also studied the stability of FNPK considering the transformation from the S-plane to the W-plane and finding the unstable and stable zones in the system.

Vyawahare & Nataraj (2018) present a brief development and analysis of the FNPK and NFDE models, applied to control; additionally they rewrite the neutron transport equation in its integral form, compare the kernel of the respective formal solution with the Riemann–Liouville definition of the fractional derivative operator, and solve the corresponding algebraic equation for finding the differ-integration order; their proposed equation establishes the ideas for solving transport problems in heterogeneous media with anisotropic scattering. This year, also the first artificial neural network (ANN) approximation applied to the FNPK and F-ROM was presented by Vyawahare et al. (2018), the Fractional-Space Neutron Point Kinetics (F-SNPK) and their main findings are that the ANN has good agreement with the linear FNPK models and the convergence and learning of the ANN are affected by the type of model, the value of the fractional diffusion exponent and the relaxation time. Although the F-SNPK being novel, Vyawahare & Espinosa-Paredes (2018) present a work regarding its stability using three methods, root locus, Bode plot, and unite step response applied to closed and open loop models (slab and cylindrical geometries), they compare their results with non-fractional models, finding stability for both and faster dynamics with an increase in sub-diffusivity. Aboanber et al. (2018a) present a solution method using the generalization form of the Taylor's formula involving the Caputo fractional derivatives to solve the stiffness of the nonlinear fractional differential model which includes a fractional term for the temperature feedback, finding that in *sub-difussion* greater number of fissions are produced while for *super-diffussion* smaller number of fissions are produced. On another work and based on a study by Nahla & Hemeda (2017), Aboanber et al. (2018b) present a solution method including the Mittag-Leffler function with the Padé approximations to solve the stiffness of a proposed two fractional neutron point kinetics model which include an equation for the neutron density for the core and one for the

moderator, they validate their model with a variation of reactivity insertions and found that their results agree with the Picard iteration method. Also based in a previous work (Ray & Patra, 2013), Aboanber et al. (2018c) developed the second fractional stochastic point kinetics model with multi-group of precursors and temperature feedback, applying a split-step method which considers the Laplace transforms, Mittage–Leffler function, eigenvalues of the coefficient matrix, and its corresponding eigenvectors for the solution of the fractional stochastic matrix differential equation; their results agree with the normal Neutron Point Kinetics model. Another stochastic neutron point kinetics model with temperature feedback effects is presented by Singh & Saha Ray (2019), where the solution is obtained by higher-order approximation where the fractional stochastic for neutron density and concentration of precursors were presented in the work of Ray & Patra (2013).

Rafiei et al. (2019a) present a stability analysis of the FNPK model with three groups of delayed neutrons and reactivity feedback effects, their solution method is by transformation to the W-domain, they find negative effects by Xenon on the stability and that stability highly depends on the values of the fractional derivative and relaxation time. The same authors (Rafiei et al., 2019b) apply a PID controller based to their previous work, Genetic Algorithm is used for the optimization of the PID controller, the model was applied during power maneuvering transients considering Xenon concentration changes and results find good performance and stability compared to the conventional PID and FOPID (not-tuned) controllers. Roul et al. (2019a) also studies the FNPK model considering *non-leakage probability* ($P_{NL} \neq 1$), and named it, the extended fractional neutron point kinetics (EFNPK), they apply a nonstandard finite difference scheme and compare the FNPK with the EFNPK applying the same numerical scheme by Hamada & Brikaa (2017). Furthermore, in another

work, Roul et al. (2019b) present the numerical solution of the Aboander & Nahla (2016) model (CFNPK), they compare the results of neutron density with the FNPK original model, the difference in the neutron density increases as sub-diffusion increases or when the simulation time increases, but for short times of the simulation where the dynamics analysis NPPs are paramount, the difference is relatively small. Based on the work of Aboanber et al. (2018c), Singh & Ray (2019) present another fractional Stochastic Point Kinetics Equations (SPKEs) including Newtonian temperature feedback effects, they solve their model using a higher-order approximation scheme, the results were compared against previous integer stochastic models finding good agreement among them. Finally, a dynamics analysis of a PWR was presented by Zarei (2019) where the coupling of integer and fractional order models is studied, their results show instability issues when the fractional derivative value decreases, i.e., in more sub-diffusive regions.

3.2 Contemporary stage

The modified FNPK Hamada (2017a) model is solved by Polo-Labarrios et al. (2020a,b) for sinusoidal reactivity and during transient, applying a numerical solution based on the Edwards et al. (2002) method, they compare their results against Hamada's (2017a) and the normal neutron point kinetics, finding evident differences mainly because the fractional derivative term of the neutron density was considered as a differential operator and solved by implicit difference by Hamada (2017a), while the current authors consider it as an integro-differential operator. Once again Hamada (2020) applies fractional derivatives to nuclear reactor analysis and proposed a fractional telegraph point reactors kinetics (FTPRK) model considering two new terms for the neutron density, $\frac{\alpha}{\Lambda}\frac{d\rho_n(t)}{dt}I_{t_0}^{1-\alpha}n(t)P_{NL}$ and

$\tau^{\alpha}\gamma D_n B_g^2 \frac{d^{\alpha}n(t)}{dt}$, applies the model to a TRIGA reactor and to the Three Miles Island PWR for different reactivity insertions (step, ramp and sinusoidal); his results agree with those of literature, large values of the relaxation time (τ) increases rapidly the neutron density and the value of the fractional derivative order affects directly the behavior of the neutron density. Roul et al. (2021) present a numerical method to solve the FNPK, using the L1 approximation technique for the discretization of the fractional time derivative; convergence and stability analyses are reported. Another numerical solution is proposed for solving the FNPK by Sadeghi (2020), a mesh-free numerical scheme, their main finding is that the method is accurate and efficient. Zare et al. (2020) present another reactor power FPID controller using Matlab/Simulink and the FNPK finding robustness in the controller against disturbances and uncertainties.

The model developed in the present work (Espinosa-Martínez et al., 2020) integrates the first novel model since the F-SNPK Espinosa-Paredes (2017) model, and constitutes a state of the art Time-Space Fractional Neutron Point Kinetics (TSFNPK) model,

$$\tau^{\alpha}\frac{d^{\alpha+1}n(t)}{dt^{\alpha+1}}+\frac{dn(t)}{dt}+\tau^{\alpha}\sum_{a\gamma}\upsilon\frac{d^{\alpha}n(t)}{dt^{\alpha}} = \left[\frac{(\rho(t)-\beta)+\rho_{\kappa}}{\Lambda}\right]n(t)+\lambda C(t)+\tau^{\alpha}\frac{d^{\alpha}S(t)}{dt^{\alpha}} \tag{3.14}$$

The development of the model is presented in the following chapter.

Finally, in the present year a few accepted papers and a book dealing within the present's work scope can be found. At the beginning of 2021, Espinosa-Paredes (2021) publishes a book in which its scope is the importance of the non-Fickian

diffusion in heterogeneous systems and variations of the diffusion processes in nuclear reactors as well as issues regarding fractional modeling in nuclear reactors. The prolific authors, Aboander et al. (2021) present a Fractional two energy groups kinetics equations with multi-group of delayed neutron precursors (2EFPKE) and its solved analytically based on the Laplace transform, eigenvalues, and eigenvalues of the coefficient matrix; their main findings are that for sub-diffusion processes the accumulation in the neutron density increases, and for super-diffusive processes the accumulation decreases. Roul et al. (2021) expand their numerical method (Roul et al., 2020) to solve the NFDE, considering in addition to the L1 approximation technique, a collocation method based on quintic B-spline (QBS); they report results of benchmark problems showing a convergence of the solution. The most current work, Nikan et al. (2021) present the solution of the TFTE in in two "stages", the first contemplates a semi-discrete algorithm and the second is a full discretization, approaching the derivatives to a given point producing a sparse matrix and reducing the computational effort, the stability and convergence are confirmed with the results.

As an advice for the reader, I would like to point out that since the last update of the existing literature and the writing of the present thesis, other works might have been submitted and published.

4. TIME-SPACE FRACTIONAL NEUTRON POINT KINETICS (TSFNPK) MODEL

In the present chapter, the mathematical derivation of the Time-Space Fractional Neutron Point Kinetics Model is presented in detail. The TSFNPK model was derived considering a non-Fickian law for the neutron density current where the differential operators, one dependent in time and another dependent in space, are both of fractional order, thus being an extended model with respect to other fractional models and the classical neutron point kinetics equations due to the consideration of such two diffusion exponents.

4.1 Development of the TSFNPK Model

The conservation equation that governs the neutron collision and reaction processes in a multiplying-system, as well as the initial conditions and boundaries at interfaces are given by,

$$\frac{1}{\upsilon}\frac{\partial\phi(\mathbf{r},t)}{\partial t}+\nabla\cdot\mathbf{J}_n(\mathbf{r},t)+\Sigma_a(\mathbf{r})\phi(\mathbf{r},t)=S(\mathbf{r},t) \tag{4.1}$$

$$\frac{1}{\upsilon}\frac{\partial\mathbf{J}_n(\mathbf{r},t)}{\partial t}+\frac{1}{3}\nabla\phi(\mathbf{r},t)+\Sigma_{tr}(\mathbf{r})\mathbf{J}(\mathbf{r},t)=\mathbf{S}_1(\mathbf{r},t) \tag{4.2}$$

where Σ_{tr} is the transfer cross section.

Initial condition,

$$\phi(\mathbf{r},0)=\phi_0(\mathbf{r}) \tag{4.3}$$

The *boundary conditions* are depending in general on the type of physical system we are studying. However, to local scale (moderator-γ and fuel rod-σ) continuity of the neutron

flux and continuity of the neutron current vector can be applied at the interface between the moderator and fuel rod,

$$-\mathbf{n}_{\gamma\sigma}\cdot D_{n\gamma}\nabla\phi_{\gamma} = -\mathbf{n}_{\gamma\sigma}\cdot D_{n\sigma}\nabla\phi_{\sigma} \quad \text{at} \quad \gamma\sigma\text{ - interface} \tag{4.4.1}$$

$$\phi_{\gamma} = \phi_{\sigma} \quad \text{at} \quad \gamma\sigma\text{ - interface} \tag{4.4.2}$$

where $D_n\gamma$ is the neutron diffusion coefficient at the coolant, $D_{n\sigma}$ is the neutron diffusion coefficient at the fuel rod and $\mathbf{n}_{\gamma_\sigma}$ ($-\mathbf{n}_{\gamma_\sigma}$) is the unit normal vector directed from the moderator towards the fuel. These equations are known as *one-speed neutron diffusion equation*.

From a fundamental point of view, the neutron processes in nuclear reactors are not instantaneous phenomena. Then in order to considers the time-and space-memory effects, in this work we propose that the vector of the neutron current density $\mathbf{J}_{n\gamma}$ for subdiffusive process, is given by,

$$\tau^{\alpha}\frac{\partial^{\alpha}\mathbf{J}_{n\gamma}(\mathbf{r},t)}{\partial t^{\alpha}} + \mathbf{J}_{n\gamma}(\mathbf{r},t) = -D_{k\gamma}\nabla^{\kappa}\phi_{\gamma}(\mathbf{r},t) \tag{4.5}$$

For subdiffusive process $0<\alpha<1$ and $0<\kappa<1$, where α is the time dependent anomalous diffusion exponent, τ is the relaxation time, and κ is the space dependent anomalous diffusion exponent. In this equation τ^{α} has units of s^{α}, $D_{k\gamma}$ of cm^{κ}, and ∇^{κ} of $\mathrm{cm}^{-\kappa}$. The analysis of this fractional constitutive law indicates that when $\alpha\to 1$ and $\kappa\to 1$, the P1 approximation of transport theory of neutron is recovered. The P1 approximation considers normal diffusion with relaxations effects (Espinosa-Paredes et al., 2019), i.e., with memory process. Now, when $\tau\to 0$ and $\kappa\to 1$ the so-called Fick's law

(Duderstadt and Hamilton, 1976) is recovered, that is normal diffusion where this law is memoryless process. Now, when $\kappa \to 1$ and $0 < \alpha < 1$, the time-fractional constitutive law of vector current is recovered (Espinosa-Paredes et al., 2008), finally when $\tau \to 0$ and $0 < \kappa < 1$ the space-fractional constitutive law of vector current is recovered (Espinosa-Paredes, 2017). Another fundamental characteristic is that the nuclear reactor models based on fractional-order differential operators are by nature non-local.

The relaxation time for the neutronic process is defined as,

$$\tau = \frac{3D_{n\gamma}}{\upsilon} \tag{4.6}$$

and the neutron diffusion coefficient,

$$D_{n\kappa\gamma} = \frac{1}{3^{\kappa}\left(\Sigma_{tr}\right)^{\kappa}} = \frac{1}{3^{\kappa}[\Sigma_t - \bar{\mu}_0\Sigma_s]^{\kappa}} \tag{4.7}$$

where $\bar{\mu}_0$ is the average scattering angle cosine and, Σ_{tr}, Σ_t, and Σ_s are respectively, the transport, total and scattering cross sections for the coolant γ.

Next, combining Eqs. (4.1) and (4.5) yields a fractional neutron diffusion equation,

$$\begin{aligned} &\frac{\tau^{\alpha}}{\upsilon}\frac{\partial^{\alpha+1}\phi_{\gamma}(\mathbf{r},t)}{\partial t^{\alpha+1}} + \tau^{\alpha}\Sigma_{a\gamma}\frac{\partial^{\alpha}\phi_{\gamma}(\mathbf{r},t)}{\partial t^{\alpha}} + \frac{1}{\upsilon}\frac{\partial\phi_{\gamma}(\mathbf{r},t)}{\partial t} + \Sigma_{a\gamma}\phi_{\gamma}(\mathbf{r},t) \\ &\quad = D_{n\kappa\gamma}\nabla^{\kappa+1}\phi_{\gamma}(\mathbf{r},t) + \tau^{\alpha}\frac{\partial^{\alpha}S(\mathbf{r},t)}{\partial t^{\alpha}} + S(\mathbf{r},t) \end{aligned} \qquad \text{for} \quad \begin{cases} 0 < \alpha < 1 \\ 0 < \kappa < 1 \end{cases} \tag{4.8}$$

For the particular case when $\tau \to 0$ and $\kappa \to 1$, as stated before, the Fick's law is recovered, thus resulting in the classical form of the diffusion equation,

$$\frac{1}{\upsilon}\frac{\partial \phi}{\partial t} - \Sigma_a \phi + D_{n\gamma} \nabla \phi = S \tag{4.9}$$

The source term is given by (Glasstone and Sesonske, 1981),

$$S(\mathbf{r},t) = (1-\beta) k_\infty \Sigma_{a\gamma} \phi(\mathbf{r},t) + \sum_{i=1}^{m} \lambda_i C_i(\mathbf{r},t) \tag{4.10}$$

where k_∞ is the infinite multiplication factor and the subindex (i) indicates the precursor of delayed neutron of the $i-th$ group, given by,

$$\frac{dC_i(\mathbf{r},t)}{dt} = \beta_i \, k_\infty \, \Sigma_{a\gamma} \, \phi_\gamma(\mathbf{r},t) - \lambda_i C_i(\mathbf{r},t) \tag{4.11}$$

where C_i is the concentration of neutron precursors of the $i-\text{th}$ group, $\Sigma_{a\gamma}$ is the macroscopic absorption cross section at the coolant, β_i is the total fraction of delayed neutrons of the $i-\text{th}$ group, k_∞ is the infinite medium neutron multiplication factor, and λ_i is the decay constant of delayed neutron of precursors of the $i-\text{th}$ group.

Using the presented equations, we will derive the *Time-Space Fractional Neutron Point Kinetics* (TSFNPK) model, first we substitute Eq. (4.10) into Eq. (4.8),

$$\begin{aligned} \frac{\tau^\alpha}{\upsilon}\frac{\partial^{\alpha+1}\phi_\gamma(\mathbf{r},t)}{\partial t^{\alpha+1}} + \tau^\alpha \Sigma_{a\gamma}\frac{\partial^\alpha \phi_\gamma(\mathbf{r},t)}{\partial t^\alpha} + \frac{1}{\upsilon}\frac{\partial \phi_\gamma(\mathbf{r},t)}{\partial t} = D_{\kappa\gamma}\nabla^{\kappa+1}\phi_\gamma(\mathbf{r},t) \\ + \left[(1-\beta)k_\infty - 1\right]\Sigma_{a\gamma}\phi(\mathbf{r},t) + \sum_{i=1}^{m}\lambda_i \hat{C}_i(\mathbf{r},t) + \tau^\alpha \frac{\partial^\alpha \hat{S}(\mathbf{r},t)}{\partial t^\alpha} \end{aligned} \tag{4.12}$$

where the differential operator of fractional order in the diffusive term was proposed by Espinosa-Paredes (2017),

$$\nabla^{\kappa+1}\phi_\gamma(\mathbf{r},t) \approx -B_g^{k+1}\phi_\gamma(\mathbf{r},t) \tag{4.13}$$

The above assumption, known as the fractional geometrical buckling (B_g^{k+1}) which is related to the deviation of the ideal flux map (cosine in an infinite slab) inside the reactor, was first conceived when fractional divergence was noticed (anomalous diffusion), also gives birth to fractional criticality when used with the classical multiplication factor k_∞ (Das 2008; Das and Biswas, 2007). The geometrical buckling is a measure of neutron leakage and depends on the geometry of the core, thus the approximation is valid for subdiffusive processes, when $\kappa \to 1$ the classical flux profile is obtained, (i.e., normal diffusion).

Introducing the fractional geometrical buckling into Eq. (4.12), leads to,

$$\begin{aligned} &\frac{\tau^\alpha}{\upsilon}\frac{\partial^{\alpha+1}\phi_\gamma(\mathbf{r},t)}{\partial t^{\alpha+1}} + \tau^\alpha \Sigma_{a\gamma}\frac{\partial^\alpha \phi_\gamma(\mathbf{r},t)}{\partial t^\alpha} + \frac{1}{\upsilon}\frac{\partial \phi_\gamma(\mathbf{r},t)}{\partial t} \\ &= \left[(1-\beta)k_\infty \Sigma_{a\gamma} - \Sigma_{a\gamma} - D_{\kappa\gamma}B_g^{k+1}\right]\phi_\gamma(\mathbf{r},t) + \sum_{i=1}^{m}\lambda_i \hat{C}_i(\mathbf{r},t) + \tau^\alpha \frac{\partial^\alpha \hat{S}(\mathbf{r},t)}{\partial t^\alpha} \end{aligned} \tag{4.14}$$

Next, representing the flux, precursor concentrations and source term as separable functions of space and time,

$$\phi_\gamma(\mathbf{r},t) = \upsilon n(t)\,\psi(\mathbf{r}) \tag{4.15}$$

$$\hat{C}_i(\mathbf{r},t) = C_i(t)\,\psi(\mathbf{r}) \tag{4.16}$$

$$\hat{S}(\mathbf{r},t) = S(t)\,\psi(\mathbf{r}) \tag{4.17}$$

Thus, Eq. (4.14) can be re-written solely as a function of time,

$$\begin{aligned} &\tau^\alpha \frac{d^{\alpha+1}n(t)}{dt^{\alpha+1}} + \tau^\alpha \Sigma_{a\gamma}\upsilon\frac{d^\alpha n(t)}{dt^\alpha} + \frac{dn(t)}{dt} \\ &= \left[(1-\beta)k_\infty \Sigma_{a\gamma} - \Sigma_{a\gamma} - D_{n\kappa\gamma}B_g^{k+1}\right]\upsilon n(t) + \sum_{i=1}^{m}\lambda_i C_i(t) + \tau^\alpha \frac{d^\alpha S(t)}{dt^\alpha} \end{aligned} \tag{4.18}$$

Substituting the acknowledged nuclear definitions in Table 4.1 of reactivity, effective neutron multiplication factor, neutron diffusion length, neutron mean life in the reactor core, non-leakage probability and neutron mean generation time (Lamarsh and Baratta 2001), we obtain,

$$\tau^{\alpha}\frac{d^{\alpha+1}n(t)}{dt^{\alpha+1}}+\tau^{\alpha}\Sigma_{a\gamma}\upsilon\frac{d^{\alpha}n(t)}{dt^{\alpha}}+\frac{dn(t)}{dt}$$
$$=\left[\frac{\left(\rho_n(t)-\beta\right)}{\Lambda}+\upsilon\left(D_{\gamma}B_g^2-D_{\kappa\gamma}B_g^{\kappa+1}\right)\right]n(t)+\sum_{i=1}^{m}\lambda_i C_i(t)+\tau^{\alpha}\frac{d^{\alpha}S(t)}{dt^{\alpha}} \tag{4.19}$$

Table 4.1. Nuclear definitions

Description	Variable	Definition
Reactivity	ρ_n	$\frac{k_{eff}-1}{k_{eff}}$
Effective neutron multiplication factor	k_{eff}	$\frac{k_{\infty}}{(1+L^2B_g^2)}$
Neutron diffusion length	L	$\left(\frac{D_{\gamma}}{\Sigma_{a\gamma}}\right)^{1/2}$
Mean lifetime of neutron in reactor	l	$\frac{P_{NL}}{\Sigma_{a\gamma}\upsilon}$
Non-leakage probability	P_{NL}	$\frac{1}{(1+L^2B_g^2)}$
Mean neutron generation time	Λ	$\frac{\ell}{k_{eff}}$

Finally, for simplification we conglomerate the terms containing the fractional geometrical buckling and normal geometrical buckling in the following definition of

reactivity for the fractional term of order κ, which is associated to neutron leakage in the system, i.e., $\rho_\kappa < 0$.

$$\rho_\kappa = \Lambda\upsilon\left(D_{n\gamma}B_g^2 - D_{n\kappa\gamma}B_g^{\kappa+1}\right) \tag{4.20}$$

where B_g^2 is the geometrical buckling.

Thereby the TSFNPK equation model,

$$\begin{aligned}&\tau^\alpha \frac{d^{\alpha+1}n(t)}{dt^{\alpha+1}} + \tau^\alpha \Sigma_{a\gamma}\upsilon \frac{d^\alpha n(t)}{dt^\alpha} + \frac{dn(t)}{dt} \\ &= \left[\frac{(\rho_n(t)-\beta)+\rho_\kappa}{\Lambda}\right] n(t) + \sum_{i=1}^{m}\lambda_i C_i(t) + \tau^\alpha \frac{d^\alpha S(t)}{dt^\alpha}\end{aligned} \tag{4.21}$$

It is important to note that this equation has no restrictions regarding the *non-leakage probability* discussed in previous works, due that the source term is in implicit form (last term in the right side) (Aboanber & Nahla, 2016; Espinosa-Paredes, 2016).

Applying the elements that led to the time-fractional order model, we re-write Eq. (4.10) for neutron source,

$$S(t) = \frac{(1-\beta)}{\Lambda} n(t) + \sum_{i=1}^{m}\lambda_i c_i(t) \tag{4.22}$$

It can be demonstrated that starting with concentration of delayed neutron precursors given by Eq. (4.11), and following the same procedure applied previously, leads to,

$$\frac{dC_i(t)}{dt} = \frac{\beta_i}{\Lambda} n(t) - \lambda_i C_i(t), \qquad i = 1,2,...m \tag{4.23}$$

This condition in all cases is fulfilled due that $D_{n\gamma}B_g^2 < D_{n\kappa\gamma}B_g^{\kappa+1}$. This can be explained considering that the diffusion processes are carried out in the moderator (γ) with a characteristic length ℓ_γ, which is the distance between two fuel rods, and the characteristic length of the system is L_a (fuel assembly), in this sense the Fickian and non-Fickian diffusion approximations are valid as long as the scale restrictions fulfill $\ell_\gamma << L_a$. The orders of magnitude of the current density vectors, normal and fractional, are,

$$\overbrace{\nabla = O\left(\frac{1}{L_\phi}\right)}^{normal} \qquad \overbrace{\nabla^\kappa = O\left(\frac{1}{L_\phi^\kappa}\right)}^{fractional}$$

$$\mathbf{J}_\gamma = O\left(\ell \times \frac{\phi_\gamma}{L_\phi}\right) \qquad \mathbf{J}_\gamma = O\left(\ell^\kappa \times \frac{\phi_\gamma}{L_\phi^\kappa}\right)$$

$$D_\gamma = O(\ell) \qquad D_{\kappa\gamma} = O\left(\ell^\kappa\right)$$

respectively. Then it can be clearly shown that $\left(\frac{\ell}{L_\phi}\right)^\kappa > \left(\frac{\ell}{L_\phi}\right)$ for $\ell_\gamma^\kappa << L_\phi^\kappa$ and $\ell_\gamma << L_\phi$.

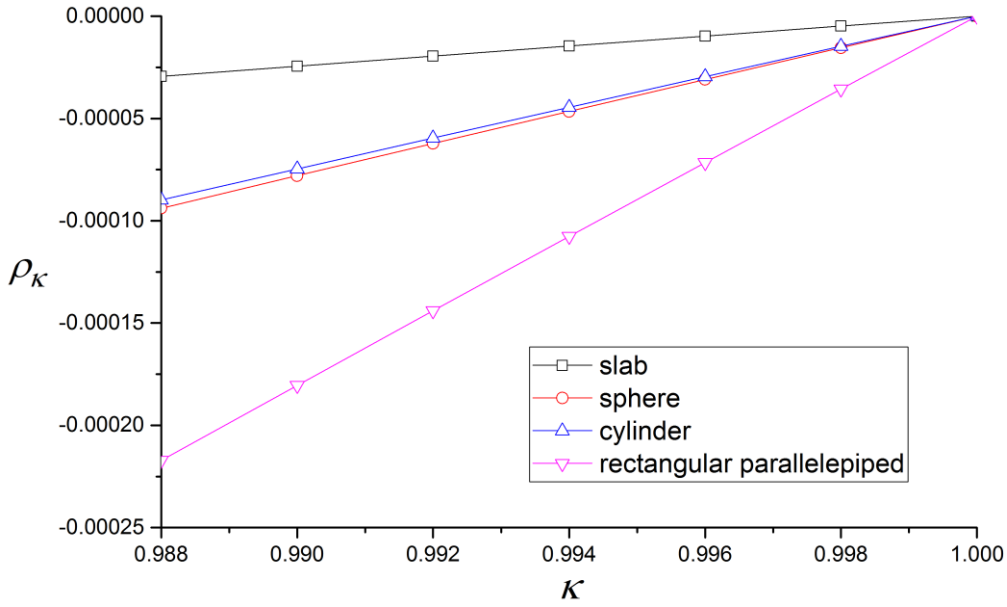

Figure 4.1. Value of ρ_κ in pcm for different reactors. Slab reactor, sphere reactor, cylinder reactor and rectangular parallelepiped reactor. Values were: thickness a = 100 cm for slab, radius R = 50 cm for a sphere and cylinder, length a = b = 50 cm and c = 100 cm for rectangular parallelepiped.

It is important to stress that the definition of leakage reactivity (ρ_κ) given by Eq. (4.20) contains a term of integer order, and a term of fractional order, which depends of the geometry and size of the reactor which is analyzed in Figure 4.1 using the calculated geometric buckling of fractional order from Table 4.2. The integer order term is due to classic diffusion whose approximation is $\nabla^2\phi_\gamma(\mathbf{r},t) = -B_g^2\phi_\gamma(\mathbf{r},t)$, while the fractional order term is due to anomalous diffusion (subdiffusion), i.e., $\nabla^{\kappa+1}\phi_\gamma(\mathbf{r},t) = -B_g^{\kappa+1}\phi_\gamma(\mathbf{r},t)$. Performing a dimensional analysis, we can observe that the quantity $D_{n\kappa\gamma}B_g^{\kappa+1}$ has the dimensions of $length^{-1}$, since $D_{n\kappa\gamma}$ is a $length^{\kappa}$ and $B_g^{\kappa+1}$ is a $length^{-(\kappa+1)}$.

Table 4.2. Geometric Buckling of fractional order

Reactor Geometries	${}^{*}B_g^{\kappa+1}$
Slab	$\left(\frac{\pi}{a}\right)^{\kappa+1}$
Sphere	$\left(\frac{\pi}{R}\right)^{\kappa+1}$
Rectangular parallelepiped	$\left(\frac{\pi}{a}\right)^{\kappa+1}+\left(\frac{\pi}{b}\right)^{\kappa+1}+\left(\frac{\pi}{c}\right)^{\kappa+1}$
Cylinder	$\left(\frac{2.405}{R}\right)^{\kappa+1}+\left(\frac{\pi}{H}\right)^{\kappa+1}$

For the introduction of temperature feedback effects, derived from the ideas of Hetrick (1993) and Glasstone & Sesonske (1994), we introduce a temperature dependent reactivity,

$$\rho_n(t)=\rho_{n0}-r_c\left[T(t)-T_0\right] \tag{4.24}$$

where ρ_0 is the initial reactivity, r_c is the reactivity coefficient, T_0 is the initial fuel temperature, and the prompt temperature is given by,

$$\frac{dT(t)}{dt}=K_c n(t) \tag{4.25}$$

where K_c is the reciprocal of thermal capacity of the fuel.

Differentiating Eq. (4.24) and substituting it in Eq. (4.25) yields the temperature feedback model,

$$\frac{d\rho_n(t)}{dt}=-r_c K_c n(t) \tag{4.26}$$

In previous works feedback effects have been studied with models of fractional order for neutron point kinetics approximation, mainly with the FNPK model but not exclusive (e.g., Espinosa-Paredes et al., 2014; Nowak et al., 2015; Vyawahare & Nataraj, 2015; Schramm et al., 2016; Singh & Ray, 2019).

4.1.1 Temperature feedback effects

For the numerical experiments only one group of delayed neutrons is considered. The complete set of equations and initial conditions of the space-time fractional point reactor with feedback effects are,

Space-time Fractional neutron density equation

$$\tau^{\alpha}\frac{d^{\alpha+1}n(t)}{dt^{\alpha+1}}+\frac{dn(t)}{dt}+\tau^{\alpha}\Sigma_{a\gamma}\upsilon\frac{d^{\alpha}n(t)}{dt^{\alpha}}=\left[\frac{(\rho_n(t)-\beta)+\rho_{\kappa}}{\Lambda}\right]n(t)+\lambda C(t)+\tau^{\alpha}\frac{d^{\alpha}S(t)}{dt^{\alpha}} \tag{4.27}$$

Precursor concentration

$$\frac{dC(t)}{dt}=\frac{\beta}{\Lambda}n(t)-\lambda C(t) \tag{4.28}$$

Reactivity feedback

$$\frac{d\rho_n(t)}{dt}=-r_c K_c n(t) \tag{4.29}$$

Neutron source

$$\frac{dS(t)}{dt}=\frac{(1-\beta)}{\Lambda}\frac{dn(t)}{dt}+\lambda\frac{dC(t)}{dt} \tag{4.30}$$

The initial conditions at $t=0$ are,

$$n(0)=n_0 \tag{4.31}$$

$$C(0) = C_0 = \frac{\beta}{\Lambda\lambda} n_0 \tag{4.32}$$

$$\rho_n(0) = \rho_{n0} = -\rho_k \quad \text{for } 0 < \kappa < 1 \tag{4.33}$$

$$S(0) = S_0 = \frac{n_0}{\Lambda} \tag{4.34}$$

$$\frac{d^{\alpha+1} n(0)}{dt^{\alpha+1}} = 0 \tag{4.35}$$

$$\frac{d^{\alpha} n(0)}{dt^{\alpha}} = 0 \tag{4.36}$$

$$\frac{d^{\alpha} S(0)}{dt^{\alpha}} = 0 \tag{4.37}$$

It is important to note that Eq. (4.27) is written in terms of differential operators, due to strategies of the numerical solution in the applied method, as presented in the next section.

4.2 Numerical Solution

The present solution uses the Caputo version of the fractional derivative instead of the Riemann-Liouville fractional derivative, due that the initial conditions correspond to physical states, i.e., initial condition of the integer-order model can be considered. Additionally, this numerical solution is based on the idea of solving the fractional differential equation as a system of equations, thus, reducing the problem to a much easier one.

For a function $f : [a, +\infty[\to \Re$, the α order Caputo fractional derivative is defined by Podlubny (1999),

$${}_{a}^{C}D_{t}^{\alpha} f(t) = \frac{1}{\Gamma(n-\alpha)} \int_a^t \frac{f^{(n)}(\tau)}{(t-\tau)^{\alpha+1-n}} d\tau, \qquad n-1 < \alpha < n \tag{4.38}$$

where $\Gamma(n-\alpha)$ is the gamma function, whose argument is $n-\alpha$, and $f^{(n)}=\frac{d^n}{dt^n}$.

The numerical solution of the fractional point reactor model is obtained applying linear multi-term fractional differential equations for systems of equations developed by Edwards et al. (2002). The fractional kinetics model can be represented as a multi-term high-order linear fractional differential equation, which is calculated by writing the problem as a system of ordinary and fractional differential equations. This numerical method is attractive for the fractional nuclear reactor dynamics analysis, because the implementation is relatively direct and it has been applied in previous works (e.g. Espinosa-Paredes et al., 2011; Nowak et al., 2014; Polo-Labarrios et al., 2014). Regarding to discreditation of the derivatives to solve; for the first-order differential equations, the trapezium rule is applied; and to discretize the fractional derivative, the Diethelm's method is applied (Diethelm, 1997),

$$D^{\alpha}y=\frac{1}{{}^{\alpha}\gamma_i}\left(\sum_{k=0}^{i}{}^{\alpha}\omega_{k,i}\ y_{i-k}+\frac{y_0}{\alpha}\right) \tag{4.39}$$

where ${}^{\alpha}\gamma_i=(ih)^{\alpha}\Gamma(-\alpha)$, h is the size step, y_0 is the initial condition, and ${}^{\alpha}\omega_{k,0},...,{}^{\alpha}\omega_{k,i}$ are convolution weights calculated by (Diethelm, 1997),

$${}^{\alpha}\omega_{k,i}=\begin{cases}-1 & , \quad for \quad k=0\\ 2k^{1-\alpha}-(\alpha-1)^{1-\alpha}-(\alpha+1)^{1-\alpha} & , \quad for \quad k=1,2,\cdots,i-1\\ (\alpha-1)k^{\alpha}-(k-1)^{1-\alpha}+k^{1-\alpha} & , \quad for \quad k=i\end{cases} \tag{4.40}$$

In this analysis, the fractional neutron point kinetics equations, considering one group of delayed neutron precursors with reactivity feedback effects, are given by a set of

fractional-order and integer-order ordinary differential, Eqs. (4.27)-(4.29) that are rewritten of the following form,

$$D^{\alpha+1}n + a_3 Dn + a_2 D^{\alpha} n + a_1 n = b_1 C + D^{\alpha} S \tag{4.41}$$

$$DC + b_2 C = a_0 n \tag{4.42}$$

$$DS = a_4 Dn + b_2 DC \tag{4.43}$$

$$D\rho = -r_c K_c n \tag{4.44}$$

In these equations it was changed $\frac{d}{dt}$ for D and the coefficients are defined in Table 4.3.

Table 4.3. Coefficients of Eqs. (4.41)-(4.44)

Coefficient	Value
a_0	$\frac{\beta}{\Lambda}$
a_1	$-\frac{\rho - \beta + \rho_\kappa}{\tau^{\alpha}\Lambda}$
a_2	$\Sigma_a \upsilon$
a_3	$\frac{1}{\tau^{\alpha}}$
a_4	$\frac{1-\beta}{\Lambda}$
b_1	$\frac{\lambda}{\tau^{\alpha}}$
b_2	λ

Applying the following change of variables, $x_1 = n$, $x_2 = D^{\alpha} x_1$, $x_3 = Dx_1$, $x_4 = D^{\alpha} x_3$, $y_1 = C$, $y_2 = Dy_1$, $z_1 = S$, $z_2 = D^{\alpha} z_1$, $z_3 = Dz_1$, $r_1 = \rho$ and $r_2 = Dr_1$. The discrete form of the solution of the system of equations can be presented in matrix form,

$$\mathbf{Ax} = \mathbf{b} \tag{4.45}$$

where

$$\mathbf{x} = \left(x_{1,i}\ x_{2,i}\ x_{3,i}\ y_{1,i}\ z_{1,i}\ z_{2,i}\ z_{3,i} \right)^T \tag{4.46}$$

$$\mathbf{b} = \left(u_{1,i}\ u_{2,i}\ u_{3,i}\ v_{1,i}\ w_{1,i}\ w_{2,i}\ w_{3,i} \right)^T \tag{4.47}$$

$$\mathbf{A} = \begin{pmatrix} -{}^{\alpha}\omega_{0,i} & {}^{\alpha}\gamma_i & 0 & 0 & 0 & 0 & 0 \\ 1 & 0 & -h/2 & 0 & 0 & 0 & 0 \\ -{}^{\alpha}\gamma_i a_{1,i} & -{}^{\alpha}\gamma_i a_2 & -\left({}^{\alpha}\gamma_i a_3 + {}^{\alpha}\omega_{0,i} \right) & {}^{\alpha}\gamma_i b_1 & 0 & {}^{\alpha}\gamma_i & 0 \\ -a_0 h/2 & 0 & 0 & \left(1 + b_2 h/2\right) & 0 & 0 & 0 \\ 0 & 0 & 0 & 0 & -{}^{\alpha}\omega_{0,i} & {}^{\alpha}\gamma_i & 0 \\ -a_0 b_2 h/2 & 0 & -a_4 h/2 & b_2^2 h/2 & 1 & 0 & 0 \\ r_c K_c h/2 & 0 & 0 & 0 & 0 & 0 & 1 \end{pmatrix} \tag{4.48}$$

the coefficients of the vector $\mathbf{b}$ are given by,

$$u_{1,\mathrm{i}} = \sum_{p=1}^{i} {}^{\alpha}\omega_{p,i} \cdot x_{1,i-p} + \frac{x_{1,0}}{\alpha} \tag{4.49}$$

$$u_{2,\mathrm{i}} = x_{1,i-1} + \frac{h}{2} x_{3,i-1} \tag{4.50}$$

$$u_{3,\mathrm{i}} = \sum_{p=1}^{i} {}^{\alpha}\omega_{p,i} \cdot x_{3,i-p} + \frac{x_{3,0}}{\alpha} \tag{4.51}$$

$$v_{1,i} = \frac{a_0 h}{2} x_{1,i-1} + \left(1 - \frac{b_2 h}{2}\right) y_{1,i-1} \tag{4.52}$$

$$w_{1,\mathrm{i}} = \sum_{p=1}^{i} {}^{\alpha}\omega_{p,i} \cdot z_{1,i-p} + \frac{z_{1,0}}{\alpha} \tag{4.53}$$

$$w_{2,i} = z_{1,i-1} + \frac{h}{2}\left(a_0 b_2 x_{1,i-1} + a_{4 x_{3,i-1}} - b_2^2 y_{1,i-1} \right) \tag{4.54}$$

$$w_{3,i} = z_{3,i-1} - \frac{h}{2}\left(r_c K_c x_{1,i-1} \right) \tag{4.55}$$

The problem solution is subject to the following initial conditions,

$$
\begin{aligned}
&x_{1,0} = n_0, \quad x_{2,0} = 0, \quad x_{3,0} = 0, \\
&y_{1,0} = \frac{\beta}{\Lambda\lambda} x_{1,0}, \\
&z_{1,0} = \frac{x_{1,0}}{\Lambda}, \quad z_{2,0} = 0, \quad z_{3,0} = \rho_0
\end{aligned}
\tag{4.56}
$$

4.3 Numerical Experiments

In order to establish proper values of the time- and space-anomalous diffusion coefficient with memory effects α and κ, numerous simulations were performed in which we establish the single effects of the fractional diffusion exponents i.e., for a fixed value of α and different values of κ, and for different values of α and a fixed value of κ, as well as without temperature feedback effects and then considering them.

The anomalous diffusion exponents are applicable everywhere in the homogeneous and heterogeneous reactor core due that it predicts neutrons finite velocity i.e., a value of α close to one indicates the presence of normal diffusion (Fickian) implying lesser or negligible fission reactions, such as in the moderator and reflectors; and, smaller values of α evidence highly subdiffusive conditions, strong absorbing regions, such as fuel bundles and control rods (Vyawahare and Nataraj, 2018). On the other hand, the term κ considers neutron leakage, i.e., a value of κ close to one indicates lesser leakage and smaller values of κ greater leakage, which is directly affected by cores geometry.

4.3.1. Slab geometry without temperature feedback effects

For the following numerical experiments, a homogeneous slab reactor with a thickness of $a = 100$ cm, including the extrapolation distance, was considered. Thermal neutron diffusion parameters were taken from literature (Lamarsh, 2001; Duderstadt, 1976)

for water as moderator at 20 ºC, $\Lambda = 2E - 5$ s, $\beta = 0.0065$, $v = 220{,}000$ cm/s, $D = 0.16$ cm, $\Sigma_a = 0.0197$ 1/cm, $\lambda = 0.0810958$ and $l = 0.00024$ s.

Figures 4.2 and 4.3 show the neutron density behavior of a positive reactivity insertion of $\rho_n = \beta/5$ at 0.5 s. Figure 4.2 shows clearly the effect of the spatial anomalous diffusion coefficient (κ) which can be important for short transients, i.e., for smaller values of κ the neutron density increases less dramatically than for bigger values or even without the term ρ_κ which contains the coefficient in the proposed fractional buckling. In Figure 4.3 the effect of the value in the fractional derivative is shown, contrary to what happens with the anomalous diffusion coefficient κ, for smaller values of α the neutron density increases more dramatically, this effect can also be important for short transients.

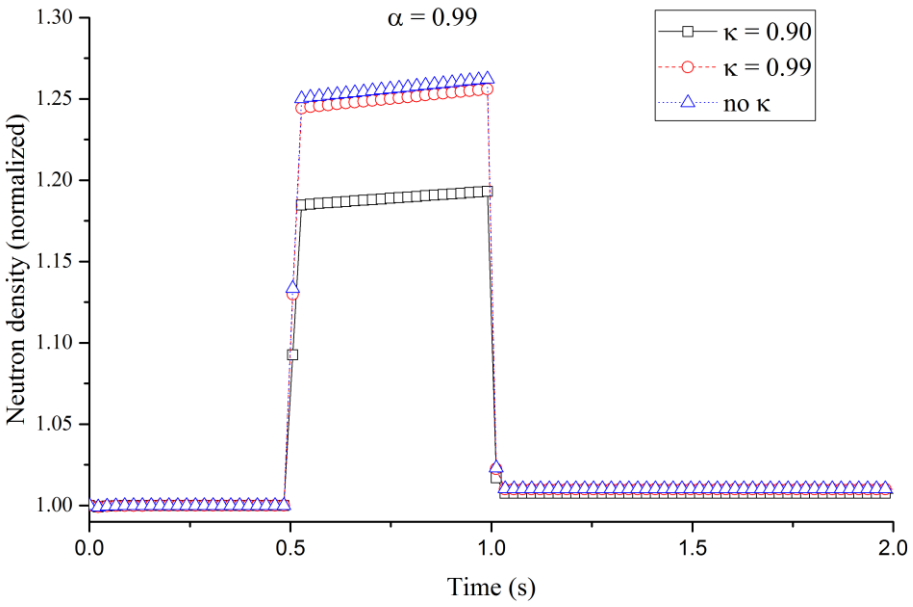

Figure 4.2. Normalized neutron density (n/n_0) when $\alpha = 0.99$ for two values of the fractional diffusion exponent κ and without its effect.

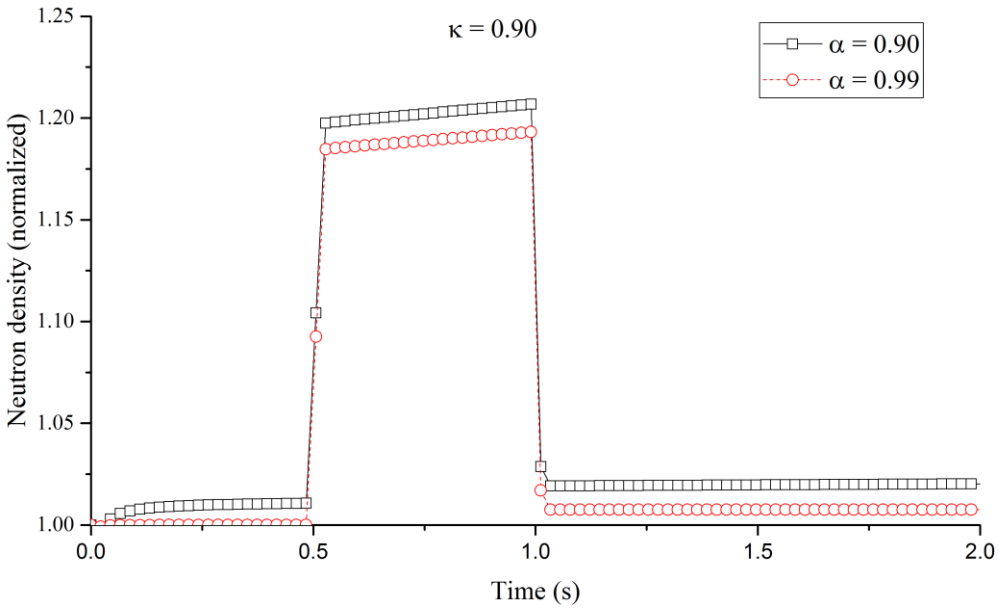

Figure 4.3. Normalized neutron density (n/n_0) when $\kappa = 0.90$ for two values of α in the fractional derivative.

Figures 4.5-4.8 show the neutron density behavior after a constant positive reactivity insertion of $\rho_n = \beta/5$, it can be observed that when α decreases, neutron leakage is greater, this can be specially noticed in Figure 4.8 where a comparison between Figures 4.4 and 4.7 is presented. With respect to the fractional diffusion exponent κ, the behavior is backwards, i.e., the neutron leakage is less when κ decreases.

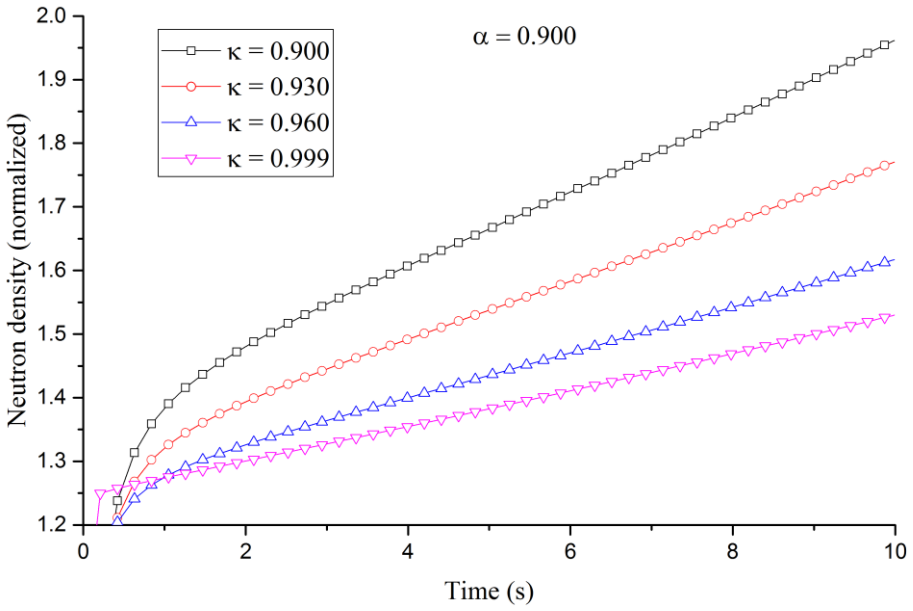

Figure 4.4. Normalized density (n/n_0) when $\alpha = 0.900$ for different values of the fractional diffusion exponent κ.

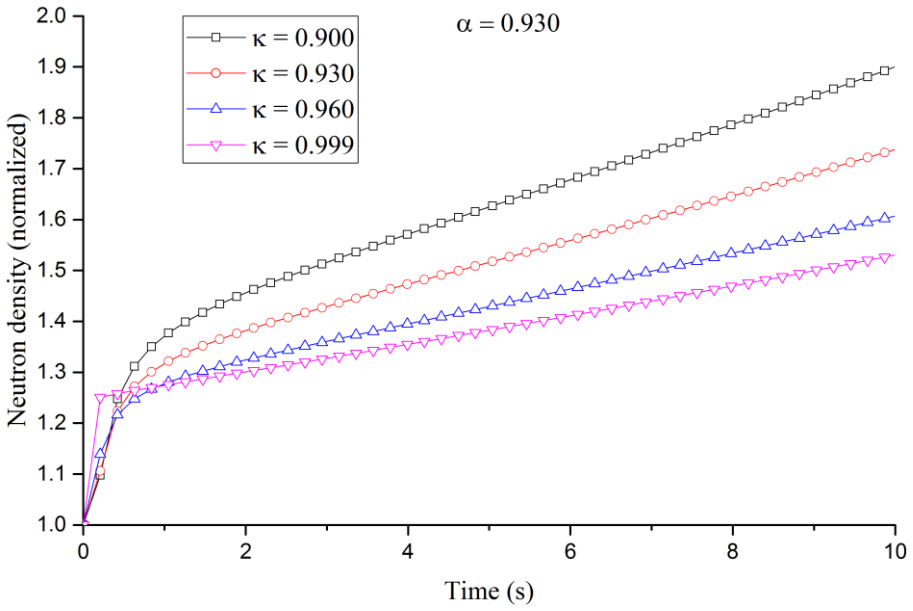

Figure. 4.5. Normalized neutron density (n/n_0) when $\alpha = 0.930$ for different values of the fractional diffusion exponent κ.

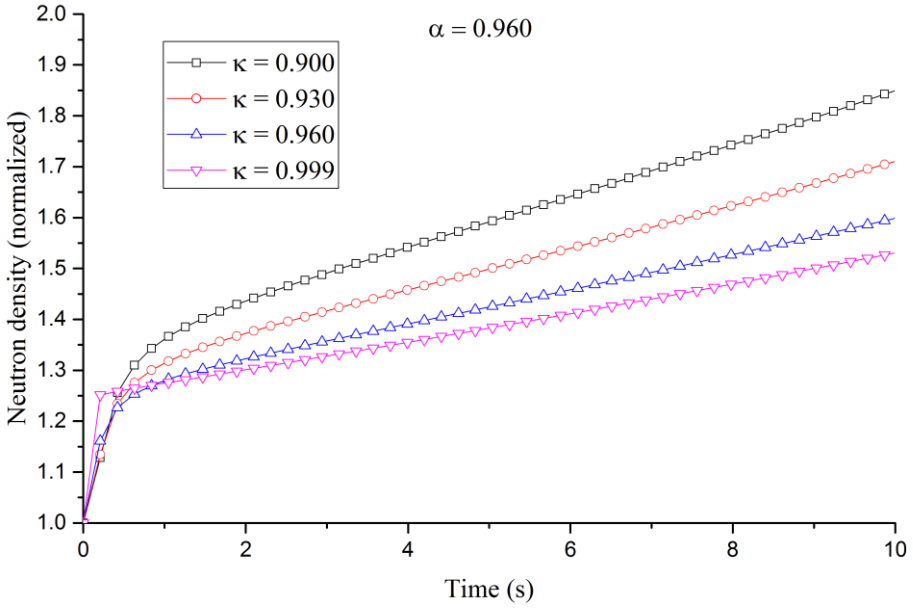

Figure.4.6. Normalized neutron density (n/n_0) when $\alpha = 0.960$ for different values of the fractional diffusion exponent κ.

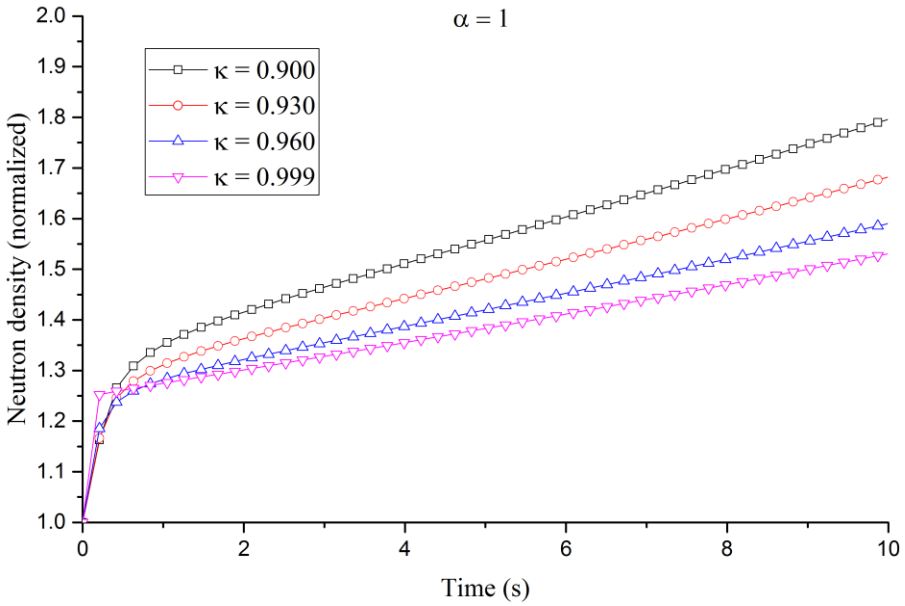

Figure. 4.7. Normalized neutron density (n/n_0) when $\alpha = 1$ for different values of the fractional diffusion exponent κ.

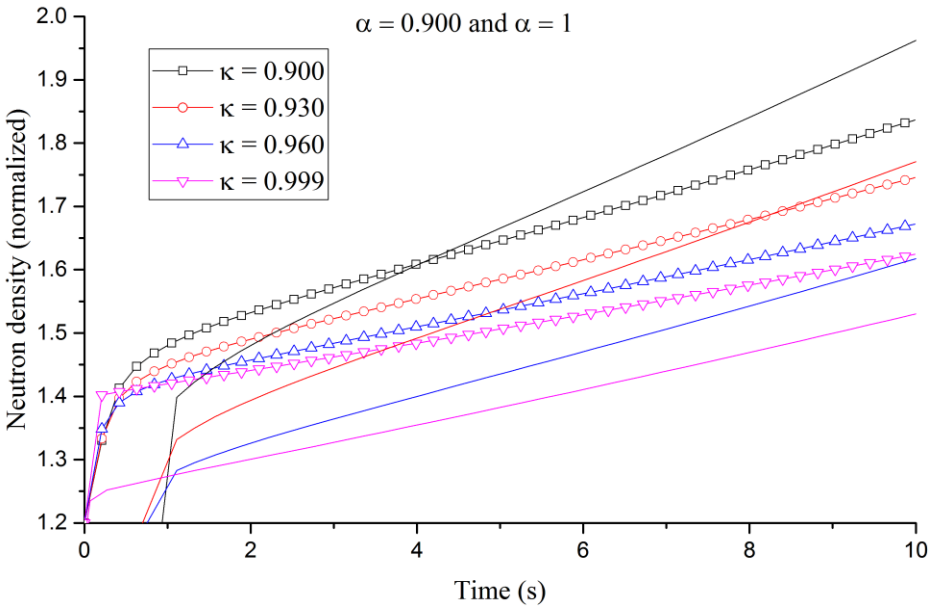

Figure. 4.8. Overlapping of Figures 4.4 and 4.7, lines with symbol represent $\alpha = 0.900$ and solid lines represent $\alpha = 1$.

Figures 4.9-4.12 show the precursors concentration behavior after a constant positive reactivity insertion of $\rho_n = \beta/5$, it can be observed that when α decreases, precursors concentration increments, this can be specially noticed in Figure 4.13 where a comparison between Figures 4.9 and 4.12 is presented. With respect to the fractional diffusion exponent κ, the behavior is consistent with the behavior of α, i.e., when κ decreases, precursors concentration increments as well.

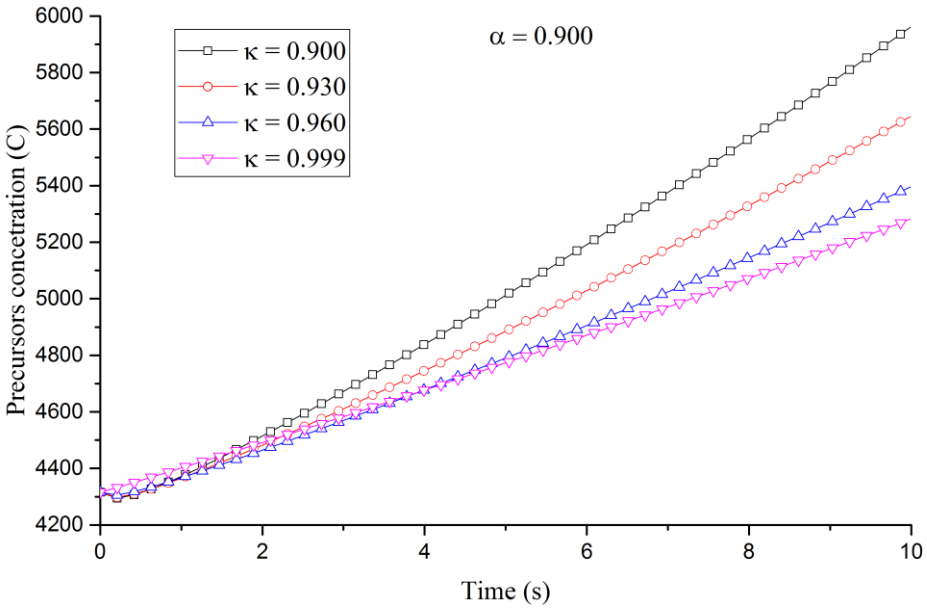

Figure 4.9. Precursors concentration (C) when $\alpha = 0.900$ for different values of the fractional diffusion exponent κ.

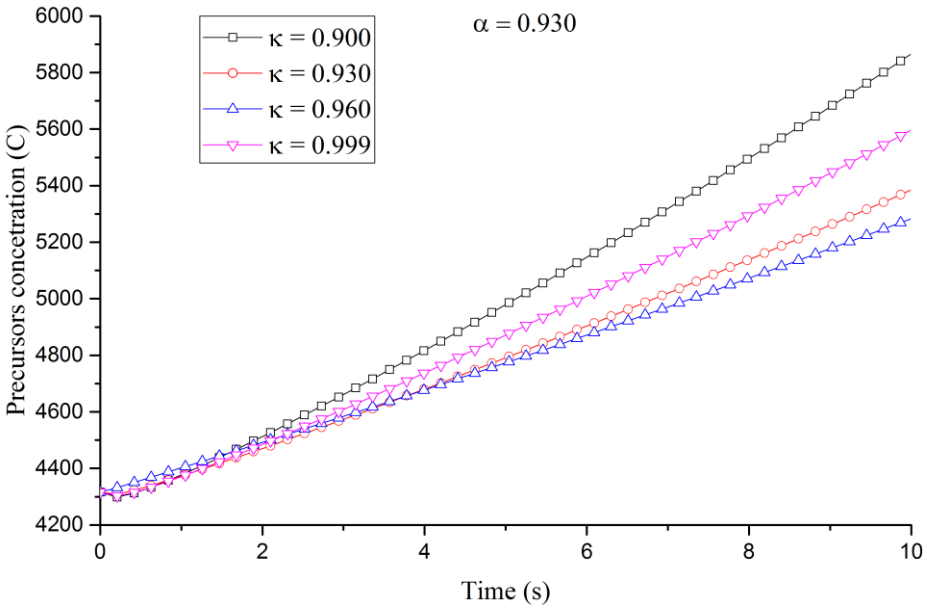

Figure 4.10. Precursors concentration (C) when $\alpha = 0.930$ for different values of the fractional diffusion exponent κ.

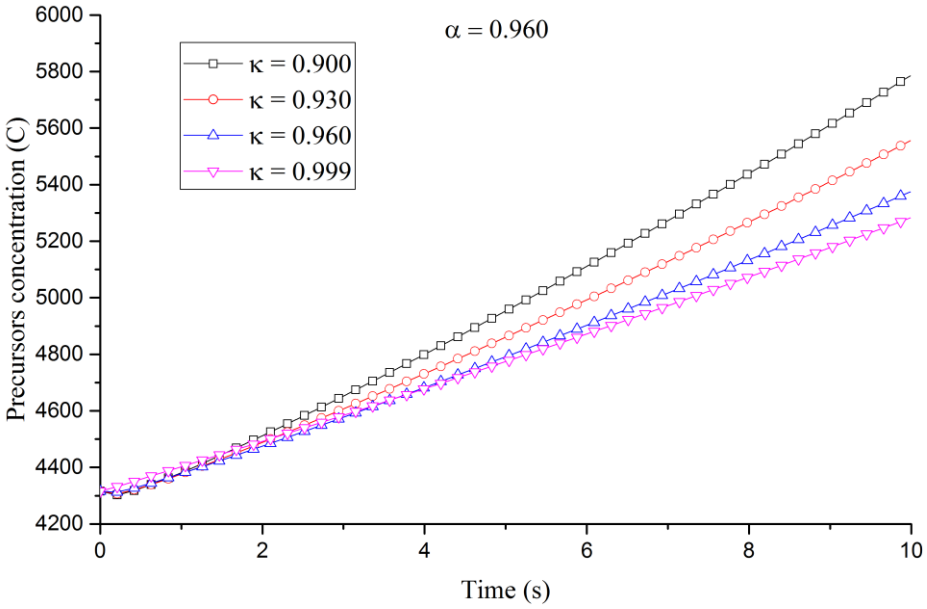

Figure 4.11. Precursors concentration (C) when $\alpha = 0.960$ for different values of the fractional diffusion exponent κ.

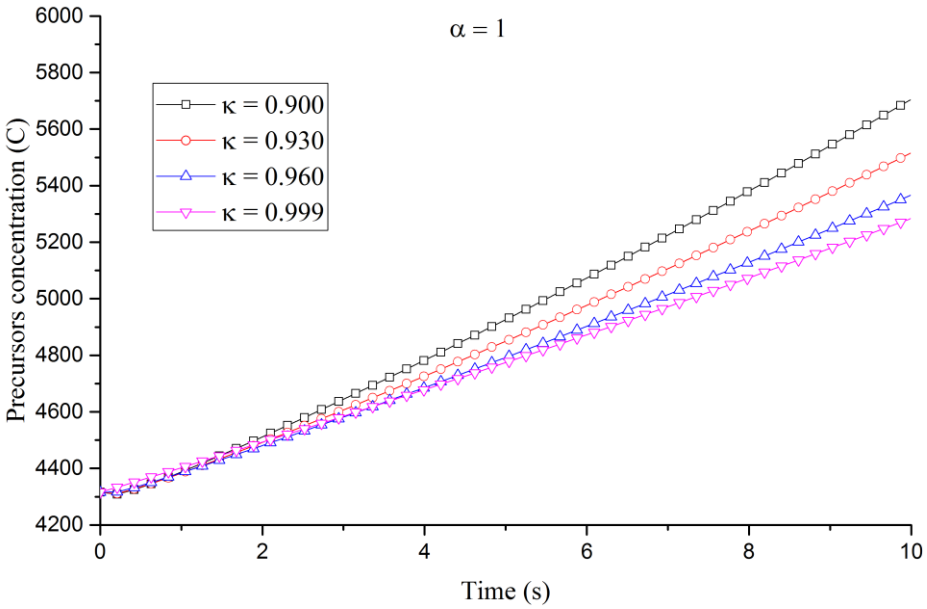

Figure 4.12. Precursors concentration (C) when $\alpha = 1$ for different values of the fractional diffusion exponent κ.

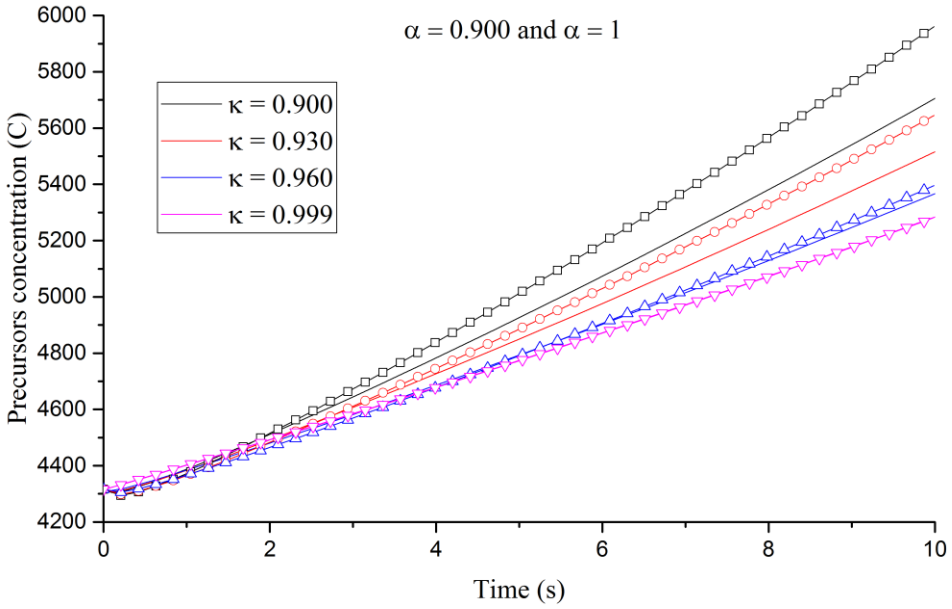

Figure 4.13. Overlapping Figures 4.9 and 4.12, lines with symbol represent $\alpha = 0.900$ and solid lines represent $\alpha = 1$.

4.3.2. Slab geometry with temperature feedback effects

For the following numerical experiments, a homogeneous slab reactor with a thickness of $a = 100$ cm, including the extrapolation distance, was considered. Thermal neutron diffusion parameters were taken from literature (Lamarsh, 2001; Duderstadt, 1976) for water as moderator at 20 ºC, $\Lambda = 2E-5$ s, $\beta = 0.0065$, $v = 220{,}000$ cm/s, $D = 0.16$ cm, $\Sigma_a = 0.0197$ 1/cm, $\lambda = 0.0810958$ and $l = 0.00024$ s.

Figures 4.14 and 4.15 show the behavior of neutron density and reactivity, respectively for an initial reactivity of $\rho_{n0} = 0.002$, a fixed $\alpha = 0.90$ and different values of κ.

Figure 4.14 shows clearly the effect of the anomalous diffusion coefficient (κ) which can be important for long transients, i.e., for smaller values of κ the neutron density increases less dramatically than for bigger values or even without the term ρ_κ which contains the coefficient in the proposed fractional buckling. In Figure 4.15 the same effect can be appreciated, i.e., for smaller values of κ the reactivity decreases less dramatically than for bigger values or even without the term ρ_κ.

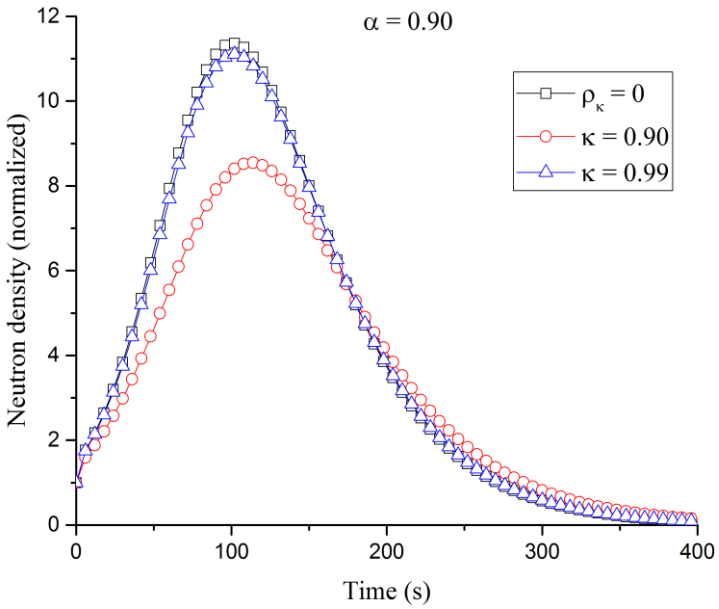

Figure 4.14. Normalized neutron density when $\alpha = 0.90$ for different values of the fractional diffusion exponent κ.

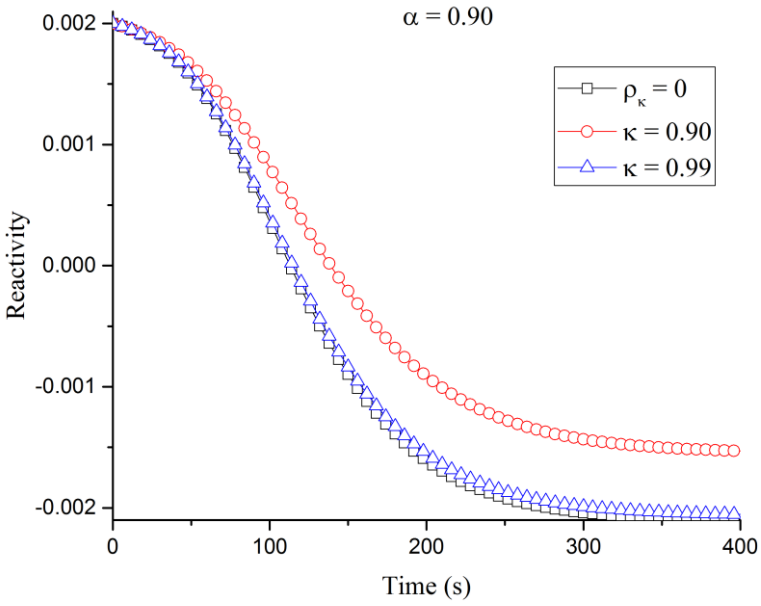

Figure 4.15. Reactivity when $\alpha = 0.90$ for two values of the fractional diffusion exponent κ and without its effect.

Figures 4.16 and 4.17 show the behavior of neutron density and reactivity, respectively for an initial reactivity of $\rho_{n0} = 0.002$, a fixed $\alpha = 0.99$ and different values of κ. Similarly to Figures 4.14 and 4.15 the behavior of the neutron density and reactivity are apparently the same in Figures 4.16 and 4.17, due that the effect of α can't be appreciated in long transients.

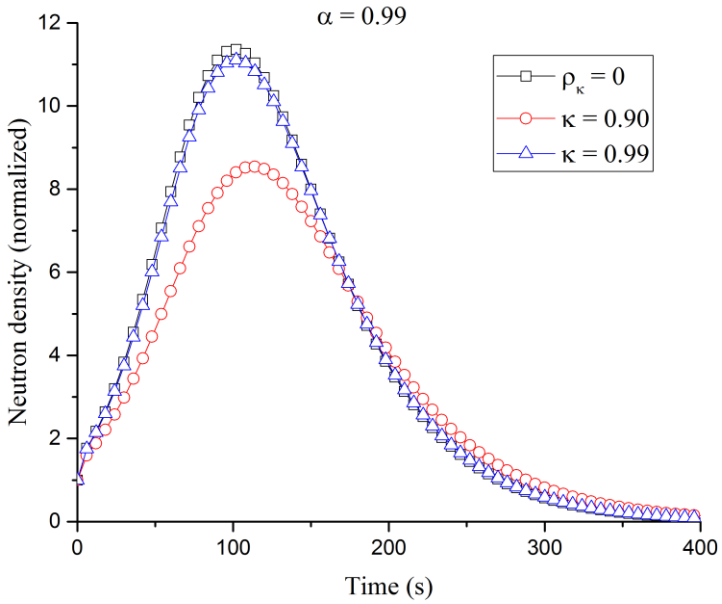

Figure 4.16. Normalized neutron density when $\alpha = 0.99$ for two values of the fractional diffusion exponent κ and without its effect.

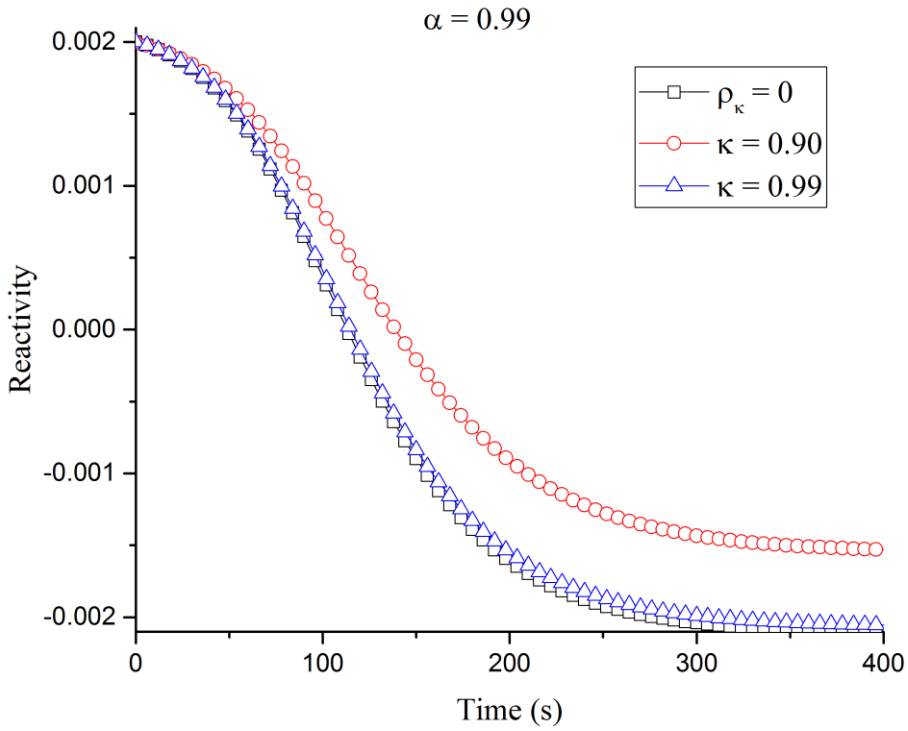

Figure 4.17. Reactivity when $\alpha = 0.99$ for two values of the fractional diffusion exponent κ and without its effect.

Figures 4.18 and 4.19 show the behavior of neutron density and reactivity, respectively for an initial reactivity of $\rho_{n0} = 0.002$, a fixed $\kappa = 0.90$ and different values of α. As stated before, the effect of α cannot be appreciated in long transients, thus simulations from a value of 0.50 up to 0.99 were performed in order to show its effect when its value moves away from 1. Figure 4.18 shows the effect of this, i.e., for very small values of α the neutron density increases more dramatically than for bigger. In Figure 4.19 its effect in the reactivity can be appreciated, i.e., for very small values of α the reactivity decreases more dramatically.

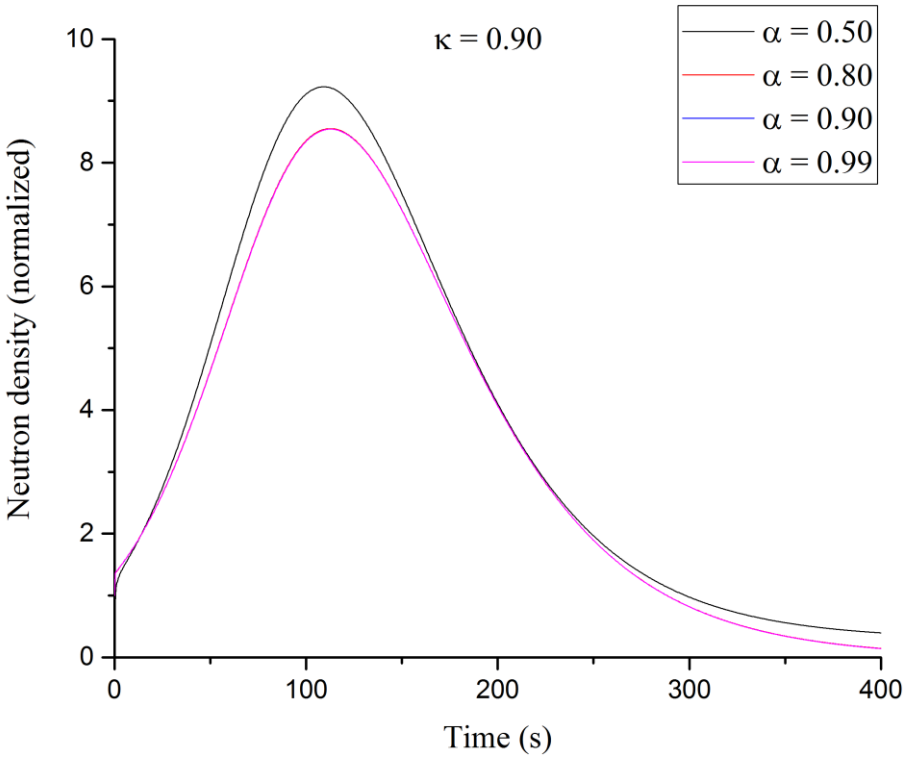

Figure 4.18. Normalized neutron density when $\kappa = 0.90$ for different values of α.

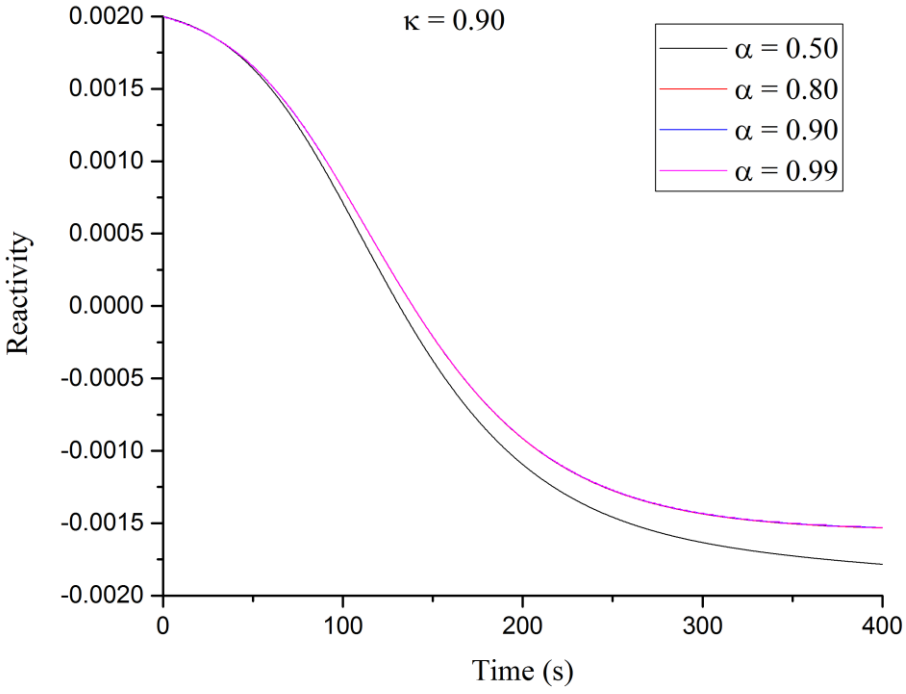

Figure 4.19. Reactivity when $\kappa = 0.90$ for different values of α.

Figures 4.20 and 4.21 show the behavior of neutron density and reactivity, respectively for an initial reactivity of $\rho_0 = 0.002$, a fixed $\kappa = 0.99$ and different values of α. As stated before, the effect of α cannot be appreciated in long transients, thus simulations from a value of 0.50 up to 0.99 were performed in order to show its effect when its value moves away from 1. Figure 4.20 shows the effect of this, i.e., for very small values of α the neutron density increases more dramatically than for bigger. In Figure 4.21 its effect in the reactivity can be appreciated, i.e., for very small values of α the reactivity decreases more dramatically.

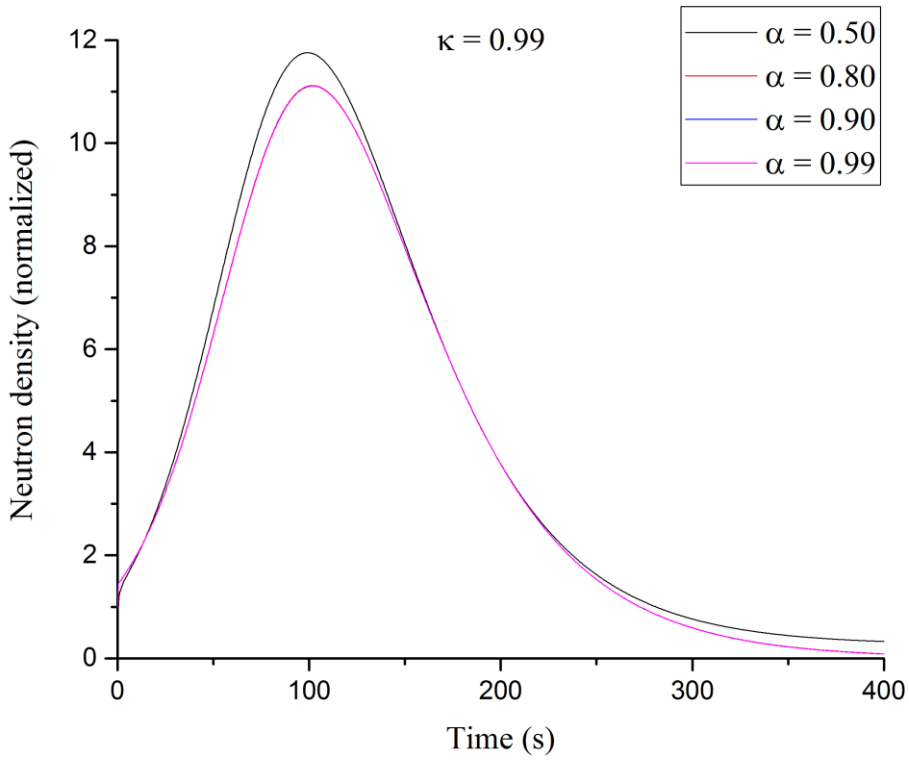

Figure 4.20. Normalized neutron density when $\kappa = 0.99$ for different values of α.

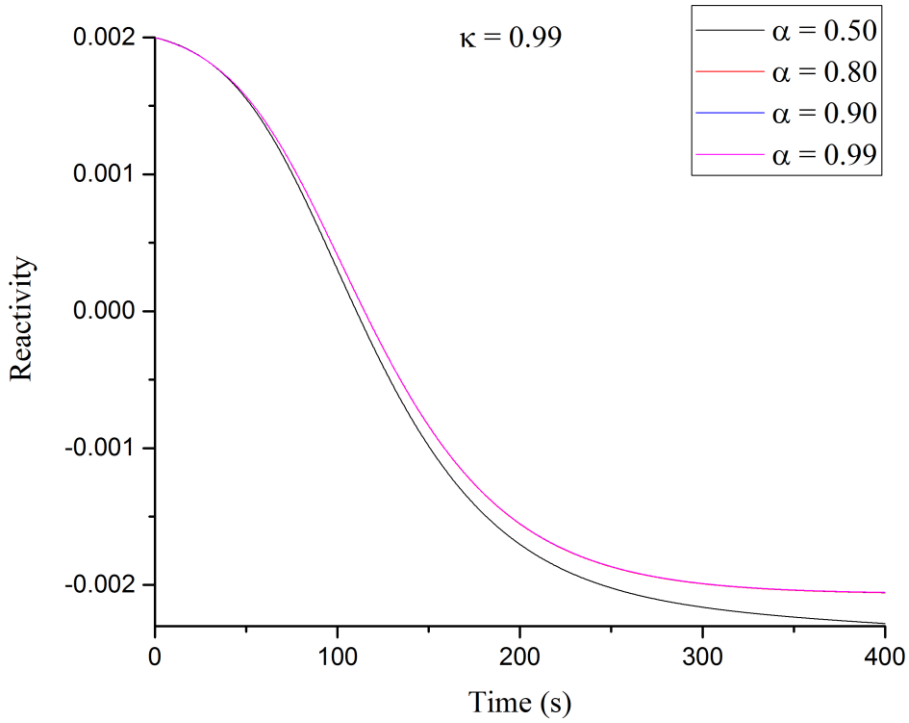

Figure 4.21. Reactivity when $\kappa = 0.99$ for different values of α.

Although the value of α should be close to 1, according to Espinosa-Paredes (2017), the experiments were performed using values as low as 0.50 in order to observe a perceivable difference. Yasser (2017) has also experimented with values of α as low as 0.2 in order to appreciate the effect of the anomalous diffusion exponent.

4.3.2. Cylindrical geometry without temperature feedback effects

For the present experiment, nuclear reactor parameters used are: $\Lambda = 2\times10^{-5}$ s, $\beta = 0.0065$, $v = 220{,}000$ cm/s, $D = 0.16$ cm, $\Sigma_a = 0.0197$ 1/cm, $\lambda = 0.0810958\ \text{s}^{-1}$, and $l = 0.00024$ s. Regarding the geometry used in the study, it corresponds to typical core dimensions of a BWR, a cylinder of 3.708 m in height and a diameter of 5.2 m.

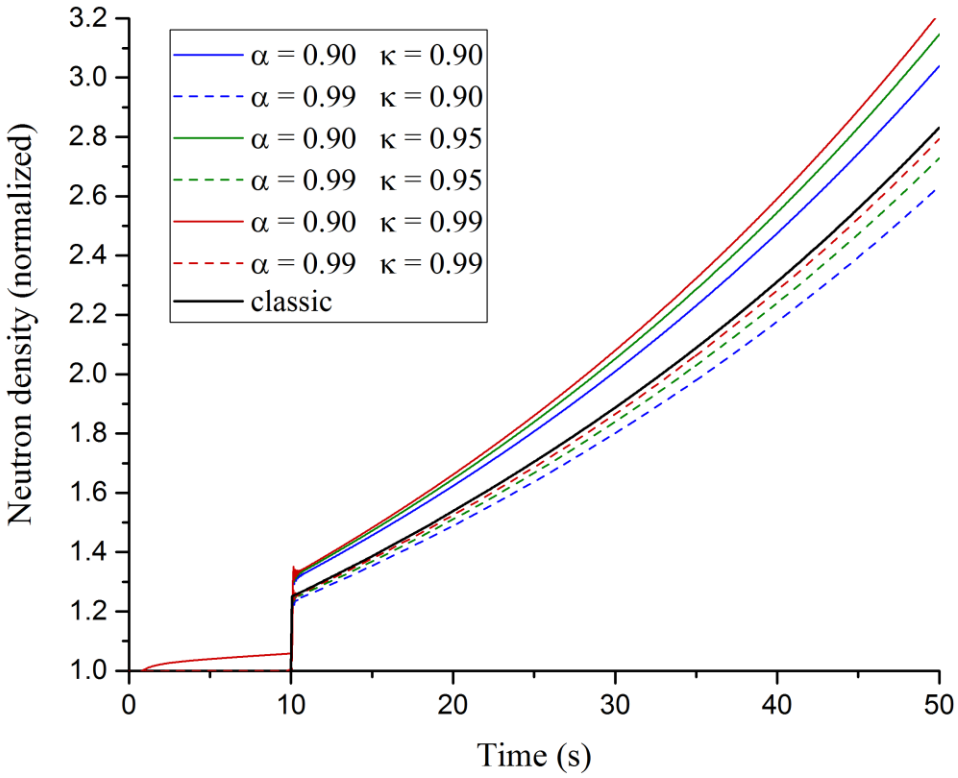

Figure 4.22. Numerical experiment without temperature feedback effects for three different values of $\kappa = 0.90, 0.95, 0.99$, two representative values of $\alpha = 0.90, 0.99$ and the classical neutron point kinetics model.

The first experiment without temperature feedback effects (Figure 4.22) considers a reactor in steady state and at $t = 10$ s, a reactivity insertion of $\rho_n = \beta/5$ is introduced. It can

be clearly observed that-the prompt jump corresponds of approximately 20-30% of nominal neutron density, which has a dependence on the value of the fractional diffusion exponent.

After numerous experiments these values of κ and α where selected due that its curves are just over and below the curve of the classic neutron point kinetics model, which was numerically solved, $\tau = 10^{-4}$ s for all cases. From this experiment, it can be observed that both terms compete with each other, for values of α closer to one (dashed lines), neutron density is lower; and for values of κ closer to one (red lines), neutron density is higher; for the case of κ, this behavior is due to neutron leakage. Table 4.4 presents the behavior of reactivity by neutron leakage ρ_κ, when $\kappa = 1$ implies that the reactivity by neutron leakage is null and corresponds to the classical approximation of the reactor point kinetics equations, additionally in Figure 4.24 the same behavior can be observed for different geometries, also it can be concluded that for bigger cores neutron leakage is less. However, as the space-anomalous diffusion coefficient decreases, i.e., neutron leakage increases. This has an important interpretation of the effect that *spatial memory* has with *spatial non-local* approximation throughout the term $(D_\gamma B_g^2 - D_{\kappa\gamma} B_g^{\kappa+1})$, i.e., for high spatial sub-diffusion (small values of κ) neutron leakage is greater (blue lines) due to two important effects, according to the order of magnitude analysis the relation among microscopic and macroscopic fractional lengths is greater with respect to the normal relation, which means that the spatial diffusion coefficient is bigger than the normal diffusion coefficient, therefore the mean free paths are greater according with κ decreasing with respect to normal diffusion (Figure. 4.23). In Table 4.5 the modified versions (for the plotting of Figure. 4.23) of the geometrical buckling are presented. For this case, the curve which fits the most to the classical model, corresponds to values of $\alpha = 0.99$ and $\kappa = 0.99$ (red dashed line).

TABLE 4.4. Behavior of neutron leakage (ρ_κ) with κ variation, for a cylindrical reactor with typical dimensions of a BWR.

κ	ρ_κ
0	-1.24E-02
0.05	-9.74E-03
0.1	-7.67E-03
0.15	-6.03E-03
0.2	-4.74E-03
0.25	-3.72E-03
0.3	-2.91E-03
0.35	-2.28E-03
0.4	-1.77E-03
0.45	-1.38E-03
0.5	-1.06E-03
0.55	-8.17E-04
0.6	-6.22E-04
0.65	-4.68E-04
0.7	-3.46E-04
0.75	-2.50E-04
0.8	-1.74E-04
0.85	-1.14E-04
0.9	-6.69E-05
0.95	-2.95E-05
1	0.00E+00

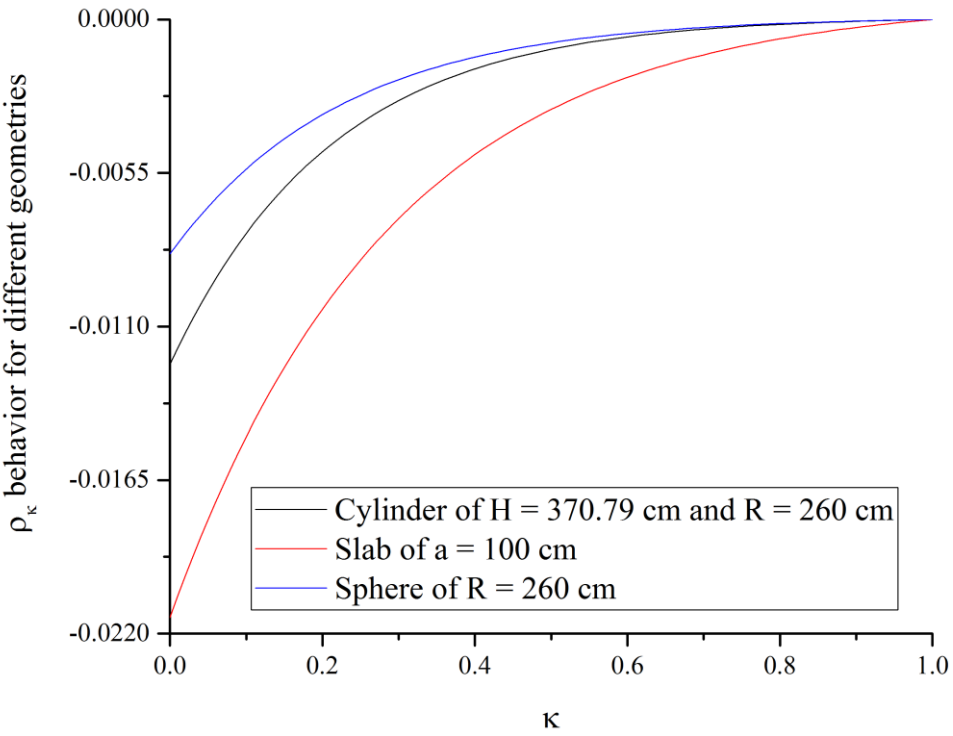

Figure 4.23. Neutron leakage (ρ_κ) behavior for different geometries.

TABLE 4.5. Fractional geometrical Buckling modified from Duderstadt and Hamilton (1976).

Geometry	Dimensions	Fractional geometrical Buckling
Cylinder	Radius R, Height H	$\left(\frac{2.405}{R}\right)^{\kappa+1}+\left(\frac{\pi}{H}\right)^{\kappa+1}$
Slab	Thickness a	$\left(\frac{\pi}{a}\right)^{\kappa+1}$
Sphere	Radius R	$\left(\frac{\pi}{R}\right)^{\kappa+1}$

4.3.3. Cylindrical geometry with temperature feedback effects

For the present experiment, nuclear reactor parameters used are: $\Lambda = 2\times10^{-5}$ s, $\beta = 0.0065$, $v = 220{,}000$ cm/s, $D = 0.16$ cm, $\Sigma_a = 0.0197$ 1/cm, $\lambda = 0.0810958\ \text{s}^{-1}$, and $l = 0.00024$ s. Regarding the geometry used in the study, it corresponds to typical core dimensions of a BWR, a cylinder of 3.708 m in height and a diameter of 5.2 m.

This experiment (Figure. 4.24) considers a reactor in steady state and at $t = i+1$ a reactivity insertion of $\rho_n = \beta/5$ is introduced, it can be observed, the prompt jump which corresponds of about 20%-30% of nominal neutron density for all cases, except for $\alpha = 0.70$ and lower values (not shown) which is only of approximately 10% of nominal neutron density.

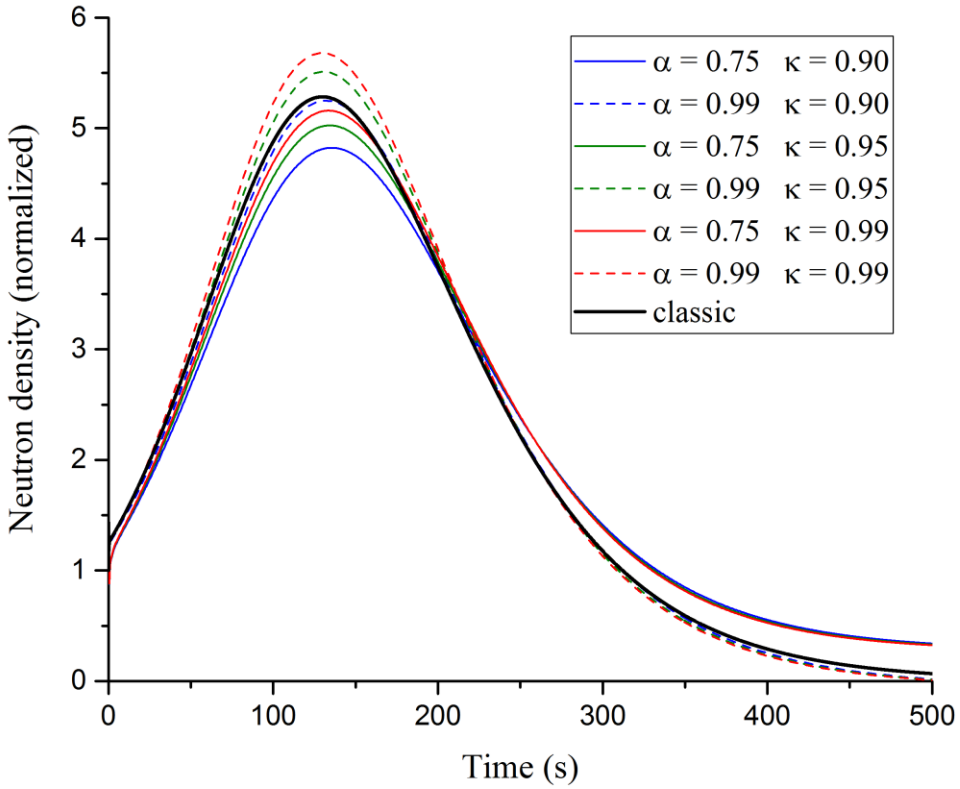

Figure 4.24. Numerical experiment with temperature feedback effects for three different values of $\kappa = 0.90, 0.95, 0.99$, two representative values of $\alpha = 0.90, 0.99$, and the classical neutron point kinetics model.

After numerous experiments these values of κ and α where selected due that its curves are just over and below the curve of the classical neutron point kinetics model, which was numerically solved, the value of $\alpha = 0.90$ is not shown due that in this scale it appears as overlapping the curve of $\alpha = 0.99$, therefore $a = 0.75$ was selected in order to show the effect of α in this experiment, additionally the curves of values between 0.75 and 0.90 were also to close to the curve corresponding to $\alpha = 0.99$, $\tau = 10^{-4}$ s for all cases. Contrary to what Schramm et al. (2016) concluded, *fractional derivative parameter effects on the neutron density are completely suppressed*, for values of $\alpha = 0.9$, $\alpha = 1.0$ and $\alpha = 1.1$ (the last value being superdifussion), we did found that temperature feedback effects are important for long (> 50s) and more important for very long times (> 100s) ; however for short (< 10s) and very short times (< 1s) they are unnoticed and a more detailed analysis is required e.g. as in transient analysis. As previously observed from previous numerical experiments and Neutron leakage (ρ_κ) behavior, for lower values of κ (blue lines), as expected, yields lower neutron density; this experiment shows that both fractional diffusion exponents α and κ are important for long (> 50s) and very long time (> 100s) transients. For this case, the curve which fits the most to the classical model, corresponds to values of $\alpha = 0.99$ and $\kappa = 0.90$ (blue dashed line).

4.3.4. Cylindrical geometry reactivity insertion pulse type experiment

For the last numerical experiment, nuclear parameters of a typical TRIGA MARK II reactor were used (Table 4.6), and a pulse type experiment was simulated with a reactivity

insertion of 2.33 dollars (Figure. 4.24), the transient occurs in 30 ms, reaching a power peak of 2250 MW with a reactor period T = 2 ms (IAEA, 2005).

TABLE 4.6. Nuclear parameters used for the pulse type experiment.

Nuclear parameter	Value
Λ	2×10^{-5} s
λ	0.0810958 s^{-1}
β	0.007
l	43×10^{-6} s

Due that the present scenario is of extremely short time duration, we used several relaxation times in order to counter for infinite velocity propagation ($\tau = 10^{-5}$ s, 10^{-6} s), this can be clearly observed (Figure 4.24), at the beginning of the transient (first 5 ms), where the blue and green lines scenarios ($\tau = 10^{-3}$ s and $\tau = 10^{-4}$ s respectively) raise evidently before the red and magenta lines scenarios ($\tau = 10^{-5}$ s and 10^{-6} s respectively). It is hard to evidence the effect of α and κ, observed from previous experiments, due that different values of α and κ (Table 4.7) were used in order to predict with little error ($<1\%$ for $\tau = 10^{-4}$ s, 10^{-5} s and 10^{-6} s) the power peak (black star). The scenario which corresponds to the black line corresponds to the classic model and presents the highest error when the transient reaches the power peak, in Table 4.7 a comparison of the power peak value of the simulated experiments against real value is presented along with its relative error.

TABLE 4.7. Values and relative error (%) of the power peak of the simulated experiments against real value.

Model	**Classical**	$\alpha = 0.947$ $\kappa = 0.900$ $\tau = 10^{-3}$	$\alpha = 0.719$ $\kappa = 0.840$ $\tau = 10^{-4}$	$\alpha = 0.839$ $\kappa = 0.990$ $\tau = 10^{-5}$	$\alpha = 0.713$ $\kappa = 0.999$ $\tau = 10^{-6}$
Power Peak	1,802.50	2,274.82	2,253.10	2252.02	2,252.87
Rel. error %	19.88	1.10	0.14	0.09	0.13

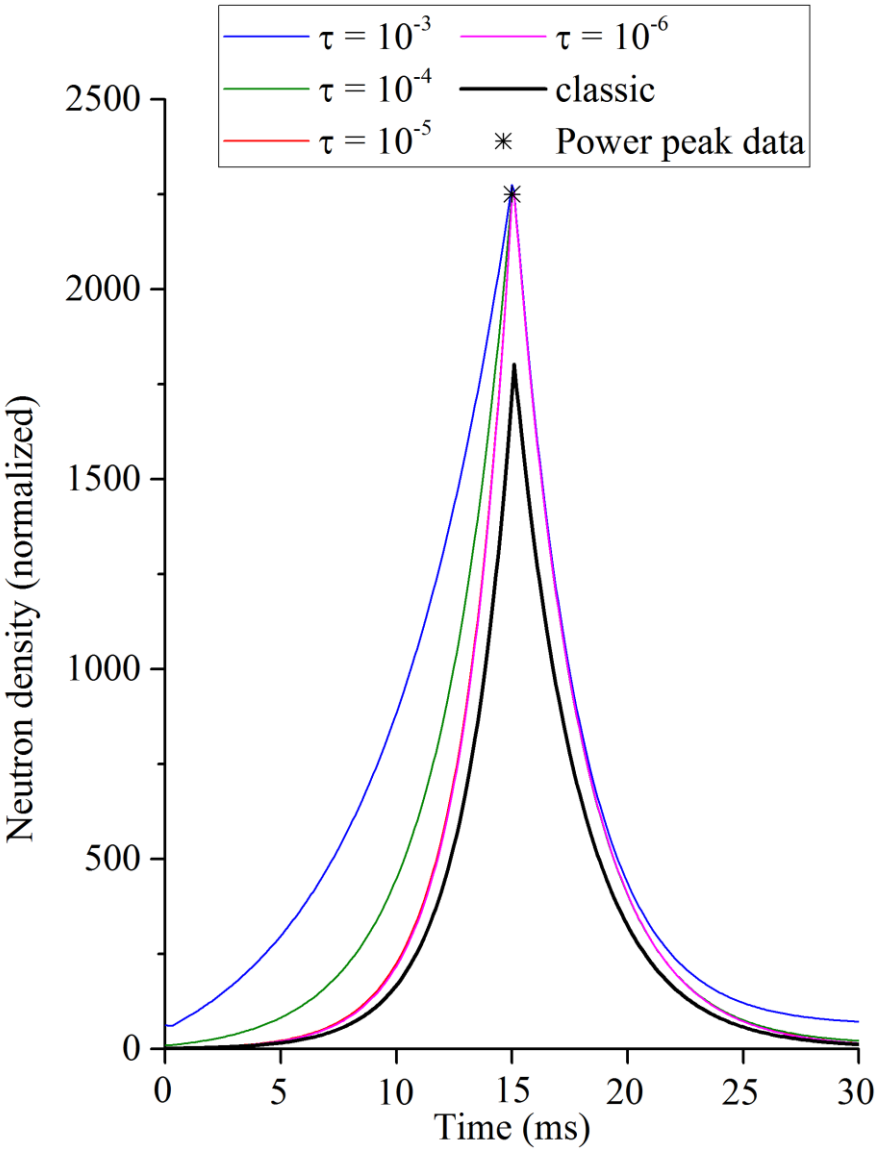

Figure 4.25. Pulse type numerical experiment for different values of τ and the classic neutron point kinetics model.

As stated before, the fractional diffusion exponent κ is related to neutron leakage, this can be explained by the fact that, as expected, “classical” diffusion violates physical principles by propagating the signal farther than the points which can be reached at the given finite speed. The consequence of this physical violation has been addressed before, Dulla et al. (2006) states that for transport, P_1 and P_3, no neutron leakage is experienced and for pulse situations the infinite velocity propagation causes a high rate flux reduction due to leakage. The latter can be observed in Figures. 4.25 even when the present model considers anomalous diffusion, i.e., a relaxation time (τ).

5. Thermal-hydraulic Coupling with neutronic fractional for SCWR

The Super Critical Water is a very high-pressure water-cooled reactor which will operate at conditions above the thermodynamic critical point. Water enters the reactor core and then exits without change of phase, i.e., no water or steam separation is necessary. There is an expected increase of thermal efficiency of current nuclear power plants from 30% – 35% to approximately 45 – 50% for Generation IV reactors (Thind, 2012; Schulenberg & Starflinger, 2012).

Figure 5.1 shows the difference in the operating conditions of current generation reactor systems in comparison to SCWRs. Compared to existing Pressurized Water Reactors (PWRs), in SCWRs the target is to increase the coolant pressure from 10 MPa– 16 MPa to about 25 MPa; the inlet temperature to about 350ºC, and the outlet temperature to about 625ºC (Pioro & Duffey, 2007).

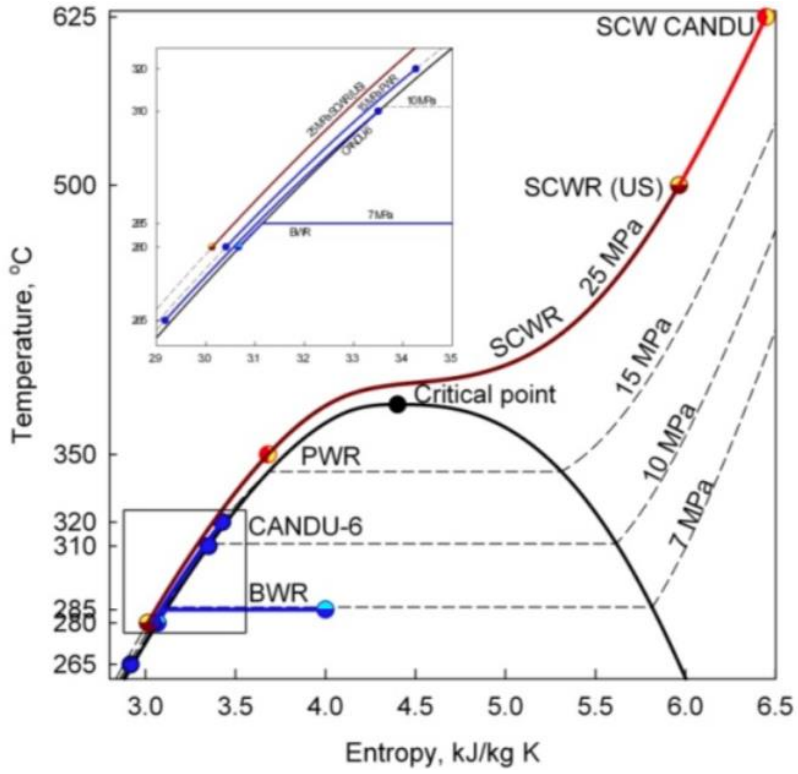

Figure 5.1. Operating conditions of current nuclear reactors and SCWRs (Pioro & Duffey, 2007).

In this work we present a numerical analysis of the effect of different heat transfer correlations on the prediction of the fuel temperature and wall cladding in a SCWR reactor which includes a Time-Space Fractional Neutron Point Kinetics (TSFNPK) (Espinosa-Martínez et al., 2018, 2020) model as a novelty, which considers a non-Fickian law for the neutron density current where the differential operators in space and time are of fractional order.

Since decades, the neutron diffusion concept is a tool commonly used to understand the complex behavior of the neutrons average motion. Most reactor studies treat the neutron motion as a diffusion process, where it is assumed that neutrons in averaged motion tend to diffuse from regions of high neutron density to low neutron density. The treatment of neutron

transport as a diffusion process has only limited validation due that neutrons tend to stream at relatively large distances between interactions.

Over the last decade fractional neutron point kinetics (FNPK) models have been developed which generalizes the classical neutron point kinetics (CNPK) model, going from integer derivatives to non-integer derivatives. These newly derived models are a useful tool to provide important information on the reactor dynamics.

In a seminal work of Espinosa-Paredes et al. (2008) a fractional wave equation for the average neutron motion in nuclear reactor was derived, which covers the full spectrum of the average neutron transport behavior, i.e., Fickian and non-Fickian effects. The fractional diffusion model retains the main dynamic characteristics of the neutron motion in which the relaxation time associated with a rapid variation in the neutron flux contains a fractional order exponent which is known as anomalous diffusion exponent. According with these authors the anomalous diffusion exponent can be manipulated to obtain the best representation of the neutron transport phenomena.

The neutronic process with temperature feedback effects, the heat transfer in the fuel rod and the thermal-hydraulics in the core were simulated. Special attention was given to the thermal hydraulics, which uses a three-pass core design with multiple heat-up steps, where each step was simulated using an average channel. The first pass called “evaporator” is located in the center of the core. In this region, the moderator water flows downward in gaps between assembly boxes and inside the moderator tubes. The moderator water, heated-up through its path downward to the lower plenum, is mixed with the coolant coming from the downcomer reaching an inlet temperature of around 583K. The evaporator heats the coolant up to 663K, flowing upward and around the fuel rods, resulting in an outlet temperature 5K higher than the pseudo-critical temperature of 557.7K at a pressure of 25MPa. The second

pass, called “superheater”, with downward flow, heats the coolant up to 706K. After a second mixing in an outer mixing plenum below the core, the coolant will finally be heated up to 803K with an upward flow in a second superheater (the third pass) located at the core periphery. A transient one-dimensional radial conduction model was applied in the fuel rod for each cell in the axial coordinate. Energy balances for the coolant have been implemented using a steady state and a one-dimensional model for the axial coordinate. Fuel lattice neutronic calculations were performed with the HELIOS-2 code and the reactivity coefficients were used to evaluate the reactivity effects due to changes in the fuel temperature and in the supercritical water density for 177 energy groups. Due to the strong variation of coolant density through the core, five densities were considered. This safety parameter is calculated in order to evaluate the variation of the reactivity due to the Doppler Effect, as a function of the fuel temperature, which is related to the resonances broadening when the fuel temperature increases. The coupling of neutronics with the heat transfer in the fuel rod, and the thermal hydraulics is presented, and numerical experiments due to changes in the mass flow rate were accomplished in this study. Effects on fuel temperature predictions with improved heat transfer correlations and classical heat transfer correlations were also compared.

5.2 Supercritical Fluids

The behavior of liquid and gas density with pressure and temperature is illustrated in Figure. 5.2. When the pressure and temperatures are low, there is a significant density difference between the liquid and the gas states. Near the critical point, the density difference

between the liquid and gas is small, and above the critical point, the densities of the liquid and the gas have become equal.

The heat transfer process, at critical and supercritical pressures, is influenced by the significant changes in thermophysical properties, as is observed in Figure. 5.3 for specific heat, thermal conductivity, and density obtained from thermal properties taken from Wagner & Kretzchmar (2008). The most significant thermophysical property variations occur near the critical and pseudocritical points. For example, the specific heat of water has a maximum value at the critical point. The exact temperature that corresponds to the specific heat peak at pressures above the critical pressure is known as the pseudocritical temperature (Pioro et al., 2004).

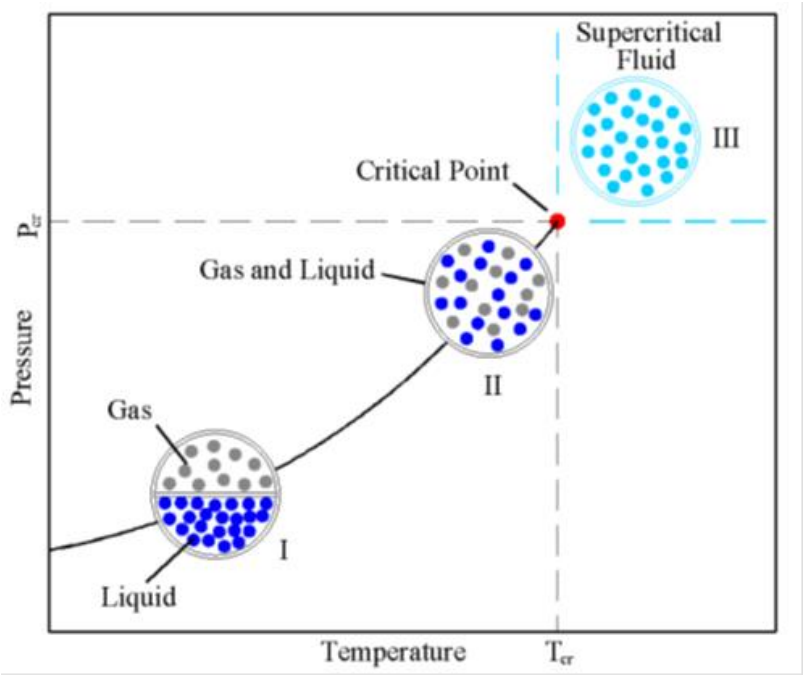

Figure 5.2. Schematic behavior of liquid and gas density with pressure and temperature (Thind, 2012).

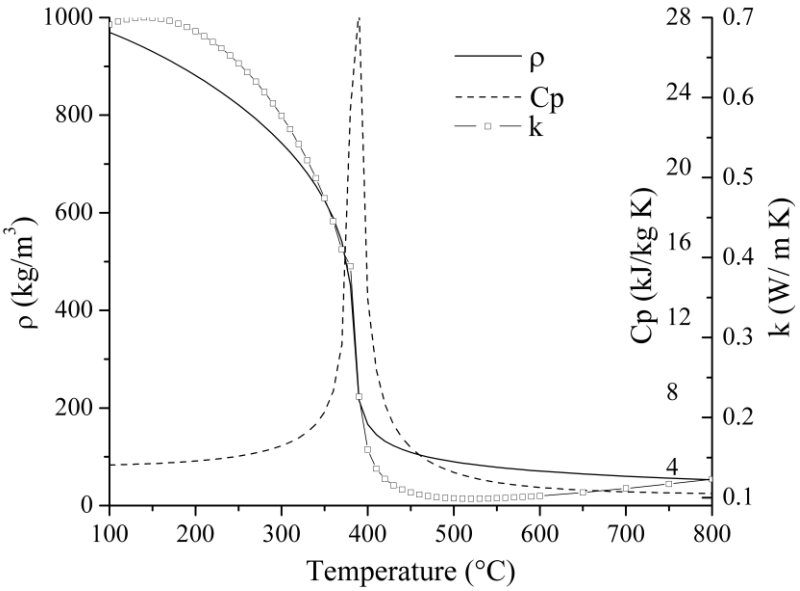

Figure 5.3. Behavior of the specific heat capacity (*Cp*), thermal conductivity (*k*) and density (ρ), as a function of temperature at 25 MPa.

5.3 Implementation

In order to analyze the effect of different heat transfer correlations on the prediction of the wall temperature of the fuel rods, the SCWR numerical code developed by Barragán-Martínez (2013) was applied using the HTCs shown in Table 5.1. The numerical model of the heat transfer processes in the fuel element of the HPLWR was obtained using the numerical model of typical reactors (Espinosa-Paredes & Espinosa-Martínez, 2009). The supercritical water reactor is integrated of cylindrical fuel elements which contain ceramic pellets inside the cladding.

Then, the effect of heat transfer correlations on the fuel temperature prediction of SCWRs was conducted with numerical experiments.

Table 5.1. Supercritical Water Heat-Transfer Correlations (HTCs)

Correlation	Reference
$Nu_b = 0.023\,Re_b^{0.8}\,Pr_b^{0.4}$	Dittus & Boelter (1930)
$Nu_b = 0.0243\,Re_b^{0.8}\,Pr_b^{0.4}$	McAdams (1942)
$Nu_b = 0.0069\,Re_b^{0.9}\langle Pr_b\rangle^{0.66}\left(\frac{r_w}{r_b}\right)^{0.43}\left(1+2.4\frac{D}{x}\right)$	* Bishop et al., (1964)
$Nu_b = 0.0069\,Re_b^{0.9}\langle Pr_b\rangle^{0.66}\left(\frac{\rho_w}{\rho_b}\right)^{0.43}$	Bishop et al., (1964)
$Nu_w = 0.00459\,Re_w^{0.923}\langle Pr_w\rangle^{0.613}\left(\frac{\rho_w}{\rho_b}\right)^{0.231}$	Swenson et al., (1965)
$Nu_b = 0.0053\,Re_b^{0.914}\langle Pr_b\rangle^{0.654}\left(\frac{\rho_w}{\rho_b}\right)^{0.518}$	Mokry et al., (2009a) preliminar
$Nu_b = 0.0061\,Re_b^{0.904}\langle Pr_b\rangle^{0.684}\left(\frac{\rho_w}{\rho_b}\right)^{0.564}$	Mokry et al., (2009a) final

*with Entrance-Region Effect (ERE) and a fit of ±15%; $\langle Pr\rangle$ is the average; *b* and *w* means bulk-fluid and *w*all temperature, respectively.

5.3.1 Fuel Heat Transfer Model

A detailed multi-node fuel pin model was developed for this study. The fuel heat transfer formulation is based on the following fundamental assumptions: (i) Axis-symmetric radial heat transfer, ii) the heat conduction in the axial direction is negligible, iii) the volumetric heat rate generation in the fuel is uniform in each radial node, and iv) storage of heat in the fuel cladding and gap is negligible. Under these assumptions, the transient temperature distribution in the fuel pin, and the initial and boundary conditions are given in the following conditions,

$$(\rho_m Cp)\frac{\partial T}{\partial t} = k\frac{1}{r}\frac{\partial}{\partial r}\left(r\frac{\partial T}{\partial r}\right) + q'''(t) \qquad \text{at} \qquad r_0 \le r \le r_{cl} \qquad (5.1)$$

$$\text{I.C.} \qquad T(r,0) = T(r) \qquad \text{at} \qquad t = 0 \qquad (5.2)$$

B.C.1. $$-k\frac{\partial T}{\partial r} = H_\infty \left(T - T_m\right) \qquad \text{at} \qquad r = r_{cl} \tag{5.3}$$

B.C.2. $$\frac{\partial T}{\partial r} = H_\infty \left(T - T_m\right) \qquad \text{at} \qquad r = r_0 \tag{5.4}$$

In Eq. (5.1) $q'''(t) = 0$, for $r_f \le r_{cl}$. In these equations, r is the cylindrical radial coordinate, r_0, r_f and r_{cl} are the centroid, fuel and clad radius, respectively, $q'''(t) = P(t)/V_f$ at each axial node, where P is the neutronic power, V_f is the fuel volume, T_w is the wall temperature, T_m is the moderator temperature, and H_∞ is the convective heat transfer coefficient.

The differential equations described previously are transformed into discrete equations using the control volume formulation technique in an implicit form (Patankar, 1980). The control volume formulation enables the equations for fuel, gap, and cladding to be written as a single set of algebraic equations for the sweep in the radial direction,

$$a_j T_j^{t+\Delta t} = b_j T_{j+1}^{t+\Delta t} + c_j T_{j-1}^{t+\Delta t} + d_j \tag{5.5}$$

where $T_{j-1}^{t+\Delta t}$, $T_j^{t+\Delta t}$ and $T_{j+1}^{t+\Delta t}$ are unknowns, a_j, b_j and c_j are coefficients, which are computed at the time t. When these equations are put into a matrix form, the coefficient matrix is tridiagonal. The solution procedure for the tridiagonal system is the Thomas algorithm, which is the most efficient algorithm for this type of matrices. The coefficients a_j, b_j and c_j are dependent on thermophysical properties, i.e., thermal conductivity, density and specific heat; and since they are function of $T_j^{t+\Delta t}$, at least one iteration is needed.

5.3.2 Thermal-hydraulic Model

The basic equations for describing the thermal hydraulic behavior in the three representative heated channels (one channel for each pass core) assuming the supercritical fluid is a single phase fluid, are presented as following. Incompressible flow was also considered in this study, i.e., the mass flux (G) is a constant. Under this consideration, the energy equation at steady state is shown as follows,

$$GCp\frac{dT_b}{dz}=\frac{q"P_H}{A_f}+\frac{G}{\rho_b}\left(\frac{dp}{dz}+\frac{fG}{D_H\rho_b}\right) \tag{5.6}$$

where T_b is the bulk temperature, f is the friction factor, P_H is the heated perimeter, and A_f is the flow area. The heat transfer from the wall to the coolant is obtained with Newton's law of cooling,

$$q"=H_\infty\left(T_w-T_b\right) \tag{5.7}$$

The temperature in each node of the channel is obtained numerically as,

$$T_{b+1}=T_{b_i}+\left(\frac{dT}{dz}\right)_i\Delta z \tag{5.8}$$

where Δz is the node length and i is the node number.

5.3.3 Reactor Power Model

The reactor power is given by,

$$P\left(t,z\right)=n\left(t\right)F\left(z\right)P_0 \tag{5.9}$$

where $F(z)$ is the axial power factor, P_0 is nominal power and $n(t)$ is the normalized neutron flux, which is calculated by using a point reactor kinetics model with six groups of delayed neutrons,

$$\tau^{\alpha}\frac{d^{\alpha+1}n(t)}{dt^{\alpha+1}}+\tau^{\alpha}\Sigma_{a\gamma}\upsilon\frac{d^{\alpha}n(t)}{dt^{\alpha}}+\frac{dn(t)}{dt} = \left[\frac{(\rho_n-\beta)+\rho_{\kappa}}{\Lambda}\right]n(t)+\sum_{i=1}^{6}\lambda_i C_i(t)+\tau^{\alpha}\frac{d^{\alpha}S_{\gamma}(t)}{dt^{\alpha}} \tag{5.10}$$

$$\rho_{\kappa}=\Lambda\upsilon\left(D_{\gamma}B_g^2-D_{\kappa\gamma}B_g^{\kappa+1}\right) \tag{5.11}$$

$$\frac{dC_i(t)}{dt}=\frac{\beta}{\Lambda}n(t)-\lambda C_i(t) \tag{5.12}$$

$$\frac{dS(t)}{dt}=\frac{1-\beta}{\Lambda}\frac{dn(t)}{dt}+\lambda\frac{dC_i(t)}{dt} \tag{5.13}$$

where C_i is a delayed neutron concentration of the $i-th$ precursor group normalized with the steady-state neutron density, ρ_n is the net reactivity, β is the neutron delay fraction, Λ is the neutron generation time and β_i is the portion of neutrons generated by the $i-th$ group. The initial conditions are given by $n(0)=n_0$ and $C_i(0)=\beta_i n_0/\Lambda\lambda_i$ According with definition given by Eq, (5.11), the reactivity is associated to neutron leakage in the system, i.e. $\rho_{\kappa}<0$. The term $D_{\kappa\gamma}B_g^{\kappa+1}$ was proposed and analyzed by Espinosa-Paredes (2017). The parameters of the kinetics model are presented in Table 5.2.

Table 5.2. Point Reactor Kinetics Model Parameters (Espinosa-Paredes, 2017)

Group	β_i	$\lambda_i (s^{-1})$
1	2.470 × 10-4	0.0127
2	1.355 × 10-3	0.0317
3	1.222 × 10-3	0.1150
4	2.646 × 10-3	0.3110
5	8.320 × 10-4	1.4000
6	1.690 × 10-4	3.8700
	$\beta = 6.5 \times 10^{-3}$	$\Lambda = 4.0 \times 10^{-5} s$

The net reactivity in this work includes three main components: Doppler effects due to fuel temperature, coolant density, and reactor control rods. The reactivity coefficient due to variations in fuel temperature was considered for the fuel assembly design which was proposed by Bishop et al. (1964). Calculations were performed for this fuel assembly along the active core height. And because of the strong variation of coolant density in the axial direction of the core, five densities: 0.74, 0.45, 0.31, 0.17 and 0.09 g/cm3 had to be considered. In order to evaluate the variation of the reactivity due to the Doppler Effect, as a function of the fuel temperature, this safety parameter is calculated, which is related to the resonances broadening when the temperature increases. The values of the reactivity as a function of the coolant density and fuel temperature are presented in Figure. 5.4. The values of the infinite multiplication factor obtained with HELIOS-2 for 177 energy groups were used to determine the reactivity.

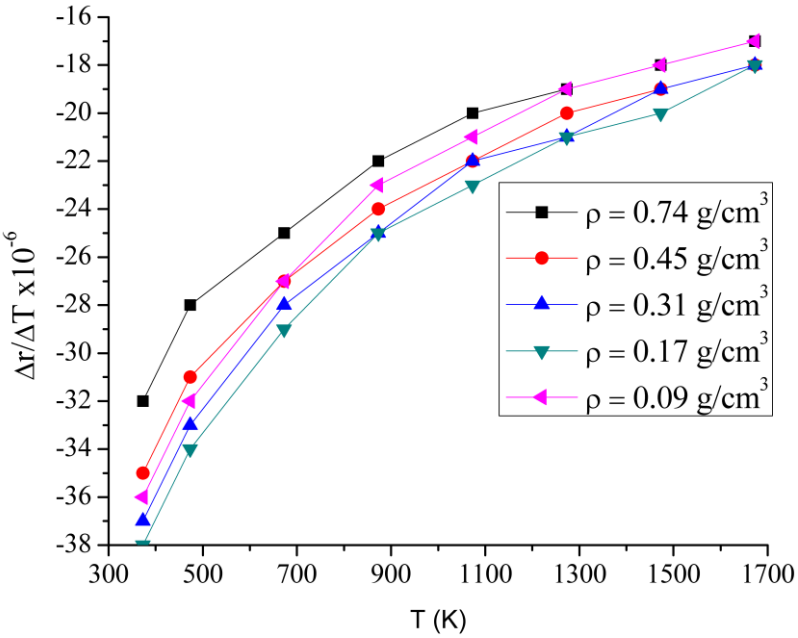

Figure 5.4. Reactivity coefficients obtained with HELIOS-2 for 177 energy groups at different densities.

5.3 Numerical Solution

The fractional neutron point kinetics equations with temperature feedback effects, considering one group of delayed neutron precursors for this analysis is given by a set of ordinary differential and algebraic Eqs, (5.10)-(5.13). The initial conditions at $t = 0$ are,

$$\begin{aligned} n &= n_0 \\ C &= C_0 = \frac{\beta}{\Lambda\lambda} n_0 \\ S &= S_0 = \frac{n_0}{\Lambda} \end{aligned} \tag{5.14}$$

Following the procedure of Edwards et al. (2002) we re-write Eqs. (5.1), (5.3), (5.4) and (5.7),

$$D^{\alpha+1}n + a_3 Dn + a_2 D^{\alpha} n + a_1 n = b_1 C + D^{\alpha} S \tag{5.15}$$

$$DC + b_2 C = a_0 n \tag{5.16}$$

$$DS = a_4 Dn + b_{2DC} \tag{5.17}$$

where D is the derivate with respect to time. The coefficients of these equations are presented in Table 5.3.

Table 5.3. Coefficients of Eqs. (5.15)-(5.17)

Coefficient	Value
a_0	$\frac{\beta}{\Lambda}$
a_1	$-\frac{\rho-\beta+\rho_K}{\tau^\alpha \Lambda}$
a_2	$\Sigma_a \upsilon$
a_3	$\frac{1}{\tau^\alpha}$
a_4	$\frac{1-\beta}{\Lambda}$
b_1	$\frac{\lambda}{\tau^\alpha}$
b_2	λ

Applying the following change of variables, $x_1 = n$, $x_2 = D^\alpha x_1$, $x_3 = Dx_1$, $x_4 = D^\alpha x_3$, $y_1 = C$, $y_2 = Dy_1$, $z_1 = S$, $z_2 = D^\alpha z_1$, $z_3 = Dz_1$, $r_1 = \rho$, $r_2 = Dr_1$, the discrete form of the solution of the system of equations can be presented in matrix form,

$$\mathbf{Ax} = \mathbf{b} \tag{5.18}$$

where

$$\mathbf{x} = \left(x_{1,i}, x_{2,i}, x_{3,i}, y_{1,i}, z_{1,i}, z_{2,i}, r_{1,i}\right)^T \tag{5.19}$$

$$\mathbf{b} = \left(u_{1,i}, u_{2,i}, u_{3,i}, v_{1,i}, w_{1,i}, w_{2,i}, p_{1,i}\right) \tag{5.20}$$

$$\mathbf{A}=\begin{pmatrix} -{}^{\alpha}\omega_{0,i} & {}^{\alpha}\gamma_i & 0 & 0 & 0 & 0 & 0 \\ 1 & 0 & -h/2 & 0 & 0 & 0 & 0 \\ -{}^{\alpha}\gamma_i a_{1,i} & -{}^{\alpha}\gamma_i a_2 & -\left({}^{\alpha}\gamma_i a_3+{}^{\alpha}\omega_{0,i}\right) & {}^{\alpha}\gamma_i b_1 & 0 & {}^{\alpha}\gamma_i & 0 \\ -a_0 h/2 & 0 & 0 & \left(1+b_2 h/2\right) & 0 & 0 & 0 \\ 0 & 0 & 0 & 0 & -{}^{\alpha}\omega_{0,i} & {}^{\alpha}\gamma_i & 0 \\ -a_0 b_2 h/2 & 0 & -a_4 h/2 & b_2^2 h/2 & 1 & 0 & 0 \\ r_c K_c h/2 & 0 & 0 & 0 & 0 & 0 & 1 \end{pmatrix} \tag{5.21}$$

5.3.1 Representative SCWR Nodalization

The fuel rod temperature distribution was obtained for the radial nodes at each of the twenty one thermohydraulic axial nodes in the core. The arrangement of the computational nodes of the thermohydraulics model is illustrated in Figure. 5.5.

Figure. 5.6 shows the grid used in calculations. Half control volume near the boundary, radial nodes 1, 2, 3, 4, and 5 for the fuel; radial node 6 was used for the gap; radial nodes 7 and 8 for the clad. Radial nodes 1 and 8 were used for the boundary condition.

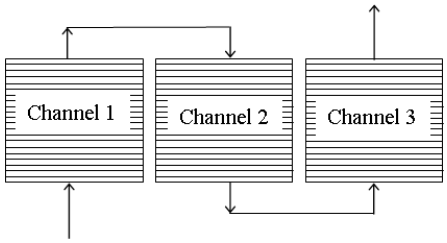

Figure 5.5. Arrangement of the computational nodes in the thermohydraulics core model of the SCWR.

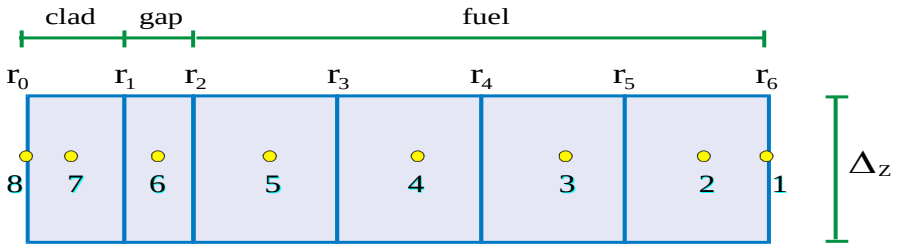

Figure 5.6. Arrangement of the computational cells of fuel, gap, and clad.

5.4 Numerical Experiments

Each channel in the core was based on a hydraulic unit cell whose parameters are: $P_H = 0.025$ m, $D_H = 0.054$ m, and $A_f = 0.34$ m^2. The parameters of the fuel element are: $r_f = 5.207\text{x}10^{-3}$m for the fuel, $r_g = 5.321\text{x}10^{-3}$m for the gap, and $r_{cl} = 6.134\text{x}10^{-3}$m for the clad. The active height of the fuel cell (4.2 m) was divided into 21 equidistant axial nodes ($\Delta z = 0.2$ m). The axial distribution of power for each channel was imposed with the idea that the heat flux is not uniform. The thermal physical properties used were taken from Wagner & Kretzschmar (2008). 73, 48 and 35 assembly clusters for Channel 1, Channel 2 and Channel 3, respectively, were used in the simulation, in order to reach a better power distribution within the core.

Fig. 5.7 presents the results for Channel 1, showing the Wall Temperature behavior for different correlations presented in Table 5.1. It should be noted that the last node temperature (at 4 m) is practically the same, and the trend is very similar for all the correlations, except for a short zone where the Swenson correlation yields a lower temperature while Mokry's correlation and TSFNPK (yield a higher temperature, the same was noted for the Bishop's correlations (with and without ERE).

In Fig. 5.8 the results for Channel 2 are presented, showing the wall temperature behavior for the correlations in Table I. Similar results were obtained, however contrary to what was observed in Channel 1, the Swenson's correlation yields slightly higher temperatures along the entire channel meanwhile the Bishop's (with and without ERE), Mokrys correlation and TSFNPK yield slightly lower temperatures along the entire channel.

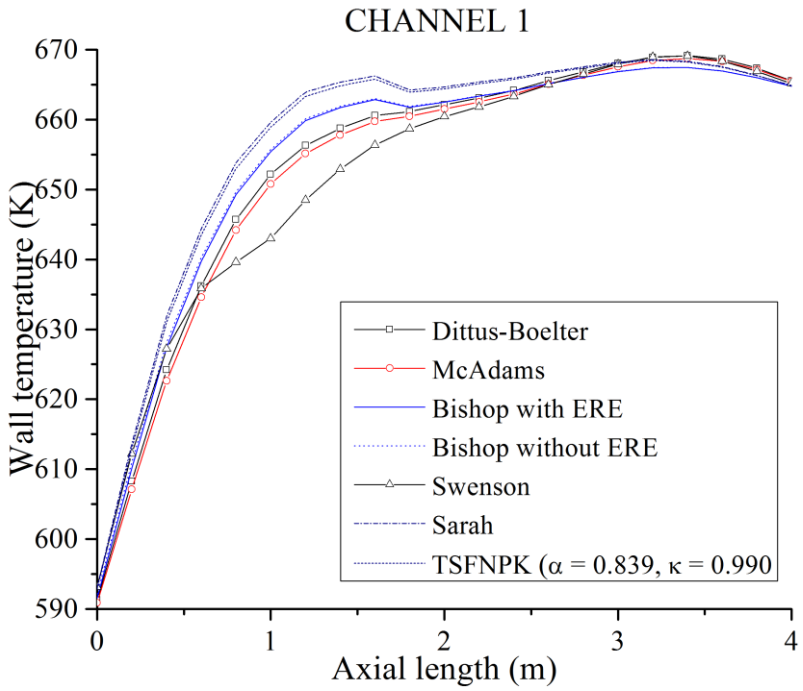

Figure 5.7. Simulation results for Channel 1 showing the wall temperature behavior for different HTCs.

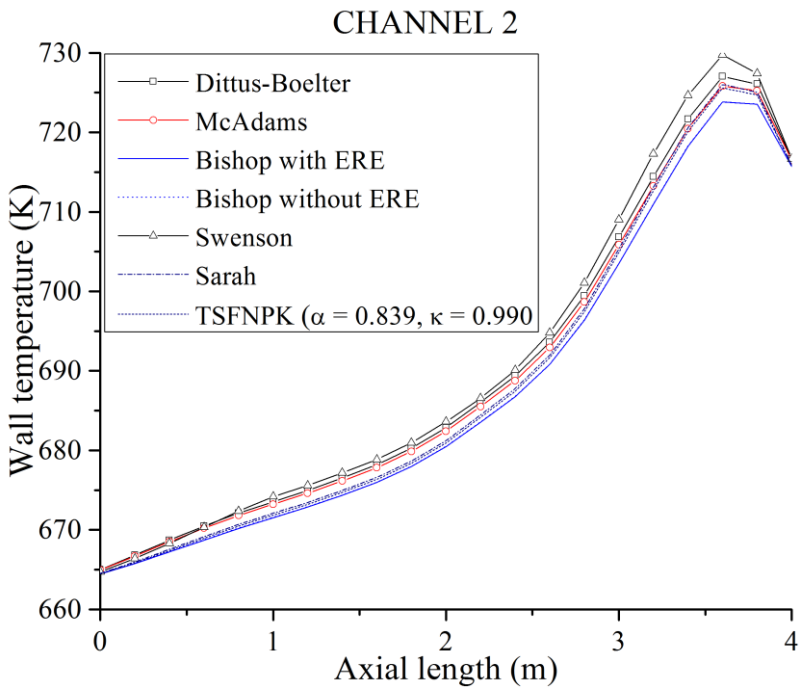

Figure 5.8. Simulation results for Channel 2 showing the wall temperature behavior for different HTCs.

Figure 5.9 presents the results for Channel 3, showing the wall temperature behavior for the correlations presented in Table 5.1. In this case, the trends that most resemble each other are presented. Again, the Swenson's correlation deviates the most, yielding slightly higher temperatures than other correlations.

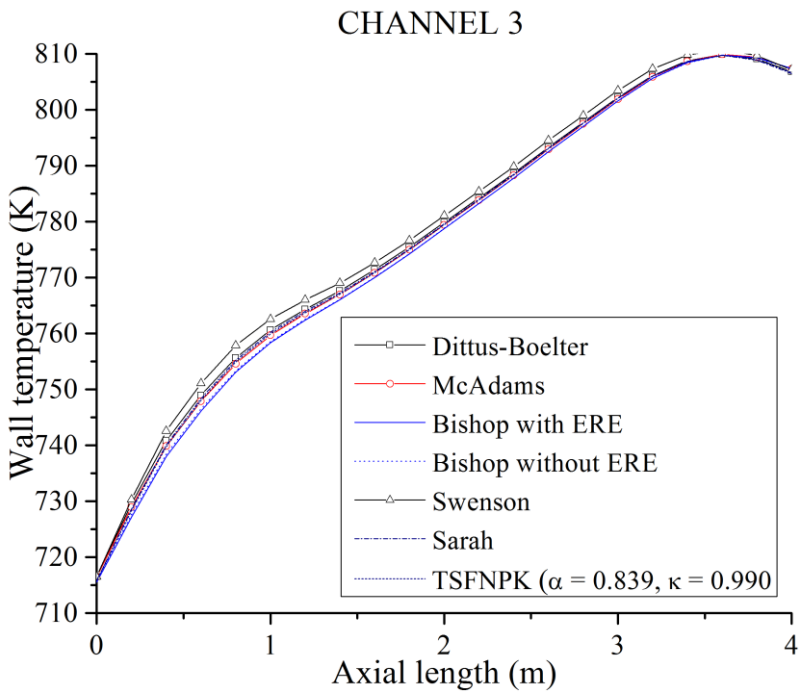

Figure 5.9. Simulation results for Channel 3 showing the Wall Temperature behavior for different HTCs.

It has been found that Bishops correlation represents more closely HTCs through the heated length but deviates significantly in the pseudocritical range, and the Dittus-Boelter correlation predicts closely experimental HTCs outside the pseudocritical region, usually experimental HTCs are compared to these correlations (Mokry et al., 2009b and 2011). Therefore, for the present study, it is correct to take both correlations as reference due that are in good agreement with experimental data, i.e., temperature and pressure above the critical point (647 K and 22.5 MPa) from Channel 1

Bishop's correlations, with and without Entrance-Region Effect (ERE) have little differences among them in the prediction of the wall temperatures, meaning that, for this simulation the ERE is not important. The latter can be observed with the naked eye in Figures 5.7-5.9 (clear blue line and clear blue dotted line) where the correspondent curves overlap. Predictions compared to the Dittus-Boelter correlation are a little higher in the first channel and slightly

lower in channels 2 and 3. With Mokrys correlation, higher temperature predictions were found in Channel 1, but were very similar to Dittus-Boelter in channels 2 and 3. Swenson's correlation showed the most deviated results, yielding lower temperatures in the first channel and higher in channels 2 and 3.

CONCLUSIONS

In this PhD thesis the development of a novel zero-dimensional mathematical model of two different fractional orders was developed and analyzed to study the simultaneous heat and neutron transport processes in nuclear power reactors. The model developed was called Time-Space Fractional Neutron Point Kinetics (TSFNPK), which considers two-anomalous diffusion exponents: one for the differential operator dependent in time and another for the dependent operator in space. It is important to note that the TSFNPK model has unique relevant characteristics, because the memory in time is of the non-local type due that the differential operator of fractional order ($D^{\alpha+1}$ and D^{α}), and the memory in space is local, i.e., it does not depend on the past and neither the future to obtain the present state, due to is a function of the fractional order reactor geometry ($B_g^{\kappa+1}$). The TSFNPK represents a model extended of the point reactor kinetics equations (PRKE), because when α and κ tend one this is recovered.

The model was assessed in order to obtain the intervals in which the fractional diffusion exponents yielded results which agreed to compared data, e.g., during positive reactivity insertion pulse type experiment. In this experiment the anomalous diffusion coefficients that were found are: $\alpha = 0.839$ and $\kappa = 0.99$ with a relative error of 0.09% vs 19.88% of PRKE. These values of the exponents of fractional order, mean that the neutronic processes in a nuclear reactor are of a subdiffusive nature.

In order to evaluate different heat transfer correlations, the TSFNPK model was coupled to a thermal-hydraulic model of a SCWR, it was found that the correlation, which agrees most with Dittus-Boelter, is McAdams. The only difference in the equation is the value of the coefficient. Mokrys correlation had higher temperature predictions in Channel 1 but were very similar to Dittus-Boelter in channels 2 and 3. And Swenson's correlation presents the most deviated results.

Challenges and recommendations

This work represents a framework for future research that is challenging.

- Develop systematic methods considering that the fractional order model is a poorly posed problem, because fractional orders in space and time are not known a priori.
- Consider problem where the effect of the fractional order spatial operator (memory in space) is non-local, as in the case of memory in time.
- Apply the PRKE model for the analysis of transients and safety in nuclear reactors, which can be compared with data from nuclear power plants.
- Explore fractional order models for neutron kinetics with complex conjugate numbers

REFERENCES

Amaral, Barbara, Vilhena, Marco T., Segatto, Cynthia F., & Malamut, C. (2003). An alternative solution for the multidimensional transport equation in cartesian geometry and unbounded domain using fractional derivative. Proceedings of the 18 ICTT: International conference on transport theory, (p. 355). Brasil

Aboanber, A. E., & Nahla, A. A. (2016a). Comment on the paper: Espinosa-Parrdes, et al., 2011. Fractional neutron point kinetics equations for nuclear reactor dynamics. Ann. Nucl. Energ. 38, 307–330. *Annals of Nuclear Energy*, *100* (88), 301-302.

Aboanber, A. E., & Nahla, A. A. (2016b). A novel fractional technique for the modified point kinetics equations. *Journal of the Egyptian Mathematical Society*, *24*(4), 666-671.

Aboanber, A. E., Nahla, A. A., & Hemeda, A. A. (2018a). Spectrum behavior for the nonlinear fractional point reactor kinetics model. *Nuclear Science and Techniques*, *29*(1), 1-14.

Aboanber, A. E., Nahla, A. A., & El Mhlawy, A. M. (2018b). Mittag-Leffler and Padé approximations to stiff fractional two point kinetics equations. *Progress in Nuclear Energy*, *104*, 317-326.

Aboanber, A. E., Nahla, A. A., & Edress, A. M. (2018c). Developed mathematical technique for fractional stochastic point kinetics model in nuclear reactor dynamics. *Nuclear Science and Techniques*, *29*(9), 132.

Aboanber A.E., Nahla A.A., & Aljawazneh S.M. (2021). Fractional two energy groups matrix representation for nuclear reactor dynamics with an external source. *Annals of Nuclear Energy*, 153, 108062.

Antaki, P.J., 1998. Importance of non-Fourier heat conduction in solid-phase reactions. Combustion and Flame. 112, 329–341.

Barragán-Martínez A. (2013). Diseño neutrónico y termohidráulico de un reactor nuclear enfriado con agua supercrítica, PhD Thesis, Universidad Nacional Autóma de México, Meixco City.

Bishop A., Sandberg R., Tong L. S. (1964). High Temperature Supercritical Pressure Water Loop: Part IV, Forced Convection Heat Transfer to Water at Near-Critical Temperatures and Super-Critical Pressures, Westinghouse Electric Corporation, Pittsburgh, Pennsylvania (1964).

Cattaneo, C. (1958). Sur une forme de l'équation de la chaleur éliminant le paradoxe d'une propagation instantanée, C.R. Acad. Sci. 247, 431–432.

Cázares-Ramírez, R. I., & Espinosa-Paredes, G. (2016). Time-fractional telegraph equation for hydrogen diffusion during severe accident in BWRs. *Journal of King Saud University-Science*, *28*(1), 21-28.

Cázares-Ramírez R. I., Vyawahare V. A., Espinosa-Paredes G., & Nataraj P. S. V. (2017). On the feedback stability of linear FNPK equations. *Progress in Nuclear Energy, 98,* 45-58.

Das, S., & Biswas, B. B. (2007). Fractional divergence for neutron flux profile in nuclear reactors. International Journal of Nuclear Energy Science and Technology, 3(2), 139-159.

Das, S., (2008). Functional fractional calculus for system identification and controls. Berlin: Springer-Verlag, 2008

Das, S., Mukherjee, S., Das, S., Pan, I., Gupta, A., (2013). Continuous order identification of PHWR models under step-back for the design of hyper-damped power tracking controller with enhanced reactor safety. Nuclear Engineering and Design, 257, 109-127.

Davijani, N. Z., Jahanfarnia, G., & Abharian, A. E. (2016). Nonlinear fractional sliding mode controller based on reduced order FNPK model for output power control of nuclear research reactors. *IEEE Transactions on Nuclear Science*, *64*(1), 713-723.

Diethelm, K., 1997. An algorithm for the numerical solution of differential equations of fractional order. Electron. Trans. Numer. Anal, 5(1), 1-6.

Dittus F & Boelter L.M. (1930). Heat transfer in automobile radiators of the tubular type, University of California, Publications in Engineering 2, 443-461.

Duderstadt, J. J., Hamilton, L.J., (1976). Nuclear Reactor Analysis. John Wiley & Sons, USA, 1976.

Dzieliński, A., Sierociuk, D., & Sarwas, G. (2010). Some applications of fractional order calculus. Bulletin of the Polish Academy of Sciences: Technical Sciences, 58(4), 583-592.

Edwards J.T., Ford N.J., Simpson A.C., 2002. The numerical solution of linear multiterm fractional differential equations. J. Comput. Appl. Math. 148, 401-418.

Espinosa-Martínez E.-G., François J.L., Martín-del-Campo C., (2018). Time-Space Fractional Neutron Point Kinetics with Temperature Feedback Effects Proceedings of Pacific Basin Nuclear Conference 2018, San Francisco, CA..

Espinosa-Martínez E.-G. François J.L., Martín-del-Campo C. (2020). Time-Space fractional neutron point kinetics: Theory and Simulations. *Annals of Nuclear Energy*, 143, 107448.

Espinosa-Paredes G., Morales-Sandoval J. B., Vázquez-Rodríguez R. & Espinosa-Martínez E. G. (2008). Constitutive laws for the neutron density current. *Annals of Nuclear Energy* 35(10), 1963-1967.

Espinosa-Paredes G., Espinosa-Martínez E.-G. (2009). Fuel rod model based on Non-Fourier

Heat Conduction Equation. Annals of Nuclear Energy. 36, 680-693.

Espinosa-Paredes, G., Polo-Labarrios, M. A., Espinosa-Martinez, E. G., & del Valle-Gallegos, E. (2011). Fractional neutron point kinetics equations for nuclear reactor dynamics. Annals of Nuclear Energy, 38(2), 307-330.

Espinosa-Paredes G., Polo-Labarrios, M.-A., 2012. Time-fractional telegrapher´s equation (P1) approximation for the transport equation. Nuclear Science and Engineering Journal, vol. 171, 258-264.

Espinosa-Paredes G, Vázquez-Rodríguez R., del Valle Gallegos E., Alonso G., Moghaddam N.M., 2013. Fractional-space law for the neutron current density. Annals of Nuclear Energy, vol. 55, 120-125.

Espinosa-Paredes G., Vázquez-Rodríguez A., Polo-Labarrios M. A., Espinosa-Martínez E.-G., Gómez-Arrieta R. (2014). The Transient Heat Transfer of a Pebble Fuel Considering Anomalous Diffusion. Energy Sources A, 36(3), 284-291.

Espinosa-Paredes G., del Valle Gallegos, E., Núnez-Carrera, A., Polo-Labarrios, M. A., Espinosa-Martínez E. G., & Vázquez-Rodríguez, A. (2014b). Fractional neutron point kinetics equation with newtonian temperature feedback effects. Progress in Nuclear Energy, 73, 96-101.

Espinosa-Paredes, G., Polo-Labarrios, M. A. (2016). Analysis of the fractional neutron point kinetics (FNPK) equation. Annals of Nuclear Energy, 92, 263-268.

Espinosa-Paredes G. (2017). Fractional-space neutron point kinetics (F-SNPK) equations for nuclear reactor dynamics, Annals of Nuclear Energy, 100, 136-143.

Espinosa-Paredes, G. (2016). Fractional-space neutron point kinetics (F-SNPK) equations for nuclear reactor dynamics. *Annals of Nuclear Energy* (Publicado en línea)

Ganapol B. D., 2008. Analytical benchmarks for nuclear engineering applications, Nuclear Energy Agency.

Glasstone, S., Sesonske, A., 1981. Nuclear Reactor Engineering, third ed. VNR, New York, United States of America.

Hamada, Y. M. (2017). Solution of the fractional neutron point kinetics equations considering time derivative of the reactivity. *Progress in Nuclear Energy*, *98*, 153-166.

Hamada, Y. M. (2017b). Modified fractional neutron point kinetics equations for finite and infinite medium of bar reactor core. *Annals of Nuclear Energy*, *106*, 118-126.

Hamada, Y. M., & Brikaa, M. G. (2017). Nonstandard finite difference schemes for numerical solution of the fractional neutron point kinetics equations. *Annals of Nuclear Energy*, *102*, 359-367.

Hamada Y., (2020). Solution of a new model of fractional telegraph point reactor kinetics using differential transformation method. *Applied Mathematical Modelling,* 78, 297-321.

Hilfer, R., 2000. Applications of fractional calculus in physics. World Scientific, Sigapore, 2000

Joseph, D.D., Preziosi, L., 1989. Heat waves. Rev. Mod. Phys. 61, 41– 73.

Joseph, D.D., Preziosi, L., 1990. Addendum to the paper "Heat waves". Rev. Mod. Phys. 62, 375–391.

Kilbas, A.A., Srivastava, H.M., Trujillo, J.J., 2006. Theory and applications of fractional differential equations. Elsevier, Amsterdam.

Lewandowska, M., Malinowski, K., 2006. An analytical solution of the hyperbolic heat conduction equation for the case of a finite medium symmetrically heated on both sides. International Communications in Heat and Mass Transfer 33, 61– 69.

Lor, W., Chu, H., 2000. Effect of interface thermal resistance on heat transfer in a composite medium using the thermal wave model, International Journal of Heat and Mass Transfer 43, 653–663.

McAdams W. (1942). Heat Transmission, 2nd ed., McGraw-Hill, New York.

Moghaddam, N. M., Afarideh, H., Espinosa-Paredes, G., 2014. On the numerical solution of the neutron fractional diffusion equation. Annals of Nuclear Energy 70, 1-10.

Moghaddam, N. M., Afarideh, H., Espinosa-Paredes, G., 2015a. Development of a 2D-Multigroup Code (NFDE-2D) based on the neutron spatial-fractional diffusion equation. Applied Mathematical Modeling 39, 3637-3652.

Moghaddam, N. M., Afarideh, H., Espinosa-Paredes, G., 2015b. Development of a 3D-Multigroup program to simulate anomalous diffusion phenomena in the nuclear reactors. Annals of Nuclear Energy 76, 378-389.

Moghaddam, N. M., Afarideh, H., Espinosa-Paredes, G., 2015c. Modifying the neutron diffusion equation using spatial fractional operators and developed diffusion coefficients. Progress in Nuclear Energy 83, 59-72.

Mokry S., Farah A., King K., Gupta S., Pioro I., Kirillov P. (2009a). Development of supercritical water heat-transfer correlation for vertical bare tubes, International Conference Nuclear Energy for New Europe 2009, Slovenia.

Mokry S., Gospodinov Y., Pioro I., Kirillov P. (2009b). Supercritical water heat-transfer correlation for vertical bare tubes, International Conference Nuclear Engineering (ICONE17), Brussels, BELGIUM.

Mokry S., Pioro I., Farah A., King K., Gupta S., Peiman W., Kirillov P. (2011). Development of supercritical water heat-transfer correlation for vertical baretubes. Nuclear Engineering and Design 241, 1126-1136.

Nahla, A. A. (2017). Analytical solution of the fractional point kinetics equations with multi-group of delayed neutrons during start-up of a nuclear reactor. Annals of Nuclear Energy 99, 247-252.

Nahla, A. A., & Hemeda, A. A. (2017). Picard iteration and Padé approximations for stiff fractional point kinetics equations. Applied Mathematics and Computation, 293, 72-80.

Nikan O., Avazzadeh Z., Tenreiro Machado J.A. (2021). Numerical approximation of the

nonlinear time-fractional telegraph equation arising in neutron transport, Communications in Nonlinear Science and Numerical Simulation

Nowak, T. K., Duzinkiewicz, K., Piotrowski, R., 2014a. Fractional neutron point kinetics equations for nuclear reactor dynamics–Numerical solution investigations. Annals of Nuclear Energy, 73, 317-329.

Nowak, T. K., Duzinkiewicz, K., Piotrowski, R., 2014b. Numerical solution of fractional neutron point kinetics model in nuclear reactor. Archives of Control Sciences 24 (2), 129-154.

Nowak, T. K., Duzinkiewicz, K., Piotrowski, R., 2015. Numerical solution analysis of fractional point kinetics and heat exchange in nuclear reactor. Nuclear Engineering and Design, 281, 121-130.

Oldham, K.B., Spanier, J., 1974. The fractional calculus, Academic Press, New York, USA.

Ozisik, M.N., Tzou D.Y., 1994. On the wave theory in heat conduction. J. Heat Transfer 116, 526–535.

Patankar S. (1980) Numerical Heat Transfer and Fluid Flow. McGraw-Hill, New York.

Patra, A., & Ray, S. S. (2015). On the solution of the nonlinear fractional neutron point-kinetics equation with Newtonian temperature feedback reactivity. Nuclear Technology, 189(1), 103-109.

Pioro I., Khartabil H. F., Duffey R. B. (2004). Heat transfer to supercritical fluids flowing in channels—empirical correlations (survey). Nuclear Engineering and Design, 230(1), pp. 69-91.

Pioro I. & Duffey R., (2007). Heat Transfer and Hydraulic Resistance at Supercritical Pressures in Power Engineering Applications, ASME Press, New York, USA.

Podlubny I., 1999. Fractional differential equations. Academic Press; San Diego, USA.

Polo-Labarrios, M. A., Espinosa-Paredes, G., 2012. Application of the fractional neutron point kinetic equation: Start-up of a nuclear reactor. Annals of Nuclear Energy, 46, 37-42.

Polo-Labarrios M. A., Quezada-García S., Espinosa-Paredes G., Ortiz-Villafuerte J. (2020a). Novel numerical solution to the fractional neutron point kinetic equation in nuclear reactor dynamics. *Annals of Nuclear Energy*, 137, 107173.

Polo-Labarrios M. A., Quezada-García S., Espinosa-Paredes G., Ortiz-Villafuerte J. (2020b). Assessment of the fractional neutron point kinetic equation to simulate core transients with Newtonian temperature feedback. *Annals of Nuclear Energy*, 138, 107197.

Rafiei, M., Ansarifar, G. R., Hadad, K., & Mohammadi, M. (2019a). Stability analysis of linear FNPK model considering reactivity feedback effects for a research nuclear reactor. *Progress in Nuclear Energy*, *117*, 103081.

Rafiei, M., Ansarifar, G. R., & Hadad, K. (2019b). Core Power Control of a Nuclear Research Reactor during power maneuvering transients using Optimized PID-Controller based on the Fractional Neutron Point Kinetics model with reactivity feedback effects. *IEEE Transactions on Nuclear Science*, 1-11.

Ray, S. S., Patra, A., 2012. An explicit finite difference scheme for numerical solution of fractional neutron point kinetic equation. Annals of Nuclear Energy, 41, 61-66.

Ray, S.S. Patra, A., 2013. Numerical solution of fractional stochastic neutron point kinetic equation for nuclear reactor dynamics. Annals of Nuclear Energy 54,154-161.

Ray, S.S., Patra, A., 2015. On the Solution of the Nonlinear Fractional Neutron Point-Kinetics Equation with Newtonian Temperature Feedback Reactivity. Nuclear Technology, 189(1), 103-109.

Ray, S. S., 2015. Fractional Calculus with Applications for Nuclear Reactor Dynamics. CRC Press.

Roul, P., Goura, V. P., Madduri, H., & Obaidurrahman, K. (2019a). Design and stability analysis of an implicit non-standard finite difference scheme for fractional neutron point kinetic equation. *Applied Numerical Mathematics, 145*, 201-226.

Roul, P., Madduri, H., & Obaidurrahman, K. (2019b). An implicit finite difference method for solving the corrected fractional neutron point kinetics equations. *Progress in Nuclear Energy 114*, 234-247.

Roul P., Rohil P., Espinosa-Paredes G., Obaidurrahman K. (2021). Design and analysis of a numerical method for fractional neutron diffusion equation with delayed neutrons. *Applied Numerical Mathematics*, 157, 634-653.

Roul P., Rohil P., Espinosa-Paredes G., Obaidurrahman K. (2021). An efficient numerical method for fractional neutron diffusion equation in the presence of different types of reactivities. *Annals of Nuclear Energy*, 152, 108038.

Sadeghi P. Darania, (2020). On the approximate solutions of the fractional neutron point kinetics equations. *Annals of Nuclear Energy*, 148, 107693.

Sallah, M., & Margeanu, C. A. (2016). Effect of fractional parameter on neutron transport in finite disturbed reactors with quadratic scattering. In Paraschiv, Irina Maria (Ed.). Proceedings of NUCLEAR 2016 the 9th annual international conference on sustainable development through nuclear research and education Part 1/3, (p. 332). Romania: Institute for Nuclear Research - Pitesti.

Samko SG, Kilbas AA, Marichev OI (1993) Fractional integrals and derivatives: theory and applications. Gordon and Breach Science Publishers, Switzerland

Sardar, T., Ray S., Bera R K., Biswas, B. B., & Das, S. (2010). The solution of coupled fractional neutron diffusion equations with delayed neutrons. *International Journal of Nuclear Energy Science and Technology*, *5*(2), 105.

Schramm, M., Petersen, C. Z., Vilhena, M. T., Bodmann, B. E. J., Alvim, A. C. M., 2013. On the Fractional Neutron Point Kinetics Equations. In Integral Methods in Science and Engineering (pp. 229-243). Springer New York.

Schramm, M., Bodmann, B. E. J., Alvim, A. C. M., Vilhena, M. T., 2016. The neutron point kinetics equation: Suppression of fractional derivative effects by temperature feedback. Annals of Nuclear Energy, 87, 479-485.

Sierociuk, D., Dzieliński, A., Sarwas, G., Petras, I., Podlubny, I., & Skovranek, T. (2013). Modelling heat transfer in heterogeneous media using fractional calculus.

Singh, S., & Ray, S. S. (2019). Higher-order approximate solutions of fractional stochastic point kinetics equations in nuclear reactor dynamics. *Nuclear Science and Techniques*, *30*(3), 49.

Shirazi, S. A. M. (2012). The theoretical simulation of a model by SIMULINK for surveying the work and dynamical stability of nuclear reactors cores (pp 175-196). In: *Nuclear Reactors*. InTech: Croatia.

Swenson H., Carver J., Kakarala C. R. (1965). Heat Transfer to Supercritical Water in Smooth-Bore Tubes," J. of Heat Transfer, Trans. ASME Series C, 87(4), pp. 477-484.

Thind H. (2012). Heat-transfer analysis of double-pipe heat exchangers for indirect-cycle SCW NPP. Master Thesis, University of Ontario Institute of Technology, Ontario.

Philosophical Transactions of the Royal Society of London A: Mathematical, Physical and Engineering Sciences, 371(1990), 20120146.

Schulenberg T., Starflinger J. (2012) High performance light water reactor – design and analyses, KIT Scientific Publishing 2012.

Stacey W. M., 2001. Nuclear Reactor Physics. John Wiley and Sons, INC, New York.

Tang, D.W., Araki, N., 2000. Non-Fourier heat conduction behavior in finite mediums under pulse surface heating. Mater. Sci. Eng. A292, 173–178.

Thind H. (2012). Heat-transfer analysis of double-pipe heat exchangers for indirect-cycle SCW NPP. Master Thesis, University of Ontario Institute of Technology, Ontario.

Todreas & Kazimi 1990. Nuclear Systems Volume I: Thermal Hydraulic Fundamentals. Hemisphere Pub. Corp. New York.

Tzou D.Y., 1997. Macro- to Microscale Heat Transfer, Taylor & Francis, Washington.

Vernotte, P., 1958. Les paradoxes de la théorie continue de l'équation de la chaleur, C.R. Acad. Sci. 246, 3154–3155.

Vyawahare, V. A., & Nataraj, P. S. V. (2013a). Development and analysis of some versions of the fractional-order point reactor kinetics model for a nuclear reactor with slab geometry. *Communications in Nonlinear Science and Numerical Simulation*, *18*(7), 1840-1856.

Vyawahare, V. A., & Nataraj, P. S. V. (2013b). Fractional-order modeling of neutron transport in a nuclear reactor. *Applied Mathematical Modelling*, *37*(23), 9747-9767.

Vyawahare, V. A., & Nataraj, P. S. V. (2015). Analysis of fractional-order point reactor kinetics model with adiabatic temperature feedback for nuclear reactor with subdiffusive neutron transport. In *Simulation and Modeling Methodologies, Technologies and Applications* (pp. 153-172). Springer, Cham.

Vyawahare, V. A., & Nataraj, P. S. V. (2016). Development of One-dimensional Fractional-order Two-Group Models for Nuclear Reactor. *IFAC-PapersOnLine*, 49(1), 260-265.

Vyawahare, V. A., Nataraj, P. S. V., Espinosa-Paredes, G., & Cázares-Ramírez, R. I. (2016). Nuclear reactor with subdiffusive neutron transport: development of linear fractional-order models. *International Journal of Dynamics and Control*, *5*(4), 1182-1200.

Vyawahare, V. A., & Espinosa-Paredes, G. (2017). BWR stability analysis with sub-diffusive and feedback effects. *Annals of Nuclear Energy, 110,* 349-361.

Vyawahare, V. A., Nataraj, P. S. V., Espinosa-Paredes, G., & Cázares-Ramírez, R. I. (2017). Nuclear reactor with subdiffusive neutron transport: development of linear fractional-order models. *International Journal of Dynamics and Control*, *5*(4), 1182-1200.

Vyawahare, V. A., & Espinosa-Paredes, G. (2018). On the stability of linear fractional-space neutron point kinetics (F-SNPK) models for nuclear reactor dynamics. *Annals of Nuclear Energy, 111*, 12-21.

Vyawahare, V., & Nataraj, P. S. (2018). Fractional-order Modeling of Nuclear Reactor: From Subdiffusive Neutron Transport to Control-oriented Models: A Systematic Approach. Singapore: Springer.

Vyawahare, V. A., Espinosa-Paredes, G., Datkhile, G., & Kadam, P. (2018). Artificial neural network approximations of linear fractional neutron models. *Annals of Nuclear Energy, 113*, 75-88.

Wagner W. & Kretzschmar H.-J. (2008). International Steam Tables. Properties of Water and Steam based on the Industrial Formulation IAPWS-IF97, Springer, Second Edition.

Zabadal, J., Vilhena, M. T., Segatto, C. F., & Pazos, R. P. (2002). Determination of a closed-form solution for the multidimensional transport equation using a fractional derivative. Annals of Nuclear Energy, 29(10), 1141-1150.

Zhang, F., Chen, W.Z., Zhao, X.W., 2009. The dynamic simulation of cold start-up based on two-group point reactor model. Ann. Nucl. Energy 36, 784–786.